CONCEPTUAL DESIGN SYNTHESIS OF FIGHTER AIRCRAFT

A THESIS SUBMITTED TO
THE GRADUATE SCHOOL OF NATURAL AND APPLIED SCIENCES
OF
MIDDLE EAST TECHNICAL UNIVERSITY

BY

MERT TOKEL

IN PARTIAL FULFILLMENT OF THE REQUIREMENTS
FOR
THE DEGREE OF MASTER OF SCIENCE
IN
AEROSPACE ENGINEERING

SEPTEMBER 2019

Approval of the thesis:

CONCEPTUAL DESIGN SYNTHESIS OF FIGHTER AIRCRAFT

submitted by **MERT TOKEL** in partial fulfillment of the requirements for the degree of **Master of Science in Aerospace Engineering Department, Middle East Technical University** by,

Prof. Dr. Halil Kalıpçılar
Dean, Graduate School of **Natural and Applied Sciences**   _____

Prof. Dr. İsmail Hakkı Tuncer
Head of Department, **Aerospace Engineering**   _____

Prof. Dr. Serkan Özgen
Supervisor, **Aerospace Engineering, METU**   _____

Examining Committee Members:

Prof. Dr. İsmail Hakkı Tuncer
Aerospace Engineering Department, METU   _____

Prof. Dr. Serkan Özgen
Aerospace Engineering, METU   _____

Prof. Dr. Yusuf Özyörük
Aerospace Engineering Department, METU   _____

Prof. Dr. Hüseyin Nafiz Alemdaroğlu
School of Civil Aviation Department, ATILIM UNI.   _____

Prof. Dr. Kürşad Melih Güleren
Faculty of Aeronautics and Astronautics, ESTU.   _____

Date: 06.09.2019

I hereby declare that all information in this document has been obtained and presented in accordance with academic rules and ethical conduct. I also declare that, as required by these rules and conduct, I have fully cited and referenced all material and results that are not original to this work.

Name, Surname: Mert Tokel

Signature:

ABSTRACT

CONCEPTUAL DESIGN SYNTHESIS OF FIGHTER AIRCRAFT

Tokel, Mert
Master of Science, Aerospace Engineering
Supervisor: Prof. Dr. Serkan Özgen

September 2019, 118 pages

The aim of this thesis is to analyze the effects of initial engine scaling (using a competitor aircraft aerodynamic performance) on fighter aircraft conceptual design activities. A design synthesis including engine scaling, configuration development, fixed aircraft analysis, fixed wing aircraft sizing and optimization methodology has been developed. Engine data has been scaled to match the competitor aircraft drag performance at the supercruise requirement. Initial configuration design including the system layout and external surfaces have been created around the scaled engine geometry. This initial computer aided design model has been called as design 0. Fixed aircraft analysis evaluation of design 0 has proven that a sizing process must be applied to any given configuration in order to create a model that is compliant with the mission profile requirement.

Using optimization methodology with parallel computation capabilities, 1500 aircraft designs with unique wing geometries have been evaluated through the proposed design synthesis and pareto-front with the size of 100 design have been found. The Pareto solutions with non-compliant requirement qualities have been eliminated. From obtained set of aircraft, "best" design has been selected using multi-criteria decision analysis. Final design result has proven that the initial engine scaling has created a basis for requirement compliant aircraft design options.

Multi-criteria decision analysis has been observed to be a useful process to determine the "best" aircraft among the set of alternative design solutions. Criteria weights have been assigned based on designer's decision on the significance of each merit. Therefore, in order to select one aircraft as a reference, a subjective "best" design selection has been found to be acceptable.

Keywords: Conceptual Design, Fighter Aircraft, Optimization

ÖZ

SAVAŞ UÇAĞI KAVRAMSAL TASARIM SENTEZİ

Tokel, Mert
Yüksek Lisans, Havacılık ve Uzay Mühendisliği
Tez Danışmanı: Prof. Dr. Serkan Özgen

Eylül 2019, 118 sayfa

Bu tezde rakip uçak aerodinamik performansı üzerinden ön motor boyutlandırılmasının savaş uçağı kavramsal tasarım süreçlerine etkisi araştırılmıştır. Motor boyutlandırılması, konfigürasyon geliştirilmesi, dondurulmuş uçak modeli analizi, kanat geometrisi sabit bir uçak boyutlandırılması ve eniyileme metodunu içeren bir tasarım sentezi geliştirilmiştir. Motor verisi belirlenen rakip uçağın süperseyir isteri koşullarındaki sürükleme kuvvetine göre boyutlandırılmıştır. Ön konfigürasyon tasarımı bünyesinde, elde edilen motor verileriyle sistem yerleşimi ve dış yüzey tasarımı geliştirilmiştir. Bu ön bilgisayar destekli çizim modeli tasarım 0 olarak isimlendirilmiştir. Tasarım 0 kullanılarak tamamlanan dondurulmuş uçak modeli analizi, geliştirilen herhangi bir ön konfigürasyon tasarımının görev profilini sağlayan bir modele dönüşümü için uçak boyutlandırma sürecinden geçmesinin gerekliliğini ortaya koymuştur.

Paralel hesaplama kabiliyetlerine sahip eniyileme metoduyla oluşturulan özgün kanat geometrine sahip 1500 uçak tasarımı önerilen tasarım sentezine göre değerlendirilmiş ve 100 tasarıma sınırlandırılmış pareto-optimumu hesaplanmıştır. Herhangi bir isteri sağlamayan sonuçlar elenmiştir. Elde edilen uçaklar arasından "en iyi" tasarım çok-kriterli karar analizi kullanılarak seçilmiştir. Böylece ön motor boyutlandırılmasının isterleri sağlayan uçak elde etme yolunda katkı sağladığı kanıtlanmıştır.

Çok kriterli karar analizinin alternatifler arasından "en iyi" uçak seçimi yolunda kullanışlı bir yöntem olduğu gözlenmiştir. Kriter ağırlıkları her öğenin önemine göre tasarımcının kararıyla atanmıştır. Bu nedenle, bir uçağı referans olarak seçebilmek adına, isterleri sağlayan uçaklar arasından "en iyi" tasarımı elde etmenin öznel bir yaklaşımla sağlanması kabul edilmiştir.

Anahtar Kelimeler: Kavramsal Tasarım, Savaş Uçağı, Optimizasyon

This thesis is dedicated to the people who believe the future is in the skies.

ACKNOWLEDGEMENTS

TABLE OF CONTENTS

LIST OF TABLES

TABLES

LIST OF FIGURES

FIGURES

xvii

LIST OF ABBREVIATIONS

ABBREVIATIONS

ATF	The Advanced Tactical Fighter
FEM	Finite Element Method
FLOPS	Flight Optimization System
AR	Aspect Ratio
QC	Quarter-Chord
ATF	Advanced Tactical Fighter
M	Mach Number
nm	Nautical Miles
cg	Center of Gravity
rad	Radians
TVC	Tail Volume Coefficient
SEP	Specific Excess Power
L/D	Lift Over Drag
NSGA II	Nondominated Sorting Genetic Algorithm II
ESF	Engine Scale Factor
THR	Thrust Ratio
CFD	Computational Fluid Dynamics
HPC	High Performance Computing

LIST OF SYMBOLS

SYMBOLS

ρ	Density (kg/m^3)
ρ_∞	Freestream Density (kg/m^3)
g	Gravitational Acceleration (m/s^2)
m	Mass (kg)
$\dot{m}$	Mass Flow (kg/s)
f	Function
Δ	Sweep Angle (deg)
S	Area (m^2)
L	Tail arm (m)
C	Chord Length (m)
$\bar{c}$	Mean Aerodynamic Chord Length (m)
b	Span (m)
d	Fuselage Diameter (m)
K	Drag Due To Lift Factor
$C_{L_{design}}$	Design Lift Coefficient
C_{L_α}	Lift Curve Slope (rad^{-1})
$C_{L_{max}}$	Maximum Lift Coefficient
C_D	Drag Coefficient
C_{D_0}	Zero-Lift Drag Coefficient
β	Compressibility Parameter
F	Fuselage Lift Factor
M_{DD}	Drag Divergence Mach Number
Re	Reynolds Number
μ	Dynamic Viscosity (Pa*s)
FF	Form Factor
C_f	Flat-Plate Skin Friction Coefficient
A_{base}	Base Area (m^2)
C_{D_i}	Drag Coefficient Due To Lift
$\dot{m}_{fuel}$	Fuel Flow (kg/s)
t_{spent}	Time Spent In Mission Segment (s)
S_{ref}	Reference Wing Area (m^2)
V_{stall}	Stall Speed (m/s)
$V_{takeoff}$	Takeoff Speed (m/s)
V_{sound}	Speed of Sound (m/s)
dt	Time Intervals (s)

NPF	Net Propulsive Force (N)
D	Drag Force (N)
L	Lift Force (N)
f_s	Ground Friction Coefficient
a	Acceleration (m/s^2)
$W_{aircraft}$	Aircraft Mass (kg)
$W_{aircraft,before}$	Aircraft Mass Before Time Interval (kg)
$W_{aircraft,after}$	Aircraft Mass After Time Interval (kg)
V_∞	Freestream Velocity (m/s)
$V_{\infty,before}$	Freestream Velocity Before Time Interval (m/s)
$V_{\infty,after}$	Freestream Velocity After Time Interval (m/s)
X_{before}	Distance Traveled Before Time Interval (m)
X_{after}	Distance Traveled After Time Interval (m)
$W_{fuel,before}$	Fuel Mass Consumed Before Time Interval (kg)
$W_{fuel,after}$	Fuel Mass Consumed After Time Interval (kg)
t_{before}	Time Spent Before Time Interval (s)
t_{after}	Time Spent After Time Interval (s)
γ_{climb}	Climb Angle (rad)
V_{∞_x}	Freestream Velocity Horizontal Component (m/s)
V_{∞_y}	Freestream Velocity Vertical Component (m/s)
H_{before}	Altitude Before Time Interval (m)
H_{after}	Altitude After Time Interval (m)
$\dot{\varphi}$	Turn Rate (rad/s)
φ_{before}	Turned Angle Before Time Interval (rad)
φ_{after}	Turned Angle After Time Interval (rad)
n	Load Factor
q	Dynamic Pressure (kg/(ms^2))
R	Turn Radius (m)
n_{guess}	Guessed Load Factor
n_{calc}	Calculated Load Factor
TAR	Transition-Arc Radius (m)
h_{TR}	Transition Altitude (m)
$h_{obstacle}$	Obstacle Clearance Altitude (m)
S_T	Transition Distance (m)
S_C	Climb Distance (m)
CAR	Circular-Arc Radius (m)
h_{FR}	Flare Altitude (m)
S_A	Approach Distance (m)
S_F	Flare Distance (m)
D_{max}	Maximum Engine Diameter (m)

CHAPTER 1

INTRODUCTION

1.1. Overview

Modern technology advancements encourage research around aircraft designs in aviation industry. Aircraft can be categorized as civil or military vehicles based on the operating purposes. Military aircraft have been designed around complex set of requirements, because these vehicles must follow the advancements in technology and include capabilities to overwhelm potential enemy aircraft or ground defense systems. An example of this is the development of Lockheed YF-22 and Northrop YF-23 to the Advanced Tactical Fighter (ATF) program. The ATF program was introduced to challenge the US aviation companies for a design that has supersonic maneuverability and supersonic flight with low observability (stealth) specifications [1]. Conceptual designs of YF-22 and YF-23 have been presented in Figure 1.1 with F-15 as a comparison to a standard U.S fighter with air superiority role. Eventually Lockheed YF-22 won the ATF program after the first flight and F-22 Raptor was manufactured through the design work presented in [2].
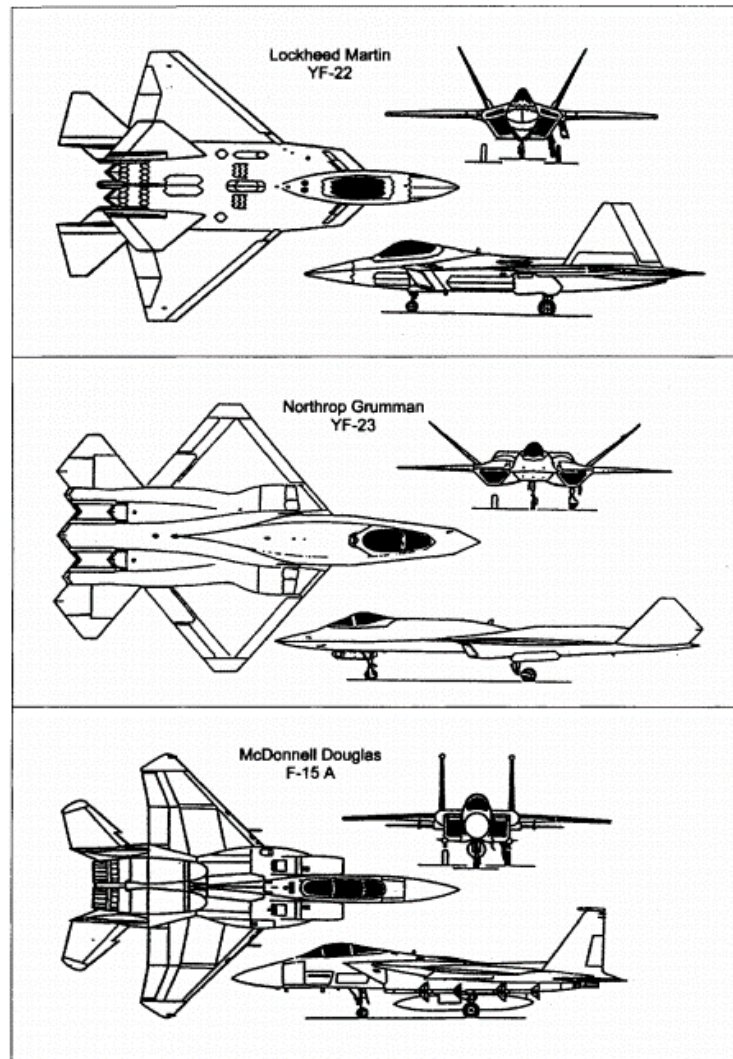
Figure 1.1. Lockheed YF-22A and Northrop YF-23A designs, with F-15A (standard U.S air superiority fighter) illustrated for comparison [2]

Aircraft design stages have conventionally been categorized by three phases in aircraft design literature; conceptual design, preliminary design and detailed design [3][4]. Conceptual design is the process where the various set of potential aircraft solutions are defined and all the trade studies to the requirements are carried out. These aircraft solutions are the sized and modified versions of unique design ideas for program requirements. Preliminary design is the phase where high fidelity analyses, wind tunnel tests and model optimization of the resulting aircraft of conceptual design phase

are carried out. Any fundamental change necessities during preliminary design might lead to a set back to the program by going back to the conceptual design stage for re-evaluation of the design and the trade studies. Detailed design is the process where the complete model of aircraft assembly is created for manufacture. Experimental tests and high-fidelity numerical analyses are carried out on the detailed models in order to model dependable pre-flight results. Ground and flight tests contribute to the purposes of the detailed design stage and component optimization.

The data produced for key defense and commercial programs (F-35, 787 Dreamliner, 747-8, A380) that witnessed significant cost variation in [5] shows the importance of the conceptual aircraft design stage. Well-structured conceptual design work can identify the weaknesses of the design and progress towards another design solution. Any major aircraft changes at the later design stages bring additional cost and risk to the program.

Conceptual design of the aircraft revolves around a conceptual aircraft model and conceptual analysis (low-fidelity methods). In order to perform the aircraft design work, conceptual design tools have been developed to work with such simple models. Some of the well-known conceptual design tools are SUAVE [6], OpenVSP [7], KEACDE [8], FLOPS [9]. An example of conceptual aircraft model generated by OpenVSP is presented in Figure 1.2.
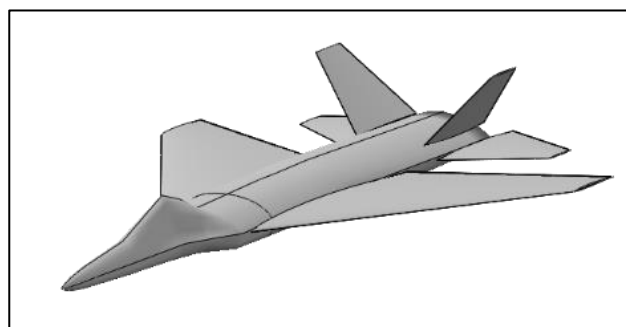
Figure 1.2. A parametric aircraft model generated by OpenVSP

Parametric aircraft model sets an opportunity for creation of increased number of aircraft designs automatically by the conceptual design framework. Conceptual methods estimate the geometry, weight, aerodynamics and performance data using the parametric models.

Each conceptual design software has its own design synthesis. Design methodologies can be evolved around "rubber" engine model (engine performance is sized with the aircraft) or constructed to work with fixed engine models (engine performance data is constant through the design work) [3]. Based on the design mission, aircraft can be sized to contain enough fuel, or the range of the design mission can be varied during design synthesis [10]. For fighter aircraft, it is hypothesized that the initial engine sizing plays a great role when finding the optimum engine size and aircraft configurations [11]. During analysis it has been proven that engines sized to the F-15 based aerodynamic model create a larger and heavier aircraft models. On the other hand, engine scaled to a F-106 based aerodynamic model, results in a smaller and lighter aircraft model that is compliant with the requirement sets. Therefore, the initial engine sizing is also included in the construction of the design synthesis proposed in this thesis.

Purpose of the design synthesis is to generate designs that contain the specifications of non-dominated optimum aircraft solutions (pareto-fronts). The selection of initial configuration from pareto-front depending on all the requirements can be achieved by using multi-criteria decision making algorithms such as analytic network process as used for trainer aircraft selection in [12].

1.2. Outline of the Thesis

Scope of this thesis is the development of a fighter aircraft design synthesis that evolves around initial engine sizing using a competitor aircraft aerodynamic model. In the design synthesis, initial configuration optimization to find pareto-front solutions

for critical performance merits and the successive design selection using multi-criteria decision are analyzed.

In chapter 2, definition of the aircraft design requirements are introduced. Requirements are split into two major categories, mission requirements and the top-level requirements. Importance of engine selection, engine net propulsive force calculation and the engine performance scaling equations are presented. Creation of aircraft configurations using the requirement sets and the internal system knowledge are shown.

In chapter 3, fixed aircraft analysis as core part of the design synthesis is introduced. All aircraft data (geometry, weight, aerodynamics and performance) are generated using the methods presented in this chapter. Geometric characteristics are calculated using the geometrical relations and mathematical algorithms suited for the analysis of 3D models generated using cross-sectional coordinates. Weights are calculated using the empirical equations for each weight breakdown element as presented in FLOPS weight estimation method [9]. Aerodynamics and performance calculations are constructed around empirical or physical equations as presented in [3][13].

In chapter 4, fixed wing aircraft sizing process is introduced. This sizing process is the modification of the aircraft geometry to include sufficient usable fuel to complete the design mission requirement successfully, respecting to the presented sizing rules. The multidisciplinary optimization methodology, the independent design variables, objectives and the constraints of the design problem are introduced. Aircraft conceptual design synthesis is constructed and the process is introduced. Estimation of the configuration selection using multi-criteria decision making is presented.

In chapter 5, an aircraft configuration is created around an engine that has been scaled with the F-15 aerodynamic data. This aircraft is sized using the synthesis presented in chapter 4, and calculations are made to find the aircraft that belong to the pareto-front of the optimization. Aircraft selection is made from this pareto-front based on the

multi-criteria decision-making methodology presented. Results are observed, compared and discussed.

In chapter 6, the conclusion regarding the scope of the thesis, importance of improvements on the design methodologies, observations from the results and the future work are presented.

CHAPTER 2

CONCEPTUAL AIRCRAFT DESIGN

2.1. Requirements

Preparations prior to the conceptual studies produce a fixed and necessary set of definitions which guide the designer team through their journey towards a target aircraft design. These set of definitions (also called the requirements) create a framework for the upcoming design stages [4]. In the present work, these set of requirements are split into two groups, mission requirements and the top-level requirements.

2.1.1. Mission Requirements

Modern advanced fighter aircraft are designed to fulfil multiple roles during their lifecycle. Therefore, the mission profile of the aircraft used during the design phases ought to be consistent with the necessities of selected role(s). In order to properly design an aircraft, the mission profile must be straightforward since an overcomplex mission profile might lead to confusion and misinterpretation during the conceptual design phase. There are multiple mission profiles corresponding to different aircraft roles used in the industry and released for the public knowledge in [14]. An example to the mission profiles that could be used for a fighter aircraft designs is presented in Figure 2.1.

The aim of the designer therefore, is to design an aircraft with sufficient fuel capacity so that the fuel required to complete the mission can be accommodated.
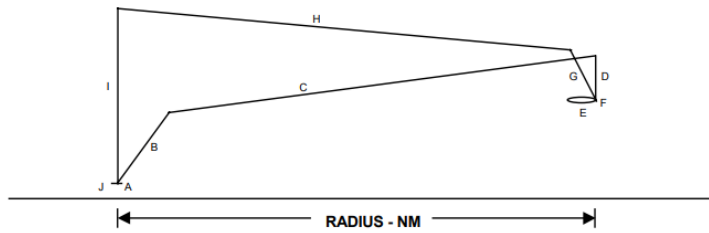
	SEGMENT	FUEL	TIME	DISTANCE	SPEED	ALTITUDE	THRUST SETTING
A	WARM-UP, TAKEOFF, AND ACCELERATE TO CLIMB SPEED	20 MIN @ GROUND IDLE + 30 SEC @ TAKEOFF / MAXIMUM / IRT (A/B IF REQUIRED) + FUEL TO ACCELERATE FROM OBSTACLE CLEARANCE TO CLIMB SPEED @ IRT. NO DISTANCE CREDIT.					
B	CLIMB (PARA 4.2.2)				MINIMUM TIME CLIMB SCHEDULE (3)	TAKEOFF TO OPTIMUM CRUISE	INTERMEDIATE
C	CRUISE (PARA 4.2.3)				OPTIMUM CRUISE	OPTIMUM CRUISE	
D	DESCENT (PARA 4.2.8)	NONE	NONE	NO CREDIT		END CRUISE TO 35,000 FEET PRESS ALT.	
E	LOITER (PARA 4.2.6)		1 HOUR	NO CREDIT	MAXIMUM ENDURANCE	35,000 FEET PRESS ALT.	
F	COMBAT (1) AND (2)	ONE 360 DEG TURN @ MACH 1.2 (MAX A/B) + TW0 360 DEG TURNS @ MACH 0.9 (MAX A/B). EXPEND HALF OF AMMO AND MISSILES. NO DISTANCE CREDIT.					
G	CLIMB (PARA 4.2.2)				MINIMUM TIME CLIMB SCHEDULE (3)	35,000 FEET PRESS ALT. TO OPTIMUM CRUISE	INTERMEDIATE
H	CRUISE (PARA 4.2.3)				OPTIMUM CRUISE	OPTIMUM CRUISE	
I	DESCENT (PARA 4.2.8)	NONE	NONE	NO CREDIT		END CRUISE TO LANDING	
J	RESERVES	20 MIN + 5% OF INITIAL FUEL		NO CREDIT	MAXIMUM ENDURANCE	SEA LEVEL	
K							
L							

NOTES: (1) SEE PARA 4.1.5 AND 4.1.7.
(2) INCLUDE FUEL TO ACCELERATE TO MACH 1.2.
(3) CLIMB SCHEDULE ENDS AT OPTIMUM CRUISE SPEED/ALTITUDE.

Figure 2.1. Mission profile: Combat Air Patrol [14]

2.1.2. Top-Level Requirements

Top-level requirements of the aircraft can be multiple set of definitions that are treated as drivers of the design. Some examples of these top-level requirements are presented below:

- Point performance requirements: Aircraft list of unique performance characteristics at a given flight regime, weight and configuration.
- System installation requirements: Aircraft to be designed to contain the list of predefined systems. For example, in order to increase the stealth characteristics, installation of the internal weapons bays can be named as a requirement instead of carrying external stores. Another example could be the wing folds or limit to the wing span of the carrier-based aircraft.

8

- Cost requirements: Aircraft's unit cost and/or direct operating cost.

The list can be expanded to variety of requirements, depending on the future aircraft's operating intention, technology advancements and environmental conditions.

2.2. Engine Selection and Scaling

Engine selection can be a multifaceted and time-consuming process of the aircraft design. If an off the shelf engine is an option, the design synthesis can be carried out for the list of selected engine models. However, most of the modern aircraft designs have unique engine designs developed alongside with the aircraft design and has an off the shelf interim engine option. The interim engine is used for testing and operations until the unique engine design is developed and manufactured. Details of aircraft engine design can be found in [4], however it is beyond the scope of this thesis.

The importance of the initial engine selection and its effects on the final aircraft design are presented in [11]. Therefore, the method presented in [11] is adopted into the design routine presented in this thesis. The method proposes that the size of the initial engine of the aircraft is dependent on the aerodynamic data set of the competitor aircraft. Selecting a competitor aircraft with higher supersonic drag leads to oversized engine specifications when compared to an aircraft with lower supersonic drag. Larger and heavier engine leads to larger and heavier overall aircraft configuration while achieving the same set of requirements.

Available engine data has been scaled to meet the top-level design requirements using the basic scaling laws as defined in [3]. These scaling laws are the functions of variable engine scale factor (ESF) and have been shown below.

$$L = L_{actual}(ESF)^{0.4} \tag{1}$$

$$D = D_{actual}(ESF)^{0.5} \tag{2}$$

$$\dot{m} = \dot{m}_{actual}(ESF)^{0.5} \tag{3}$$

$$W = W_{actual}(ESF)^{1.1} \tag{4}$$

In equation 1 to 4, L is the length of the engine, D is the fan diameter of the engine, $\dot{m}$ is the engine mass flow and the W is the weight of the engine. ESF is the engine scale factor and ESF equal 1.0 is the baseline engine data.

Once the engine has been sized to required scale, in order to evaluate aircraft flight performance at different mission segments with varius thrust settings, specific fuel consumptions at various max dry thrust ratios (THR) are estimated using equation 5.

$$SCF_{THR} = \left(\left(\frac{0.1}{THR} \right) + \left(\frac{0.24}{(THR)^{0.8}} \right) + 0.66((THR)^{0.8}) + 0.1M \left(THR - \frac{1}{THR} \right) \right) SFC_{\max\,dry}$$

$$\tag{5}$$

Uninstalled engine performance data is obtained by cycle analyses or empirical relations [3]. SFC values are based on this uninstalled engine thrust. Installed engine thrust is the actual thrust generated by the engine once it is installed in an aircraft and it is affected by the actual inlet pressure recovery, bleed, power extraction, distortion effects and actual nozzle performance. The thrust-drag bookkeeping is required in order to prevent double accounting or ignoring the drag contribution. Thrust value after this thrust-drag bookkeeping is called the installed net propulsive force. Installed net propulsive force is estimated including inlet drag, nozzle drag and throttle-dependent trim drag contributions in the engine dataset. This process is presented in Figure 2.2 [3].
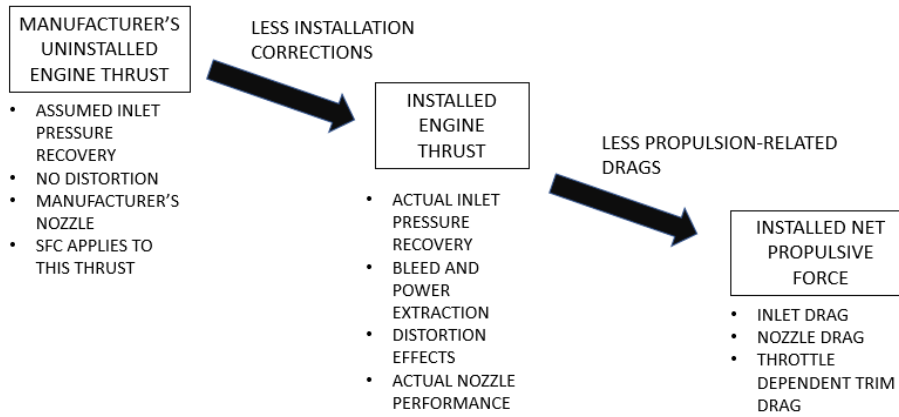
Figure 2.2. Installed thrust methodology [3]

To complete thrust-drag bookkeeping with preliminary analysis of the inlet drag, Figure 2.3 is used [3].
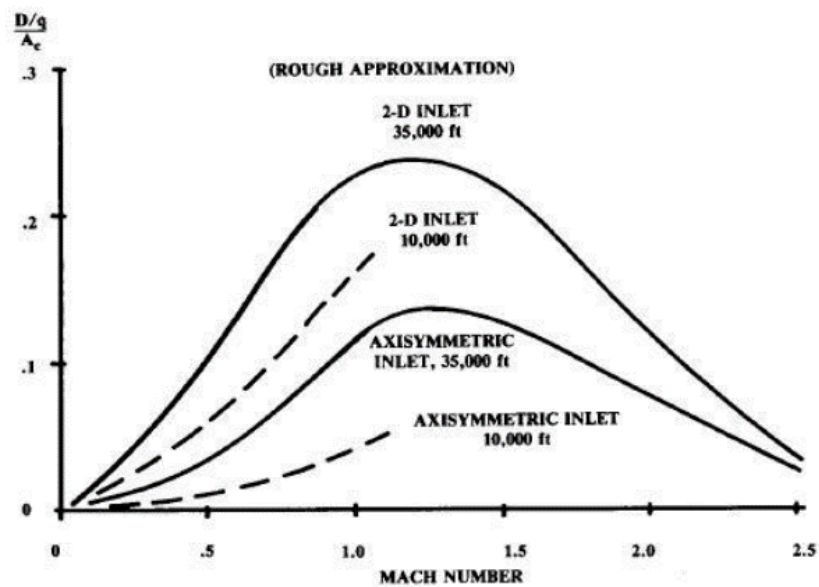
Figure 2.3. Inlet drag trends [3]

Last contribution of the thrust-drag bookkeeping is the estimation of the nozzle drag and the following table is used [3].

Table 2.1. *Nozzle incremental drag* [3]

Nozzle Type	Subsonic $\Delta C_{D_{Fuselage}}$*
Convergent	.036-.042
Convergent iris	.001-0.02
Ejector	.025-.035
Variable ejector	.01-.02
Translating plug	.015-.02
2-D nozzle	.005-.015

*Referenced to fuselage maximum cross-section area

Final engine dataset is concluded with the addition of inlet and nozzle drag to the scaled engine dataset as presented in appendix A.

2.3. Aircraft Configuration Design

Unique design solutions at the conceptual phase can be formed by variety of aircraft configurations. Quality of these aircraft configurations are dependent on design team's experience and creativity. In this thesis, configuration designs are produced following a basic design methodology:

- Internal arrangement of the main systems: Major avionics, cockpit, landing gears, internal weapons bay, engine, fuel system and duct.
- Parametric external fuselage surface creation using NASA's design tool called OpenVSP [7].

If the details of the components are not available, then a rough geometry can be created using the basic tools (rectangle and circle cross sections). General shapes of the systems used in the present work are presented in Figure 2.4.
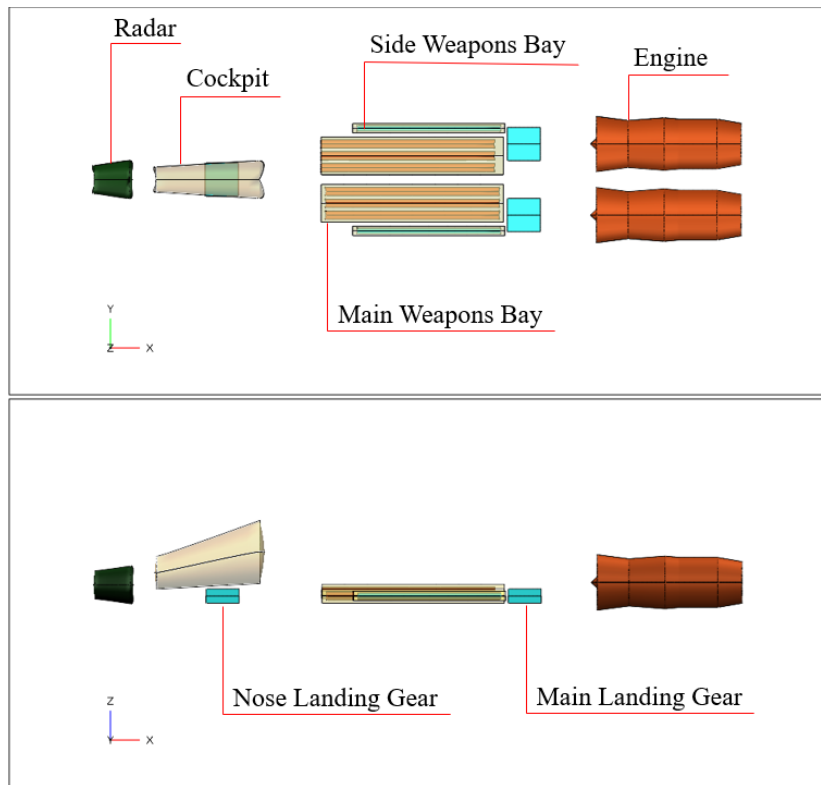
Figure 2.4. Internal systems arrangement created using OpenVSP. (Top view at top, side view at bottom)

General shapes of fuselage cross sections and their locations for a modern combat aircraft are presented in Figure 2.5 [15]. Using the examples presented in [15] and external surface definition of competitor aircraft, a parametric geometry is generated using OpenVSP.

13
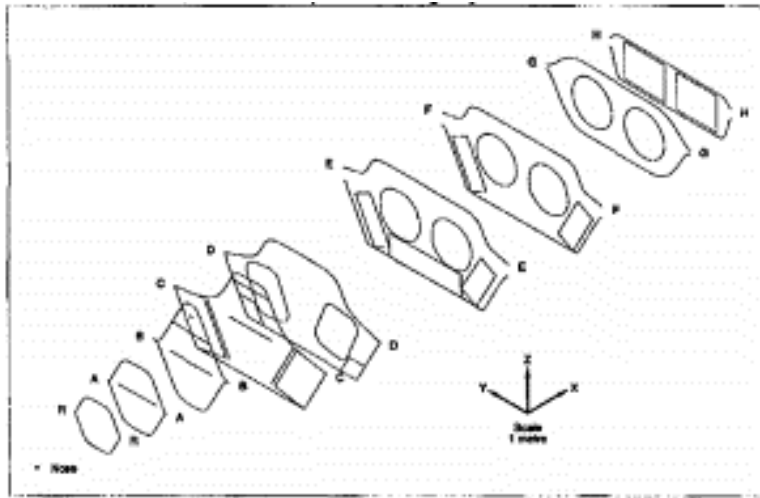
Figure 2.5. Key fuselage cross sections positioned along fuselage [15]

Cross sections of the fuselage have been created using "GENERAL_FUSE" option. In this option, the fuselage cross section is defined using a list of following parameters: Height, width, maximum width location, corner radius, top tangent angle, bottom tangent angle, top strength, bottom strength, upper strength and lower strength parameters. An example of the effects of these parameters on a cross-sectional shape is presented in Figure 2.6. Default cross-section is modified by each parameter presented in the lower side of the figure and resulting cross-sectional shape is presented around that parameter.
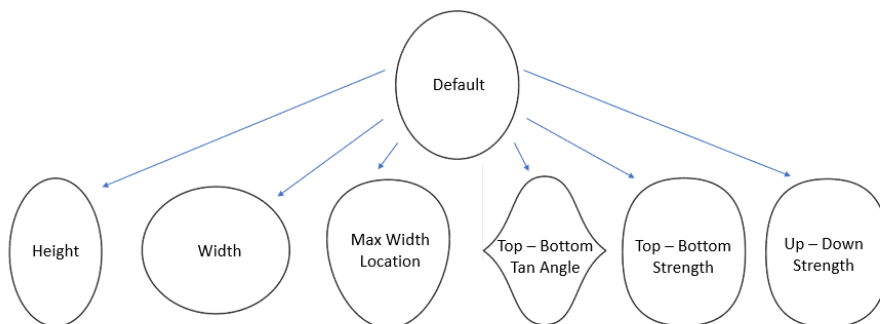
Figure 2.6. Effect of general fuselage cross-section parameters

14

Variation of the general fuselage cross-section parameters change the control points of a Bézier curves that define the cross section [7]. An example of Bézier curve with five control points has been shown in Figure 2.7.
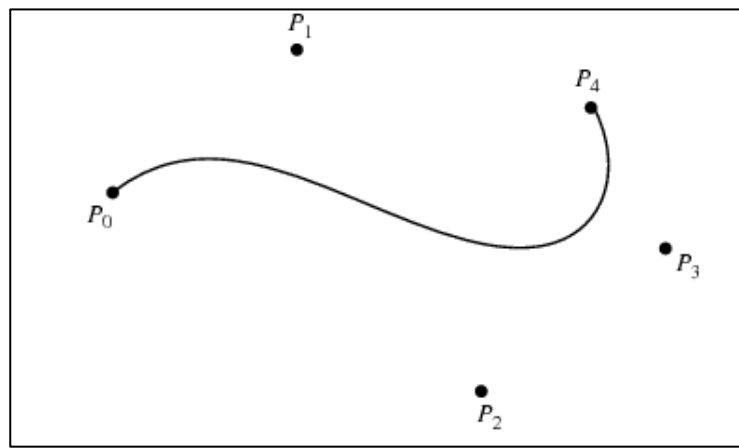
Figure 2.7. Cubic Bézier curve with five control points [16]

An example of fuselage geometry created using OpenVSP tool with the internal systems arrangement is shown in Figure 2.8.
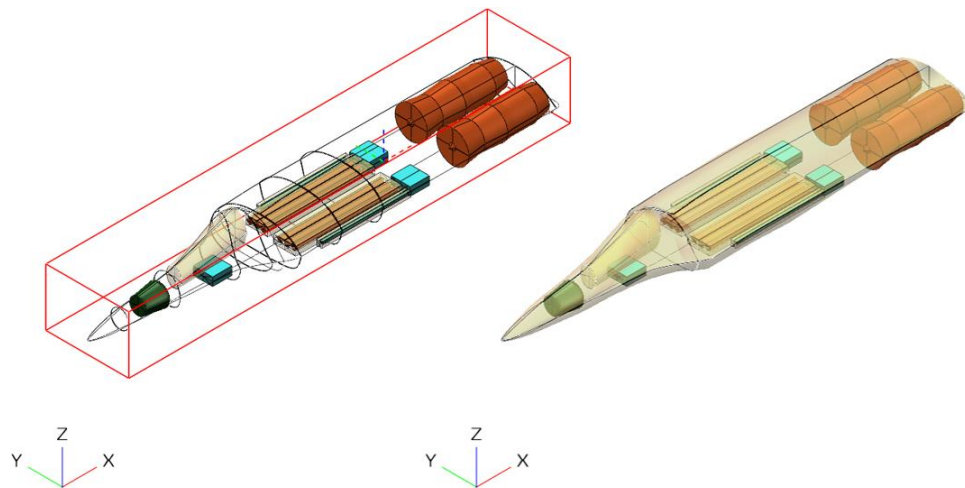
Figure 2.8. Fuselage CAD geometry in OpenVSP with internal systems arrangement (only cross sections of fuselage on left, and shaded fuselage surface on right)

The wing and the tails are sized during the proposed design synthesis. Therefore, the determination of location and size of these flying surfaces are discussed in fixed wing aircraft sizing and multidisciplinary design optimization chapters.

CHAPTER 3

FIXED AIRCRAFT ANALYSIS

Fixed aircraft analysis specifies that aircraft's geometrical analysis, weight analysis, aerodynamics analysis, mission performance analysis and point performance analysis is assessed without any changes to the aircraft geometry. In other words, geometry is not sized during the evaluation of fixed aircraft analysis.

3.1. Design Inputs

At starting phase of the conceptual design, some of the design inputs are set according to requirements, competitor aircraft and literature. These design inputs construct the design space. Design inputs and what these inputs are based on are listed in Table 3.1.

Table 3.1. *Design inputs and their sources*

Design Input	*Source*
Max. Mach Number	Requirements
Design Lift Coefficient	Competitor Study
Maximum Altitude	Requirements
Maximum Load Factor	Requirements
Ultimate Load Factor	Requirements
Flap Area Factor	Competitor Study
Number of Engines	Requirements
Armament Weight	Requirements
Design Mission Payload Weight	Requirements
Maximum Payload Weight	Requirements
Paint Weight Per Square Meters	Competitor Study
Empty Weight Margin	Literature [9]
Fuel Density	Literature [9]
Number of Fuel Tanks	Competitor Study

Fuselage Fuel Volume Ratio	Literature [15]
Total of Main System Volumes	Requirements
Base Area	Conceptual Design
Supersonic Drag Factor	Conceptual Design & Literature [3]
Conceptual CG Location	Conceptual Design
Wing Location	Competitor Study
Volume Coefficients	Literature [3]

3.2. Engine Inputs

Fundamentally, there are two ways of using engine geometry and performance data during a conceptual aircraft design – rubber engine and fixed engine [3]. Rubber engine data allows modification on the engine geometry, performance and aircraft geometry based on a parameter called engine scale factor. Thrust, fuel flow, weight and length are functions of engine scale factor, and these functions are supplied by the engine manufacturer. However, in cases where engine scale functions are not present, propulsion scaling methodology defined in [3] can be used for the purposes of initial design studies. An overall aircraft geometry sizing methodology that is related to the engine scale factor must also be adopted in order to introduce rubber engine to the design synthesis. Fixed engine data means that the engine geometry and performance data are frozen throughout the assessments (or constant engine scale factor of 1.0). In present study, design synthesis based on the fixed engine data is introduced.

Engine length (without the nozzle), engine fan-face diameter, and the engine weight are required for the analyses. Necessary engine performance data are the fuel flow and the net propulsive force with respect to thrust settings, altitudes and Mach numbers that cover the flight envelope, which altogether constitute an engine deck.

3.3. Geometry Analysis

The geometry in the present study is defined using the cross sections of the fuselage, wing and tail. For fuselage, these cross sectional coordinates can be generated using

the Bézier curve created by the methodology used in OpenVSP [7]. List of fuselage inputs are presented below:

- Fuselage cross section coordinates or OpenVSP "GENERAL_FUSE" parameters and fuselage stations of the cross sections.
- Intake area and intake fuselage station.
- Nozzle area and nozzle fuselage station.

For wings and tails, the airfoil coordinates are estimated using JavaFoil [17]. List of flying surface inputs are presented below:

- Non-dimensional airfoil geometry coordinates and thickness-to-chord ratio distribution.
- Airfoil leading-edge coordinates with respect to the fuselage nose.
- Chord length of the airfoil.

With all available coordinates that define the aircraft, the geometry analysis can be concluded to estimate necessary parameters. The perimeter of the cross sections are estimated by adding up the distances between the coordinate points (planes) iteratively. During the estimation of area and volume of aircraft components with cross sectional coordinates, mathematical models of shoelace formula [18] and convex hull [19] are used. Definitions of these mathematical models are presented in following sections.

3.3.1. Shoelace Formula

A simple polygon is a flat shape with non-intersecting line segments. Shoelace's formula is a mathematical algorithm used for estimation of the area of a simple polygon whose vertices are defined by its Cartesian coordinates in the plane. One calculates area of the encompassing polygon by cross-multiplying the corresponding coordinates and subtracting it from the surrounding polygon. An example of this is presented in Figure 3.1, a simple polygon is defined by three points. The area of this simple polygon (A) is estimated by the calculating the area of three surrounding

triangles (E, D and C) and subtracting these areas from the surrounding rectangle area [18].
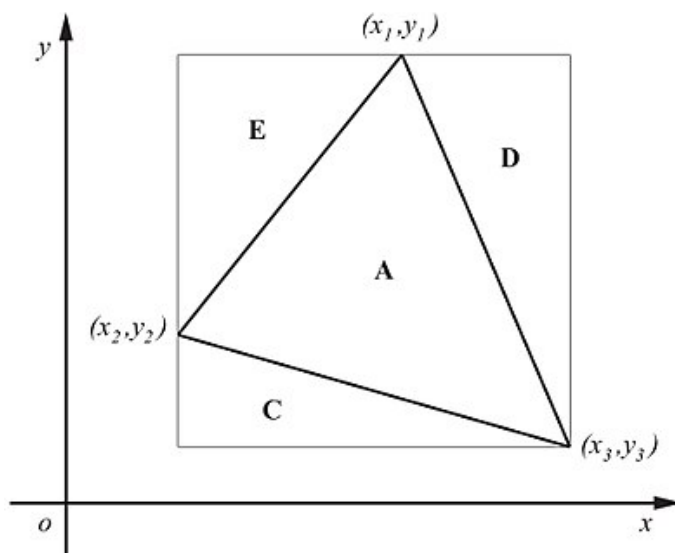
Figure 3.1. Given coordinates of a triangle [18]

The shoelace formula can be represented with the following equation [18]:

$$Area = \frac{1}{2} \left| \sum_{i=1}^{n} x_i (y_{i+1} - y_{i-1}) \right| \tag{6}$$

Where $x_{n+1} = x_1$ and $x_0 = x_n$, as well as $y_{n+1} = y_1$ and $y_0 = y_n$.

3.3.2. Convex Hull

The convex hull is the smallest convex set that contains the set of point clouds in given space. An example of convex hull is presented in Figure 3.2.
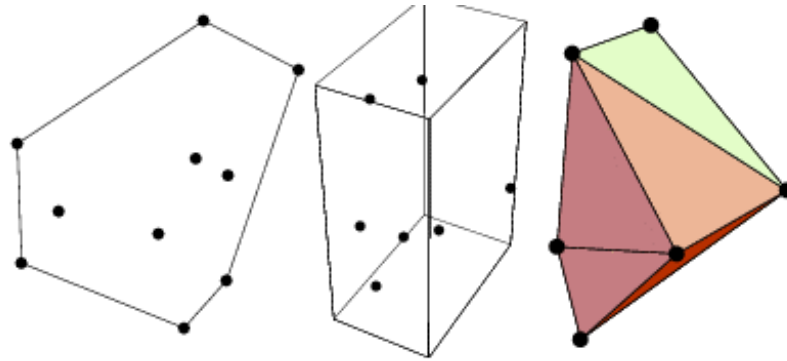
Figure 3.2. 3D convex hull of 120 point cloud [19]

A python module called "SciPy.spatial.ConvexHull" is used during calculations to estimate the convex hull of cross sections of components. The volume and area of the hull are calculated within the module itself as defined in [20].

3.3.3. Fuselage Geometrical Analysis

Rest of fuselage geometrical analysis is carried through using the geometrical relations and the cross-sectional points. Length of the fuselage is estimated by the following equation:

$$Fuselage\ length = |x_n - x_0| \tag{7}$$

In equation 7, x is the fuselage station of the cross section, n is the number of cross sections, 0th cross section is the first point and the nth cross section is the last fuselage station.

Max width and depth of the fuselage is estimated by checking maximum and minimum values of points then finding the absolute difference between these points in the y and z planes respectively.

3.3.4. Flying Surface Geometry Analysis

The surface volume and area of the flying surface is estimated using the convex hull module as presented previously. Thickness-to-chord average ratio of the flying

surfaces is calculated as the average of the thickness to chord ratios of all airfoils along the span. Leading edge coordinates, chord lengths of airfoils must be present as shown in Figure 3.3. Similarly, non-dimensional airfoil profile must be selected.

(x_1,y_1,z_1) (known)

Tip chord length (input)

Root chord length (input)

(x_0,y_0,z_0) (known)
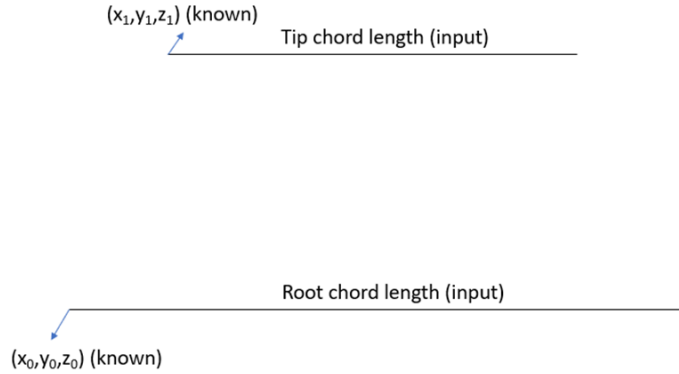
Figure 3.3. Flying surface inputs used for planform parameter calculations

Exposed semi span (b_{exp}) length of the flying surface is estimated using equation 8.

$$b_{exp} = y_1 - y_0 \tag{8}$$

The leading-edge sweep angle $(\Delta_{leading-edge})$ of the flying surface is estimated using equation 9.

$$\Delta_{leading-edge}(rad) = \arctan\left(\frac{x_1-x_0}{y_1-y_0}\right) \tag{9}$$

Exposed semi span length of the flying surface is the absolute difference of the y-coordinates of the leading edges of tip and the root airfoils. Exposed taper ratio is the ratio of the tip chord length to the exposed root chord length. The area of the exposed planform corresponds to the trapezoidal area calculated using tip and root chord lengths and the semi span length. The mean aerodynamic chord length and mean aerodynamic center location along the fuselage station, equivalent planform geometry

parameters of these flying surfaces (planform up to the aircraft centerline) are estimated using the relations proposed in [21].

Once all the parameters of exposed and equivalent planforms of the flying surfaces are estimated, then the volume coefficients can be calculated as well. Volume coefficients of the vertical and horizontal tails are estimated using the exposed tail area and the equivalent planform wing area as presented in equation 10 and 11 respectively.

$$TVC_{vertical} = \frac{S_{exposed,vertical}L_{vertical}}{b_{wing}S_{wing}} \qquad (10)$$

$$TVC_{horizontal} = \frac{S_{exposed,horizontal}L_{horizontal}}{\overline{c}_{wing}S_{wing}} \qquad (11)$$

In equation 10 and 11, TVC is the tail volume coefficient, S is the area, L is the tail arm, b is equivalent wing planform span and $\overline{c}$ is the equivalent wing mean aerodynamic chord length. The tail arm (L) is the absolute distance between the mean aerodynamic center location of the wing and the tail.

3.3.4.1. Wing Geometry Pitch-Up Tendency Avoidance

Aircraft in subsonic or transonic flight condition may be in risk of stall depending on the wing's high aspect ratio and high sweep due to the outflow from the high sweep causing the wing tips to lose lift first and because of high aspect ratio, the lift still present ahead of the center of gravity cause pitch-up (an uncontrollable nose-up divergence) [10]. Pitch-up avoidance charts presented in [3] are based on the wind tunnel testing that produced curves of reasonable combinations of aspect ratio and sweep, Figure 3.4.
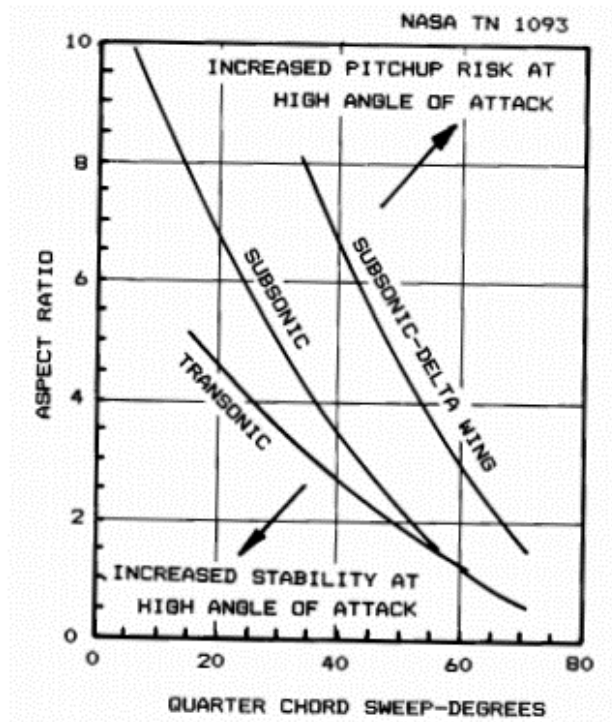
Figure 3.4. Tail-off pitch-up boundaries [3]

With the aim of pitch-up avoidance, following equation [10] is used to estimate maximum aspect ratio of the wing.

$$AR_{max} = 10.0^{(0.842-0.435*\tan(\Delta_{QC})}$$ (12)

In equation 12, AR_{max} is the maximum aspect ratio and Δ_{QC} is the quarter chord sweep angle.

3.4. Weight Analysis

During early conceptual phases of aircraft design, weight breakdown estimation can be challenging. High-fidelity methods require comprehensive set of inputs and analysis (parametric geometry, mesh generation, load calculations, finite element method (FEM) analysis). A process is presented for high-fidelity weight estimation in [22] as shown in Figure 3.5. Due to of the necessity of detailed set of inputs, diverse

aircraft configurations, increasing computation time, high-fidelity weight estimation process is not employed in this thesis.
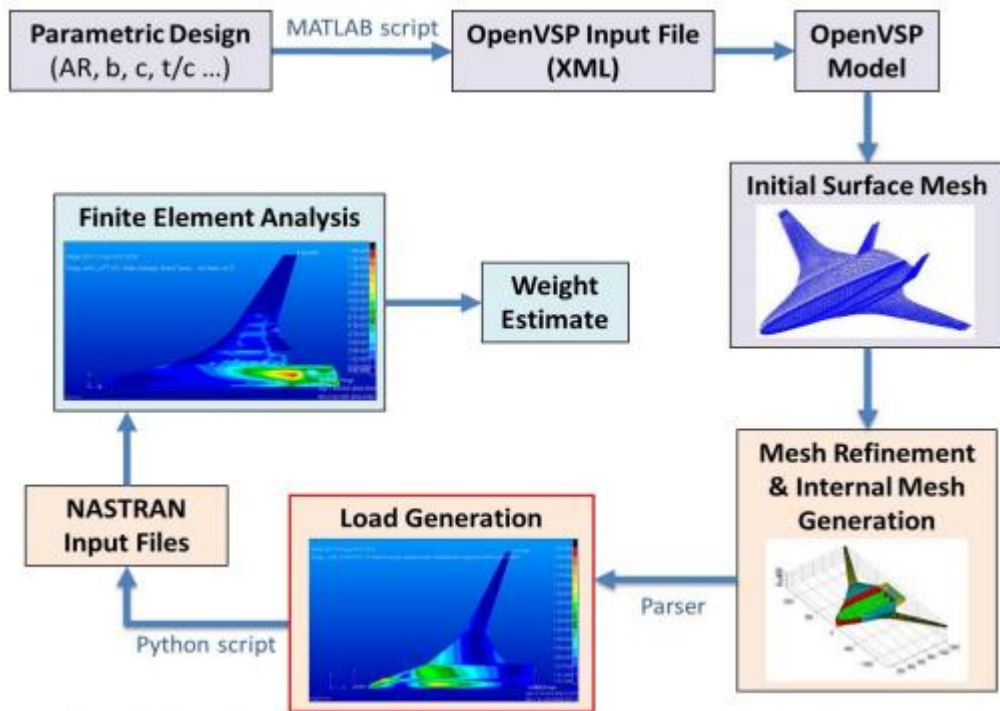
Figure 3.5. High-fidelity weight estimation process [22]

In order to generate aircraft weight breakdown based on the parameters related to the requirements and the aircraft configuration, low fidelity parametric equations generated from the historical aircraft data can be used as in [3], [15]. Once the design has matured into late conceptual aircraft design stage, high fidelity approach can be used to calibrate the low fidelity weight breakdown estimations. However, this calibration approach is beyond the scope of this thesis.

Three low fidelity parametric weight estimation methods (FLOPS [9], Raymer [3], Roskam [23]) are compared in [24]. It is observed that FLOPS requires less number of inputs compared to other two methods, while it is also capable of capturing overall

trends in component weight and provides a reasonably accurate prediction of component weight [24]. Therefore equations presented for fighter/attack aircraft in Appendix B [9] are used during weight breakdown calculations for the purposes of this thesis.

3.4.1. Structural Components

- Inputs of wing weight estimation are aircraft design gross weight, reference wing taper ratio, span, area, weighted average of the thickness to chord ratio along span, quarter-chord sweep angle, structural ultimate load factor, fraction of load carried by the wing, total movable surface area, number of wing mounted engines, wing strut bracing factor, aeroelastic tailoring factor, variable sweep penalty factor, composite utilization factor, multiple fuselage factor, and advanced composites fudge factor.

- Inputs of fuselage weight estimation are aircraft design gross weight, total fuselage length, number of fuselage mounted engines, wing variable sweep penalty factor, number of fuselages, and advanced composites fudge factor.

- Inputs of horizontal tail weight estimation are aircraft design gross weight, horizontal tail theoretical area, structural ultimate load factor, and advanced composites fudge factor.

- Inputs of vertical tail weight estimation are aircraft design gross weight, number of vertical tails, vertical tail taper ratio, area, aspect ratio, quarter-chord sweep angle, and advanced composites fudge factor.

- Inputs of canard weight estimation are aircraft design gross weight, canard area, taper ratio, and advanced composites fudge factor.

- Inputs of main landing gear weight estimation are aircraft design landing weight (also referred to as maximum payload weight), total fuselage length, and advanced composites fudge factor.

- Inputs of nose landing gear weight estimation are aircraft design landing weight, total fuselage length, and advanced composites fudge factor.

- Inputs of air induction system weight estimation are rated thrust of each engine, number of fuselage mounted engines, maximum fuselage width, maximum fuselage depth, maximum Mach number, and advanced composites fudge factor.
- Inputs of paint weight estimation are area density of the paint for all wetted areas including wing, horizontal tail, vertical tail, fuselage, canard wetted areas.

Fudge factors are multiplier to the weight estimations to include the effects of the advancements in technology. Advanced composites fudge factors are presented in Table 3.2 [3].

Table 3.2. *Advanced composites fudge factors* [3]

Weight group	*Fudge factor (multiplier)*
Wing	0.85
Tails	0.83
Fuselage	0.90
Landing gear	0.95
Air induction system	0.85

3.4.2. Propulsion System Items

Weights of propulsion systems are calculated from [9]. List of these systems are listed below:

- Thrust reversers
- Engine controls
- Engine starters
- Fuel system

All inputs required during calculations are thrust of each scaled engine, number of engines, number of flight crew, aircraft maximum fuel capacity, and number of fuel tanks.

3.4.3. Systems and Equipment Items

Weights of systems and equipment items are calculated from [9]. List of these items is listed below:

- Control surfaces
- Instruments
- Hydraulics
- Electrical
- Avionics
- Furnishings and equipment
- Air conditioning

All inputs required during calculations are aircraft design gross weight, total movable wing surface area, total fuselage length, maximum fuselage depth, number of wing mounted engines, number of fuselage mounted engines, number of flight crew, number of fuselages, fuselage planform area, reference wing area, maximum Mach number, hydraulic system pressure, wing variable sweep penalty factor, wing span, and rated thrust of each engine.

3.4.4. Operating Items

Weights of operating items are calculated from [9]. List of these items are listed below:

- Crew and baggage
- Unusable fuel
- Engine oil

All inputs required during calculations are number of flight crew, total number of engines, rated thrust of each engine, and reference wing area.

3.4.5. Fuel

- Wing usable fuel weight estimation is made from [9] and the estimation requires fuel density ratio, wing fuel capacity factor, wing area, taper ratio, span and average of the thickness to chord ratio along span as inputs.
- Fuselage usable fuel is calculated with following equation taken from [15]:

$$m_{fuselage\ usable\ fuel} = 0.85\big(V_{fuselage} - V_{systems} - 0.35V_{fuselage}\big)\rho_{fuel} \quad (13)$$

In equation 13, main systems (duct, cockpit, internal weapons bay, engine, landing gear) volume and remainder volume (structure and secondary systems: avionics, electrical, hydraulics, air, etc.) are subtracted from fuselage volume. Remainder volume can be challenging to predict at the early stages of the design as neither the structure nor the secondary systems design might not be available. Therefore, based on the empirical analysis of a number of detailed aircraft designs, remainder volume is taken to be equal to the 35% of the fuselage volume [15]. Resulting volume is then multiplied by the utilization factor (0.85) and multiplied by the fuel density (ρ_{fuel}) to calculate the fuselage usable fuel ($m_{fuselage\ usable\ fuel}$) [15].

3.4.6. Aircraft Weight Breakdown Estimation

The breakdown of the aircraft weight is estimated using the summation method presented in Figure 3.6.
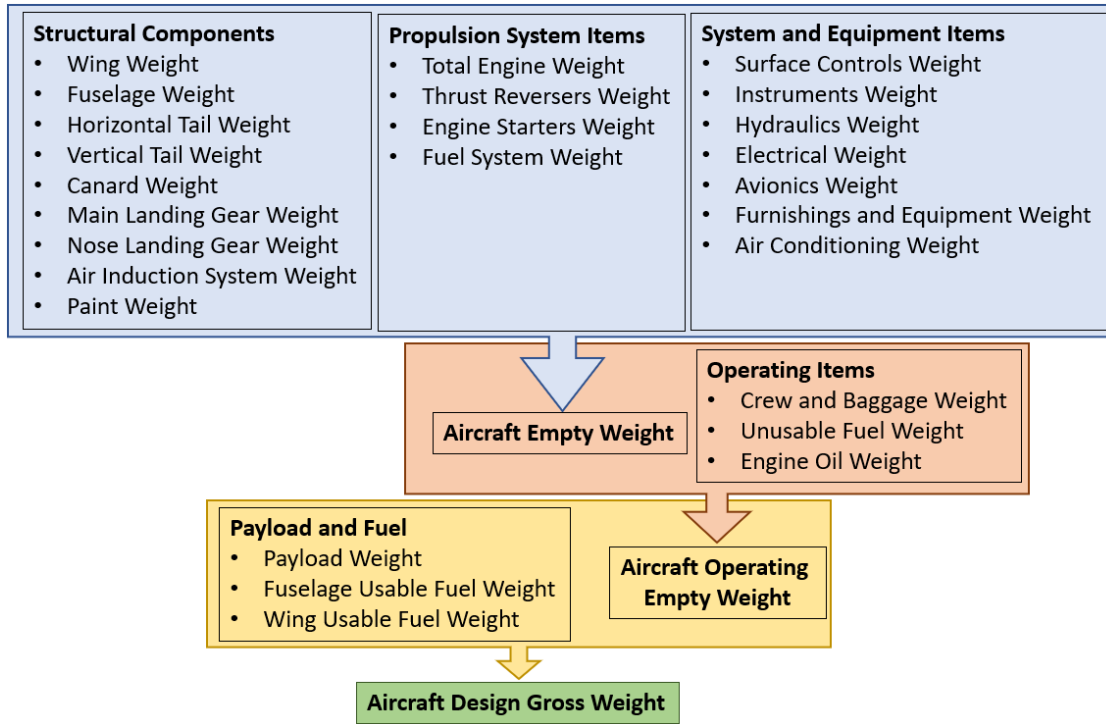
Figure 3.6. Aircraft weight breakdown estimation process

Since the number of weight estimation methods presented previously require the aircraft design gross weight of the aircraft as an input, the following equation is minimized to find correct value of the aircraft design gross weight during analysis. Minimizing the equation is accomplished using "minimize_scalar" function from SciPy module [20] with boundaries (aircraft design gross weight can be between 100. kg and 100000 kg).

$$\left| m_{initial\ design\ gross\ weight} - f_{weight\ analysis}\left(m_{initial\ design\ gross\ weight}\right)\right|$$

(14)

In equation 14, $f_{weight\ analysis}$ refers to weight analysis function that estimates the aircraft design gross weight using process presented in Figure 3.6.

3.5. Aerodynamics Analysis

Aerodynamic analysis contains the lift curve slope, the drag breakdown and drag-due-to-lift-factor (K) calculations. The aerodynamic dataset is generated for given Mach number and altitude ranges. During calculations, properties of standard atmosphere (density, speed of sounds, dynamic viscosity) are estimated for each altitude using the equations presented in [25].

Drag divergence Mach number is the Mach number at which the shock formations start to substantially affect the drag. This parameter is important for determination of the Mach number where transonic region starts during aerodynamic calculations. Drag divergence Mach number is estimated using Figure 3.7, where t/c parameter is the thickness to chord ratio average of the wing geometry. In Figure 3.7, the drag divergence Mach Number of an aircraft with design lift coefficient of 0 can be estimated. Then Figure 3.8 is used to estimate the lift adjustment (LF_{DD}) for this drag divergence Mach Number. Last, using equation 15 actual drag divergence Mach Number of the aircraft can be estimated using these parameters.
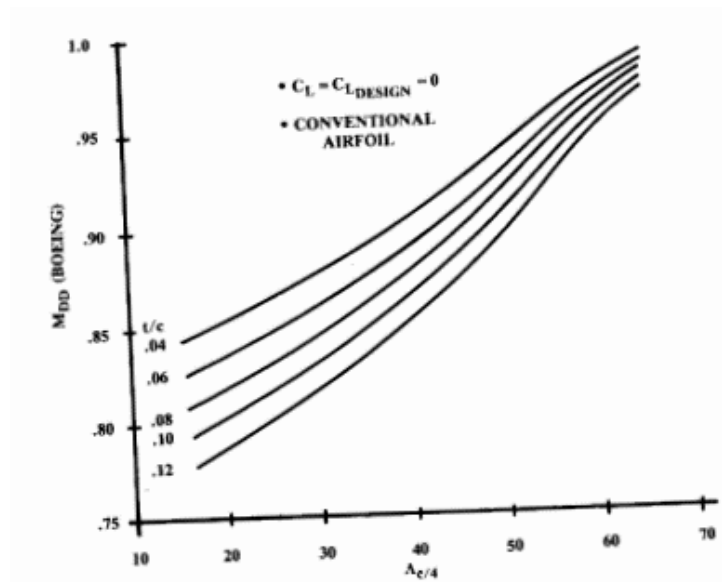
Figure 3.7. Wing drag-divergence Mach number [3]
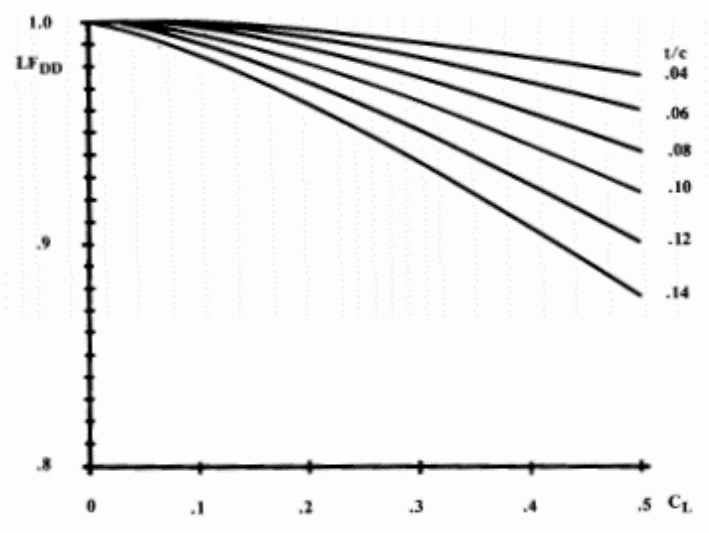
Figure 3.8. Lift adjustment for M$_{DD}$ [3]

$$M_{DD} = M_{DD_{L=0}} LF_{DD} - 0.05 C_{L_{design}} \tag{15}$$

Subsonic equations are usable when the Mach number is less than the drag divergence Mach number. Instead, supersonic equations are feasible when the Mach number is larger than 1.2.

Lift curve slope (C_{L_α}) is estimated by equation 16 for subsonic calculations and equation 17 for supersonic calculations [3]. Another option to the calculation of lift curve slope during supersonic flight is the estimation of normal force coefficient of the wing for low angles of attack [3].

$$C_{L\alpha,subsonic} = \frac{2\pi AR}{2 + \sqrt{4 + AR^2 \beta^2 \left(\frac{1 + \tan^2 \Delta_{max\_thickness}}{\beta^2}\right)}} \left(\frac{S_{exposed}}{S_{ref}}\right)(F) \quad \text{for} \quad M < M_{DD} \tag{16}$$

$$C_{L\alpha,supersonic} = 4/\beta \left(\frac{S_{exposed}}{S_{ref}}\right)(F) \qquad \text{for } M \geq 1.2 \tag{17}$$

32

Fuselage lift factor (F) is estimated using equation 18 depending on the ratio of fuselage diameter (d) to wing reference span (b).

$$F = 1.07 \left(1 + \frac{d}{b}\right)^2 \tag{18}$$

Compressibility factor (β) is estimated using equation 19 depending on the Mach number.

$$\beta = \sqrt{|M^2 - 1|} \tag{19}$$

For the transonic region $(M_{DD} < M < 1.2)$, a third order polynomial with arbitrary coefficients (A, B, C and D) is defined as equation 20:

$$y = Ax^3 + Bx^2 + Cx + D \tag{20}$$

Transonic region of the lift curve slope is estimated solving the coefficients for the third order polynomial with initial conditions presented below:

- $y(M_{DD}) = C_{L_{\alpha,subsonic}}(M_{DD})$,
- $y(1.2) = C_{L_{\alpha,supersonic}}(1.2)$,
- $y'(M_{DD}) = 0$,
- $y'(1.2) = 0$.

Aircraft drag is represented by equation 21:

$$C_D = C_{D_0} + KC_L^2 \tag{21}$$

Zero-lift drag of the aircraft (C_{D_0}) is the drag estimated without the impact of the lift generation. Zero-lift drag contributors are listed below [3]:

- Component buildup drag,
- Miscellaneous drag,
- Leakage and Protuberance drag,
- Wave drag (at M > 1.2).

Component buildup drag is estimated using equation 22.

$$C_{D_{component}} = \frac{C_{f_c} FF_c Q_c S_{wet_c}}{S_{ref}} \tag{22}$$

Flat-plate skin friction coefficient (C_{f_c}) is estimated depending on the Reynolds number (Re). Reynolds number is calculated using equation 23.

$$Re = \frac{\rho V l}{\mu} \tag{23}$$

In equation 23, ρ is the density of the air (kg/m^3), V is the air speed (m/s), l is the characteristic length (m) and μ is the dynamic viscosity (Pa.s). Characteristic length for the fuselage is taken as the fuselage length. For the wings and tails, it is taken as the mean aerodynamic chord length.

Flat-plate skin friction coefficient is estimated depending on the flow regime being laminar or turbulent. In most cases, the turbulent equation covers the whole aircraft flight regime [3] and is presented in equation 24.

$$C_{f_c} = \frac{0.455}{(\log_{10} Re)^{2.58}(1+0.144M^2)^{0.65}} \tag{24}$$

Component form factors are the factors that make flat-plate skin friction coefficient to be representative of the aircraft component. Flying surfaces and the fuselage component form factors are calculated by equation 25 & 26 [3].

$$FF_{wing,tail} = \left[1 + \frac{0.6}{\left(\frac{x}{c}\right)_m}\left(\frac{t}{c}\right) + 100\left(\frac{t}{c}\right)^4\right]\left[1.34M^{0.18}(cos\Delta_m)^{0.28}\right] \tag{25}$$

In equation 25, $(x/c)_m$ is the chordwise location of the maximum thickness, t/c is the thickness to chord ratio of the airfoil and the Δ_m is the maximum thickness location of the sweep line from root airfoil to tip airfoil.

$$FF_{fuselage} = \left(1 + \frac{60}{f^3} + \frac{f}{400}\right) \tag{26}$$

$$f = \frac{l}{\sqrt{\left(\frac{4}{\pi}\right)A_{max}}} \tag{27}$$

In equation 27, l is the fuselage length, A_{max} is the maximum cross section of the fuselage.

Parasite drag is increased because of the interference between components of the aircraft. However, for a well-designed modern fighter aircraft, interference factor Q_c, is taken as 1.0 for all components from the conceptual design advice presented in [3].

Next drag contributor to the zero-lift drag is the miscellaneous drag. There are no external stores on the configuration therefore drag due to stores are zero. Trailing-edge flap deflections must be studied carefully (proper CFD or wind tunnel testing) before adding conceptual drag area. Therefore, miscellaneous drag contributions from trailing-edge flaps deflections are neglected for fighter aircraft at this early conceptual design stage. Base area is considered to be any area of the aft fuselage surface angle to the freestream velocity larger than 20 degrees. Base drag area estimation presented in equations 28 and 29 are used [3]:

$$\text{Subsonic: } \left(\frac{D}{q}\right)_{base} = [0.139 + 0.419(M - 0.161)^2]A_{base} \tag{28}$$

$$\text{Supersonic: } \left(\frac{D}{q}\right)_{base} = [0.064 + 0.042(M - 3.84)^2]A_{base} \tag{29}$$

In equations 28 and 29, A_{base} is the base area (m^2). An example of base area calculation on fuselage cross-section is presented in Figure 3.9. The surrounding blue line is the fuselage cross-section, the red zone is the nozzle area (flow-through area). White zone is the base area where highly separated flow is experienced.
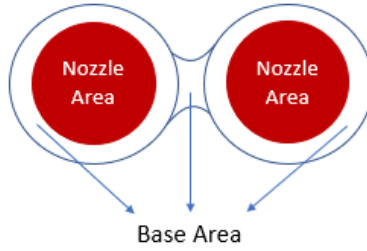
Figure 3.9. Fuselage cross-section for base area

There is no empirical method available for the estimation of leakage and protuberance drag at the early conceptual design stage. Therefore it is suggested that 5 to 10 percent of the parasite drag is to be added in order to account for leakage and turbulence drag [3]. In the present study 10 percent is used.

An ideal volume distribution is produced by the Sears-Haack body which provides the minimum drag possible for any enclosed-end body of the same length and total volume [3]. A Sears-Haack body has a wave drag defined in equation 30 [26].

$$\left(\frac{D}{q}\right)_{wave} = \frac{9\pi}{2}\left(\frac{A_{max}}{l}\right)^2 \tag{30}$$

For preliminary wave drag analysis at supersonic speeds (Mach number greater than 1.2) a modification to Sears-Haack body wave drag equation can be used as presented in equation 31.

$$\left(\frac{D}{q}\right)_{wave} = E_{WD}\left[1.0 - 0.386(M-1.2)^{0.57}\left(1.0 - \frac{\pi\Delta_{LE,deg}^{0.77}}{100}\right)\right]\left(\frac{D}{q}\right)_{Sears\_Haack} \tag{31}$$

E_{WD} is a factor that presents the aircraft's wave drag efficiency. For supersonic fighter, E_{WD} ranges between 1.4 to 2.0 [3].

Transonic region of the zero-lift drag is estimated by the graphical approach. This approach is presented in Figure 3.10 [3] for the drag rise (wave drag). Wave drag estimated at Mach number equal to 1.2 is also equal to the wave drag estimated at Mach number equal to 1.05. Wave drag at Mach number of 1.0 is half this value. Wave drag coefficient at drag divergence Mach number is 0.002. Critical Mach number is estimated from its relation to drag divergence Mach number as presented in Figure 3.10. With this approach, subsonic and supersonic drag calculations are connected and performance calculations at the transonic Mach numbers have effect of the transonic drag rise.
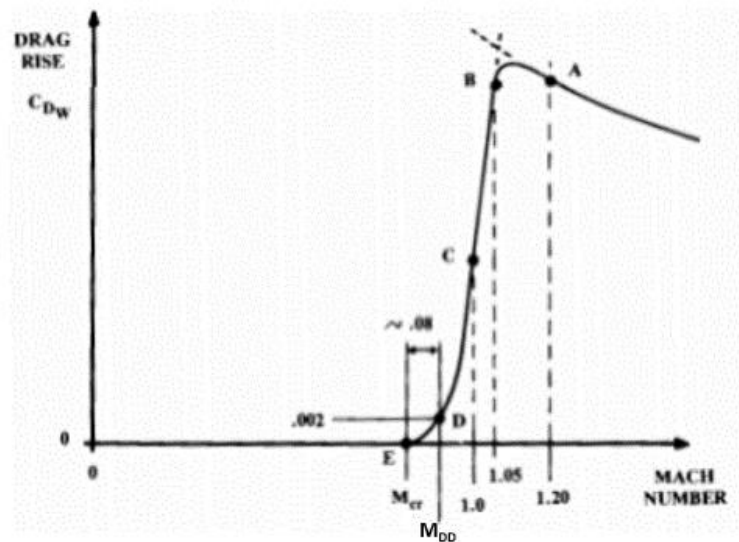
Figure 3.10. Transonic drag rise estimation [3]

After estimating the zero-lift drag, one must also calculate the drag due to lift in order to find the total drag. Drag coefficient due to lift (C_{D_i}) is expressed by equation 32.

$$C_{D_i} = K C_L^2 \tag{32}$$

37

Drag due to lift factor K can be estimated with the Oswald efficiency factor. However, leading-edge suction method is proven to be more accurate for estimation of K [3]. Leading edge suction accounts for the effect of the geometrical shape of an airfoil on pressure distribution on its surface. The curvature at the leading edge creates a pressure drop on the upper part. The reduced pressure exerts a suction force on the leading edge in a forward direction as presented in Figure 3.11. A thin flat plate would have no leading-edge suction.

Fig. 12.33 Leading edge suction definition.
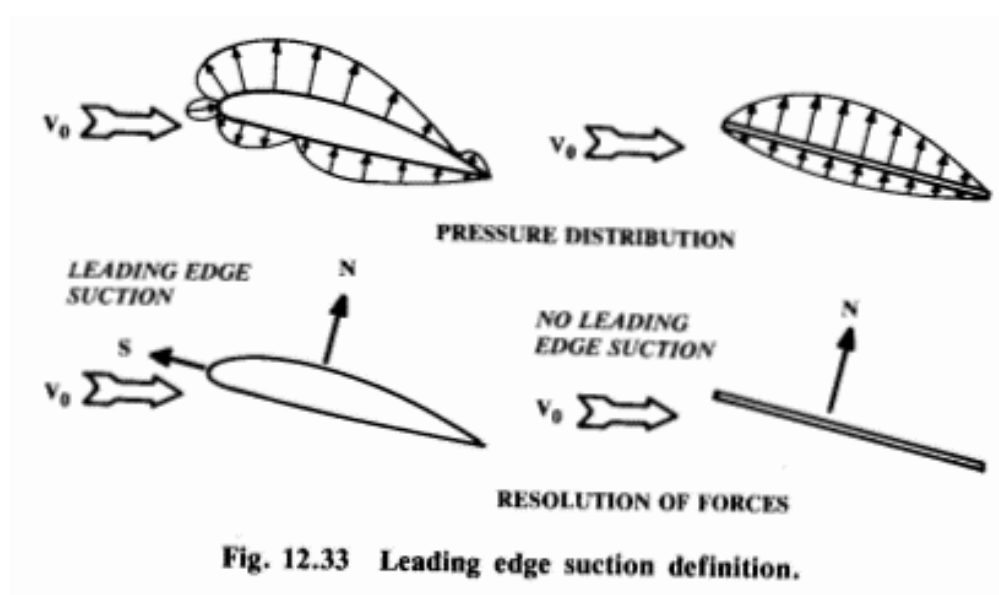
Figure 3.11. Leading edge suction definition [3]

Equation 33 is used to calculate the drag due to lift factor.

$$K = SK_{100} + (1 - S)K_0 \qquad (33)$$

K_{100} and K_0 in equation 33 are estimated using Figure 3.12. The K_0 stands for where there is no leading-edge suction, and K_{100} refers to the case where there is 100% leading edge suction. At some supersonic Mach number, both K values converge into

single value. Leading edge suction factor (S) is estimated using Figure 3.13 using the wing's design C_L and the C_L of the flight condition.
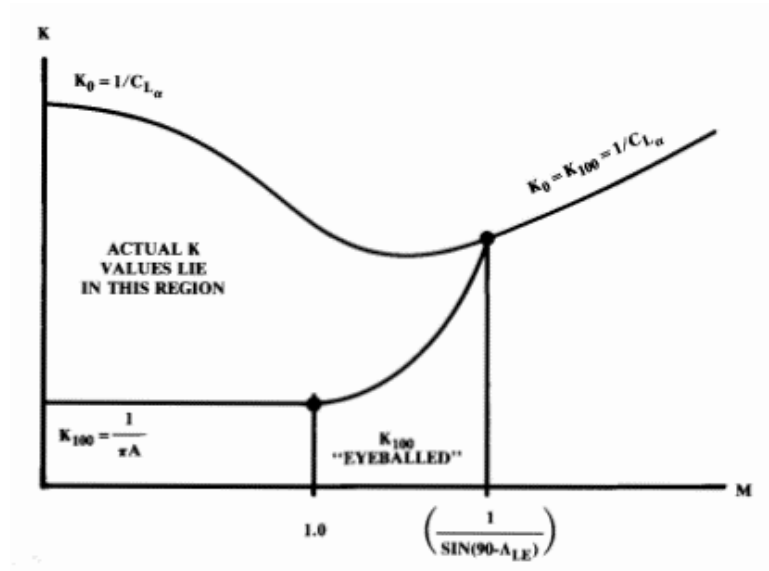
Figure 3.12. K_{100} and K_0 vs. Mach number [3]
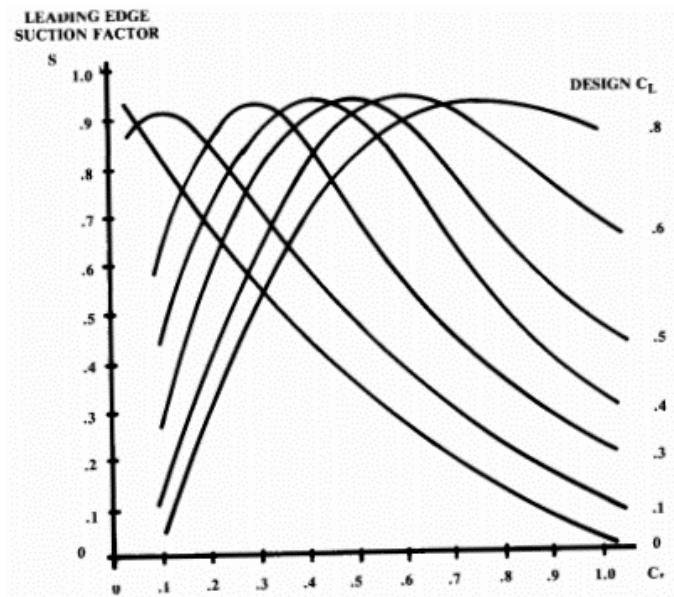
Figure 3.13. Leading edge suction vs. C_L [3]

3.6. Mission Performance Analysis

Mission performance analysis solves each mission segment separately. Each mission function calculates the fuel consumption, final speed, final altitude, time spent, distance traveled and aircraft total weight. All functions corresponding to these mission segments require the aircraft weight, reference area, aerodynamic data, engine performance data and design inputs. Therefore, these inputs are not mentioned in definitions of the functions. Following mission functions are used in this thesis:

- Consume fuel
- Takeoff
- Accelerate
- Climb
- Fly distance
- Fly setting
- Instantaneous turn
- Sustained turn
- Drop
- Loiter

3.6.1. Consume Fuel Function

Consume fuel function requires the time spent (t_{spent}) and engine setting as additional inputs. This function is usually used at the start of the mission profile to account for fuel consumption before the planned takeoff. For example, taxi or waiting with engines running in case where multiple aircraft are lined up for takeoff. Aircraft weight is estimated using equation 34.

$$W_{aircraft,final} = W_{aircraft,initial} - \dot{m}_{fuel} \, t_{spent} \qquad (34)$$

Final mass of aircraft ($W_{aircraft,final}$) (kg) is the aircraft mass after the segment is completed. Aircraft mass before the mission segment calculations is $W_{aircraft,initial}$

(kg). Fuel flow ($\dot{m}_{fuel}$) (kg/s) is estimated from the engine deck for given engine setting, Mach number and altitude information. Time spent is represented by t_{spent} (s).

3.6.2. Takeoff Function

Takeoff function for mission analysis requires the altitude, maximum lift coefficient, engine setting and ground friction (f_s) as additional inputs. Stall speed is the speed at which the aircraft can barely fly without wing losing its function to generate lift force (stall). The stall speed (V_{stall}) (m/s) of the aircraft is estimated using equation 35.

$$V_{stall} = \sqrt{\frac{W_{aircraft,initial}g}{0.5\rho_\infty C_{L_{max}}S_{ref}}} \tag{35}$$

Freestream density (ρ_∞) is estimated from the standard atmosphere module for given Mach number and altitude. Reference wing area (S_{ref}) (m^2) is calculated by the geometry module. Gravitational acceleration is represented by g and is equal to 9.81 m/s^2. The takeoff speed is taken as 1.2 times the stall speed as presented in equation 36.

$$V_{takeoff} = 1.2V_{stall} \tag{36}$$

Final distance, time, fuel consumption and weight of the aircraft are estimated with calculation of acceleration from initial speed to takeoff speed. Acceleration process is modeled for given time intervals (dt) (s). Acceleration (a) is calculated using equation 37.

$$a = \frac{\left(NPF - D - f_s\left(\left(C_L 0.5\rho_\infty V_\infty^2\right) - W_{aircraft}g\right)\right)}{W_{aircraft}} \tag{37}$$

Net propulsive force (NPF) (N) and fuel flow ($\dot{m}_{fuel}$) (kg/s) are estimated from the engine deck for given engine setting, Mach number and altitude information. Aircraft mass at the initial state is presented by $W_{aircraft}$ (kg). Aircraft speed after each time interval ($V_{\infty,after}$) (m/s) is calculated using equation 38.

$$V_{\infty,after} = V_{\infty,before} + adt \tag{38}$$

Distance traveled after each time interval (X_{after}) (m) is estimated using equation 39.

$$X_{after} = X_{before} + \frac{(V_{\infty,after} + V_{\infty,before})}{2} dt \tag{39}$$

Aircraft weight after each time interval is calculated using equation 40.

$$W_{aircraft,after} = W_{aircraft,before} - \dot{m}_{fuel} dt \tag{40}$$

Fuel consumed at each time interval is computed using equation 41.

$$W_{fuel,after} = W_{fuel,before} + \dot{m_{fuel}} dt \tag{41}$$

Total time spent after each time interval is estimated using equation 42.

$$t_{after} = t_{before} + dt \tag{42}$$

When the aircraft speed $V_{\infty,after}$ is equal to the takeoff speed $V_{takeoff}$, the function stops the estimation for next time interval and final parameters are the results.

3.6.3. Accelerate Function

Methodology for this function is identical to the takeoff function except for the estimation of the acceleration equation. Since there is no ground friction during actual flight, the friction force is dropped from equation 37, and acceleration function becomes equation 43.

$$a = \frac{(NPF - D)}{W_{aircraft}} \tag{43}$$

3.6.4. Climb Function

Aircraft must have power generated from engines greater than the power generated by the drag of the aircraft in order to perform climb. Subtracting drag power from the thrust power and dividing it by the aircraft weight is called the "Specific Excess Power" (SEP) and presented in equation 44.

$$SEP = \frac{V_\infty (NPF - D)}{W_{aircraft} g} \tag{44}$$

For flight conditions of climb, if the SEP is greater than zero, it means that the aircraft has excess power and can climb. On the other hand, if the SEP is less than zero, aircraft is descending. When the SEP is equal to zero, aircraft neither can climb or descent (level flight).

Methodology of this function requires additional inputs of initial altitude and Mach number, final altitude and engine throttle setting. The function starts with the estimation of the maximum SEP value over the aerodynamic database range in order to find the optimum climb speed at initial altitude. Then aircraft is accelerated to the resulting velocity.

Core part of the climb function is the climb loop. The loop is solved iteratively for the time intervals until the current altitude is greater than or equal to the final altitude. The climb loop starts with estimation of the SEP using equation 44. Then the climb angle is calculated using equation 45 [3].

$$\gamma_{climb}(rad) = \arcsin\left(\frac{NPF - D}{W}\right) \tag{45}$$

The horizontal component of the velocity (towards the distance traveled) is estimated using equation 46. The vertical component of the aircraft velocity (towards gaining altitude) is calculated using equation 47. Aircraft velocity components are presented in Figure 3.14.

$$V_{\infty_x} = V_\infty \cos(\gamma_{climb}) \tag{46}$$

$$V_{\infty_y} = V_\infty \sin(\gamma_{climb}) \tag{47}$$
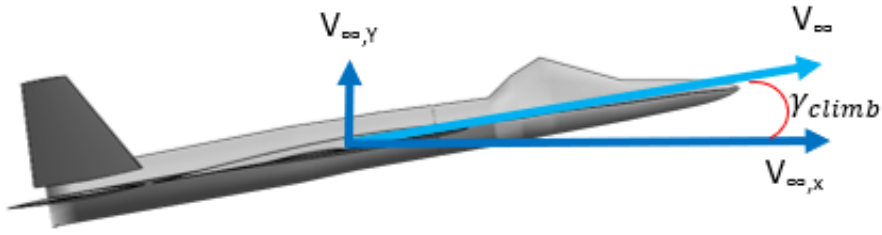
Figure 3.14. Aircraft velocity components during climb

Altitude (H) after the time interval is calculated using equation 48.

$$H_{after} = H_{before} + V_{\infty_y} dt \tag{48}$$

Distance traveled after each time interval (X_{after}) (m) is calculated using equation 49.

$$X_{after} = X_{before} + V_{\infty_x} dt \tag{49}$$

Aircraft mass after each time interval is calculated using equation 40. Fuel mass consumed at each time interval is estimated using equation 41. Total time spent after each time interval is estimated using equation 42. Then the optimum climb velocity is estimated again using equation 44 at the altitude after the time interval, the aircraft is accelerated to the optimum climb velocity and the loop is solved again until the altitude after the time interval is greater than or equal to the final altitude. A simplified version of this process is presented in Figure 3.15. The climb sequence is as follows:

- Accelerate to $M = 0.8$ at sea level, where excess power is maximum,
- Accelerate to 0.9 Mach number and climb to 2000 m altitude,
- Climb to 9000 m altitude at $M = 0.9$.
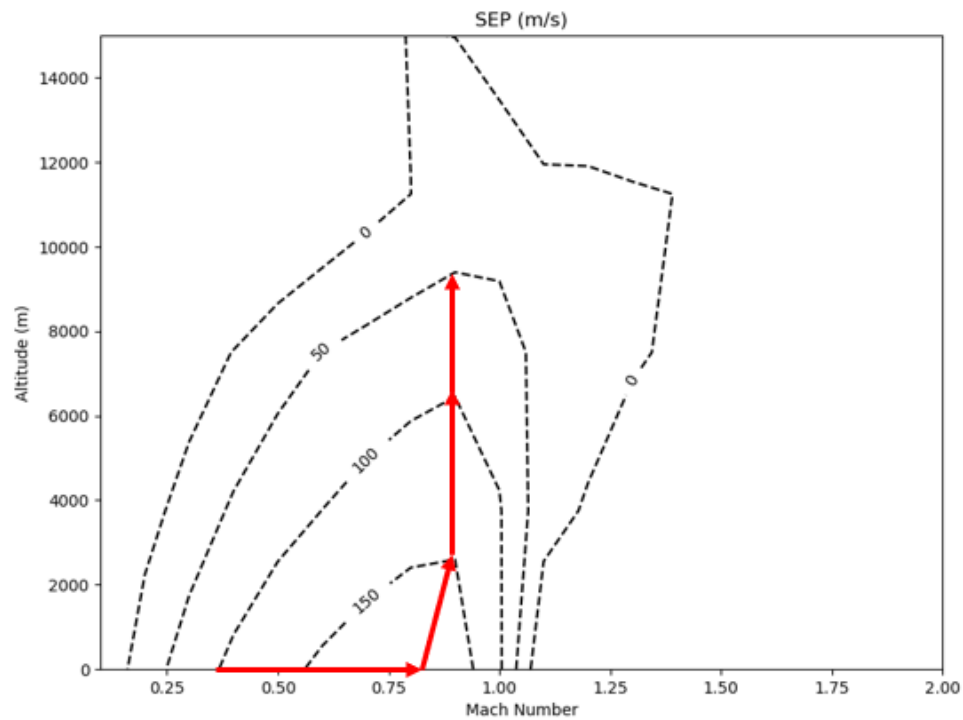
Figure 3.15. Climb function acceleration to best SEP routine

3.6.5. Fly Distance Function

According to fly distance function methodology initial Mach number, initial altitude and the distance to be flown are required. The aircraft must travel the distance with constant speed and altitude during this segment. The aircraft state is solved iteratively for time intervals until the required distance is travelled. Since the drag is equal to the net propulsive force for level flight, the aircraft is flying with constant speed. Also, the function is modeled so that the aircraft is travelling at constant altitude. The fuel flow and the net propulsive of the engines can be found for given Mach number, altitude and engine setting as presented in previous sections, and this can be mathematically written as shown in equation 50. Drag (D) of the aircraft is calculated using equation 51, where the function is the aerodynamics analysis presented in previous section and the drag is depended on the Mach Number and the altitude. Since,

45

the level flight requires a net propulsive force equal to the drag force, the engine setting must be calculated. The calculation is done by minimizing the absolute difference between the drag and the net propulsive force for variable engine setting. Mach number and the altitude are kept constant, therefore the function that is to be minimized for variable engine setting can be represented as in equation 52.

$$FF, NPF = f_{engine}(mach, altitude, setting) \qquad (50)$$

$$D = f_{aerodynamics}(mach, altitude) \qquad (51)$$

$$|NPF - D| = f_{engine\_setting}(setting) \qquad (52)$$

Estimation of engine setting allows one to calculate the distance traveled after each time interval using equation 39. The aircraft mass after each time interval has been estimated using equation 40. The mass of fuel consumed is calculated using equation 41 after each time interval. Total time spent after each time interval has been estimated using equation 42.

3.6.6. Fly Setting Function

Fly setting function methodology requires the initial Mach number, initial altitude, distance and the engine setting as additional inputs. This function is identical to the fly distance function except that the aircraft can accelerate or decelerate, and the engine setting is predetermined. Therefore, the part where the engine setting is found is not used and the aircraft acceleration is found using equation 43. Then the aircraft speed after the time interval is calculated using equation 38. Estimation of the aircraft mass, fuel mass consumption, time and distance is same as fly distance function.

3.6.7. Instantaneous Turn Function

Instantaneous turn function algorithm requires the initial Mach number, altitude, the maximum lift coefficient, the engine setting and number of turns as additional inputs. Practicality behind the instantaneous turn is to turn the aircraft from its heading direction while maintaining maximum load factor the aircraft can maintain. This

means the maneuver takes place in the minimum time possible. Performing this maneuver, the aircraft loses its speed and altitude, while changing its heading significantly faster when compared to other turn maneuvers. The function is solved iteratively for time intervals until the number of turns is achieved. The load factor of the aircraft is calculated using equation 53 [3]. If the result is greater than the design input of maximum load factor, then the maximum load factor is used in calculations instead of the result of equation 53.

$$n = \frac{0.5 S_{ref} \rho V_\infty^2 C_{L_{max}}}{W_{aircraft} g} \tag{53}$$

The turn rate is calculated using equation 54 [3].

$$\dot{\varphi} = \frac{g\sqrt{n^2 - 1}}{V_\infty} \tag{54}$$

The turned angle is estimated using equation 55. $\dot{\varphi}_{average}$ is calculated using the before and after velocity at each time interval in load factor and turn rate calculations presented above.

$$\varphi_{after} = \varphi_{before} + \dot{\varphi}_{average} dt \tag{55}$$

The vertical component of the aircraft velocity has been estimated using equation 56 [3].

$$V_{\infty,y} = V_\infty \left(\frac{NPF}{W_{aircraft} g} - \frac{C_{D_0} q S_{ref}}{W_{aircraft} g} - \frac{n^2 K W_{aircraft} g}{S_{ref} q} \right) \tag{56}$$

Dynamic pressure (q) is presented in equation 57 [3].

$$q = 0.5 \rho_\infty V_\infty^2 \tag{57}$$

Horizontal component of the aircraft velocity is estimated using the relation as shown in equation 58.

$$V_{\infty,x} = \sqrt{V_\infty^2 - V_{\infty,y}^2} \tag{58}$$

However, the heading of the aircraft is not the same as the distance direction towards range credit. Therefore, the distance traveled is estimated using the turn radius of the aircraft. Turn radius (R) has been estimated using equation 59.

$$R = \frac{V_\infty^2}{g\sqrt{n^2-1}} \tag{59}$$
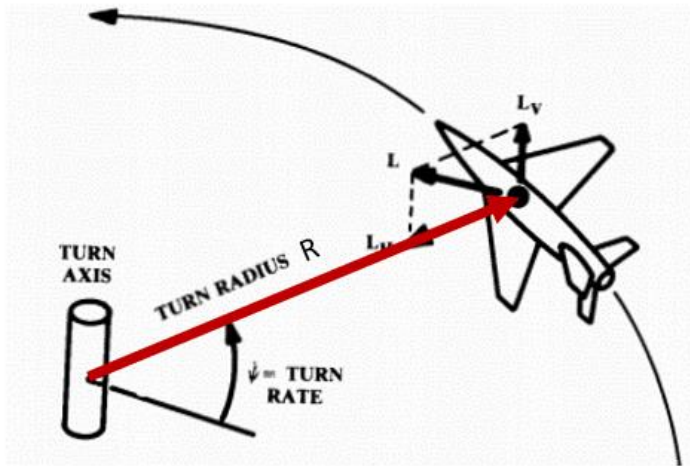
Figure 3.16. Turn radius (R) during turn performance [3]

Depending on the heading of the aircraft, the distance is calculated using equation 60. The sign becomes positive if the aircraft has positive horizontal speed component with respect to the direction of distance. The sign becomes negative once the aircraft has negative horizontal speed component with respect to the direction of the distance.

$$X_{after} = X_{before} \pm Rsin(\dot{\varphi}_{average}dt) \tag{60}$$

The acceleration of the aircraft is estimated using equation 61.

$$a = \frac{NPF-D-W_{aircraft}g\sin(\emptyset)}{W_{aircraft}} \tag{61}$$

Using this acceleration, aircraft speed after the time interval is calculated using equation 38. Aircraft mass after each time interval is calculated using equation 40. Fuel mass consumed after each time interval is estimated using equation 41. Time spent after each time interval is estimated using equation 42. Altitude after the time interval is calculated using equation 48. The function is solved iteratively until the turned angle is greater than or equal to the number of turns. One complete turn is 2π radians.

3.6.8. Sustained Turn Function

Sustained turn function requires initial Mach number, initial altitude, engine setting and number of turns as additional inputs. The sustained turn maneuver is used during operations when the aircraft must make a turn while maintaining the speed and the altitude. The function is solved iteratively for time intervals until the turned angle is greater than or equal to the number of turns. One complete turn is 2π radians.

First the load factor is estimated in order to perform the sustained turn. The load factor function requires an initial guess of the load factor, n_{guess}. The function is solved iteratively until the difference between the initial load factor and the calculated load factor is zero. First the lift coefficient is calculated using equation 62.

$$C_L = \frac{n_{guess}W_{aircraft}g}{0.5\rho_\infty V_\infty^2 S_{ref}}$$
(62)

Total drag coefficient is estimated using the lift coefficient estimated above and the aerodynamic dataset for the altitude and Mach number. Lift over drag ratio (L/D) is estimated using equation 63.

$$\frac{L}{D} = \frac{C_L}{C_D}$$
(63)

Load factor is calculated by equation 64.

$$n_{calc} = \frac{L}{D}\frac{NPF}{W_{aircraft}*g}$$
(64)

The function is minimized until the absolute difference between the n_{guess} and n_{calc} is zero. Using this load factor at each time interval, the turn rate has been estimated using equation 54. Turn radius is estimated using equation 59. Depending on the heading of the aircraft the distance is calculated using equation 60. The sign becomes positive if the aircraft has positive speed vector with respect to the direction of distance. The sign becomes negative once the aircraft has negative speed vector with respect to the direction of the distance. Aircraft mass after each time interval is calculated using equation 40. Fuel mass consumed after each time interval is estimated using equation 41. Time spent after each time interval is estimated using equation 42. Function is solved iteratively for each time interval until the angle turned is greater than or equal to the number of turns.

3.6.9. Drop

Drop function only requires the mass amount as an additional input and used to simulate the release of the external or internal stores. The drop is assumed to take place at an instant. Therefore, the velocity and altitude of the aircraft are kept constant and the time spent during drop is neglected. Final aircraft mass is estimated using equation 65.

$$W_{aircraft,final} = W_{aircraft,initial} - W_{dropped} \qquad (65)$$

3.6.10. Loiter

Loiter function requires initial Mach number, initial altitude and the endurance time as additional inputs. This function has the same methodology as the fly distance function, except that the stopping criteria for the function is not the distance but the endurance time. Therefore, the same loop is solved iteratively until the time spent is greater than or equal to the endurance time originally input.

3.7. Point Performance Analysis

Point performance is the aircraft performance merits under given flight conditions and configurations (amount of internal fuel and stores are given). Point performance

analysis is conducted by neglecting the fuel burned. Therefore, functions solved in this section (listed below) have constant aircraft mass.

- Instantaneous turn rate and the sustained turn load factor of the aircraft is calculated using the same methodology as described in the mission performance section.
- The supercruise Mach number and maximum Mach number are estimated using fly setting function described in the mission performance section. Function starts with Mach number equal to 2.0, altitude given by the point performance requirement, max dry (maximum thrust without afterburner) and max reheat (maximum thrust with afterburner) engine settings until the aircraft velocity becomes constant after iterations (acceleration equal to zero). The result with the engine setting of max dry becomes the supercruise Mach number result and the one with the engine setting of max reheat becomes the maximum Mach number result.
- Acceleration is solved in the same way as the methodology presented in mission performance section.
- The "Specific Excess Power" (SEP) is estimated using equation 44 as presented in mission performance section.

3.7.1. Takeoff Function

Takeoff function is solved in detail for accurate estimation of the takeoff distance. The function requires the altitude, maximum lift coefficient, engine setting and ground friction (f_s) as additional inputs. The function is split into three segments; ground roll, transition and climb, Figure 3.17. During ground roll the aircraft is accelerated to the 1.1 times stall speed. Then the transition segment starts where the aircraft's climb angle is solved using equation 45. The radius of the transition-arc (TAR) is solved using equation 66. Transition altitude is solved using equation 67. If the transition altitude (h_{TR}) is estimated higher than the obstacle clearance altitude ($h_{obstacle}$), then the transition distance (S_t) is calculated using equation 68. Otherwise equation 69 is

the solution for the transition distance [3]. Obstacle clearance altitude is included in the calculations for safe taking off or landing and also for compliance with airworthiness requirements. If the obstacle clearance altitude is not cleared at the transition segment, the distance traveled during the climb segment (S_C) is estimated using equation 70.

$$TAR = 0.205V_{stall}^2 \tag{66}$$

$$h_{TR} = TAR(1 - cos\gamma_{climb}) \tag{67}$$

$$S_T = \sqrt{TAR^2 - (TAR - h_{TR})^2} \tag{68}$$

$$S_T = TARsin(\gamma_{climb}) \tag{69}$$

$$S_C = \frac{(h_{obstacle} - h_{TR})}{tan\gamma_{climb}} \tag{70}$$
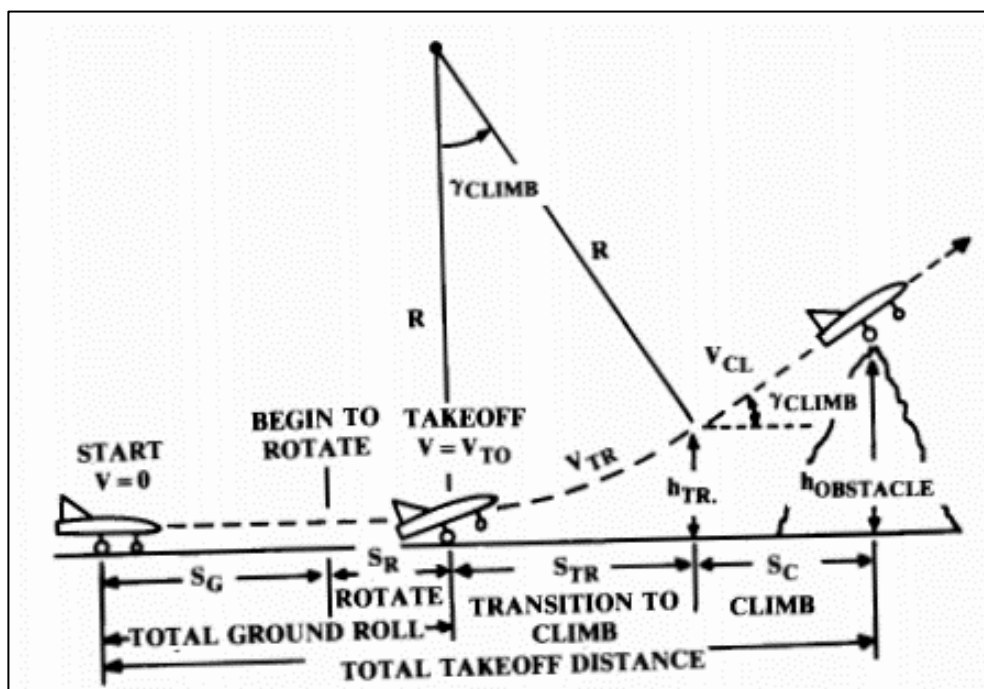
Figure 3.17. Takeoff analysis [3]

3.7.2. Landing Function

Initially, there was no landing function in the mission performance analysis as some loiter time can be added at the end of the design mission profile to account for the landing and the reserve fuel. However, a detailed model described in [3] is used in order to properly calculate the landing distance. Landing analysis is presented in Figure 3.18 [3]. Calculations start at the obstacle height with 1.2 times the stall speed the aircraft. Notice that stall speed in landing configuration may be different than takeoff configuration. Engine setting is set to idle and the drags are increased to include the effects of full flap deflections. The approach angle can be estimated from equation 45. Flare circular arc radius (CAR) is estimated using equation 66 replacing transition-arc radius (TAR) with (CAR). Then the flare altitude can be estimated from equation 67 replacing transition altitude (h_{TR}) with flare altitude (h_{FR}) and (TAR) with (CAR). The approach distance (S_A) is estimated using equation 70 with the flare altitude instead of the transition altitude. Next the flare distance (S_F) is estimated using equation 69 with replacing (TAR) with (CAR). The ground roll is estimated the same way as the takeoff distance however there is an additional 3 second allowance of free roll. Since there are brakes, flap drag and lower engine setting is slowing down the aircraft significantly, eventually aircraft stops. The process is solved for time intervals and the distance is recorded. Finally, the distance calculated for approach, flare and ground roll is added up for landing distance estimation [3].
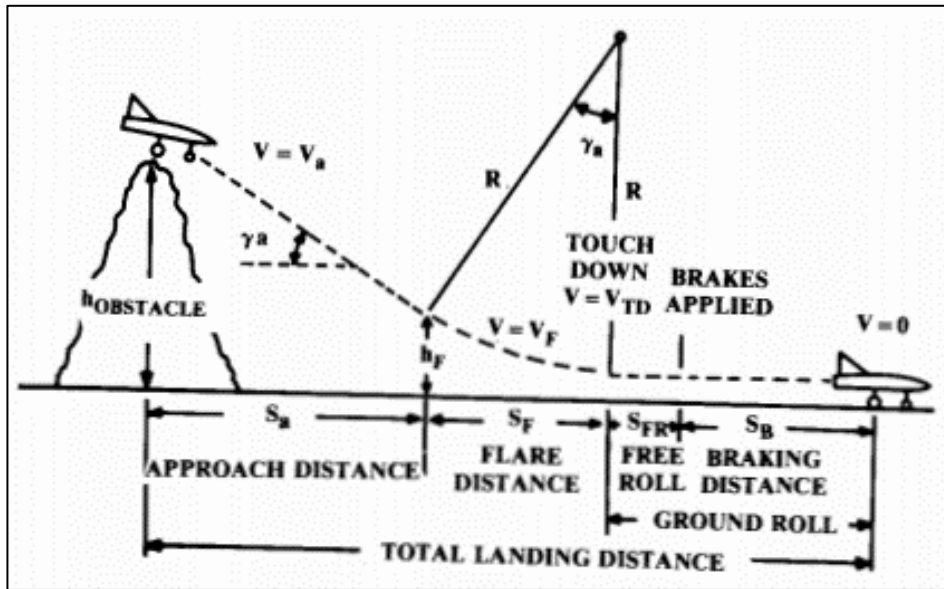
Figure 3.18. Landing analysis [3]

CHAPTER 4

AIRCRAFT CONCEPTUAL DESIGN SYNTHESIS

In the previous chapter, analysis methodology of any given aircraft has been shown. In this chapter, the methodology of aircraft sizing for the mission profile is presented. The aircraft is geometrically modified with the sizing methodology until the usable fuel within the aircraft and the fuel consumed in the mission simulation becomes equal. Fixed wing sizing means that the wing parameters are kept constant during sizing process. Since rest of the design assumptions are kept constant, the idea of fixed wing aircraft sizing presented here is the determination of aircraft characteristics that are unique to the wing shape, while the resulting aircraft is also compliant with the design mission profile.

An optimization procedure is to find the optimum or suitable solution by iterating and comparing number of solutions in the design space. Multidisciplinary concept covers combination of related disciplines and their approach to a problem. Aircraft design in this thesis includes aerodynamics, weight, geometry, performance and flight mechanics disciplines. All these disciplines have been used in order to solve for the optimum fighter aircraft for given requirements using the proposed aircraft design synthesis.

4.1. Fixed Wing Aircraft Sizing

4.1.1. Sizing Process

First, the baseline aircraft's fuselage geometry is modified to a size within predetermined limitations of the fuselage length by a parameter called plug length. The plug length is estimated by the minimization function between minimum and

maximum plug length boundaries (chosen by the user). Then the wing is relocated without changing any of the geometrical parameters so that the wing is stationed at the selected percentage location of the fuselage. Last, the tails are relocated and sized according to the initial tail volume coefficient of the aircraft. Therefore, the sizing process can be expressed as a function of variable plug length and result is the absolute difference of the usable fuel estimated by the weight analysis and total fuel consumption at the end of mission analysis. This function is then minimized to find the correct plug length. Fixed wing aircraft sizing process is presented in Figure 4.1.

Inputs

↓

Plug Length ◄─────────────────┐

↓   │

Fuselage Modification   │

↓   │ NO (New plug length)

Wing Relocation For New Fuselage Geometry

↓

Tails Are Relocated By Plug Length
&
Tails Are Sized To Meet Tail Volume Coefficients

↓

Fixed Aircraft Analysis

↓

Is Usable Fuel (Weight Analysis) Equal to Consumed Fuel (Mission Analysis)? ───┘

↓

YES (Plug length value is finalized)
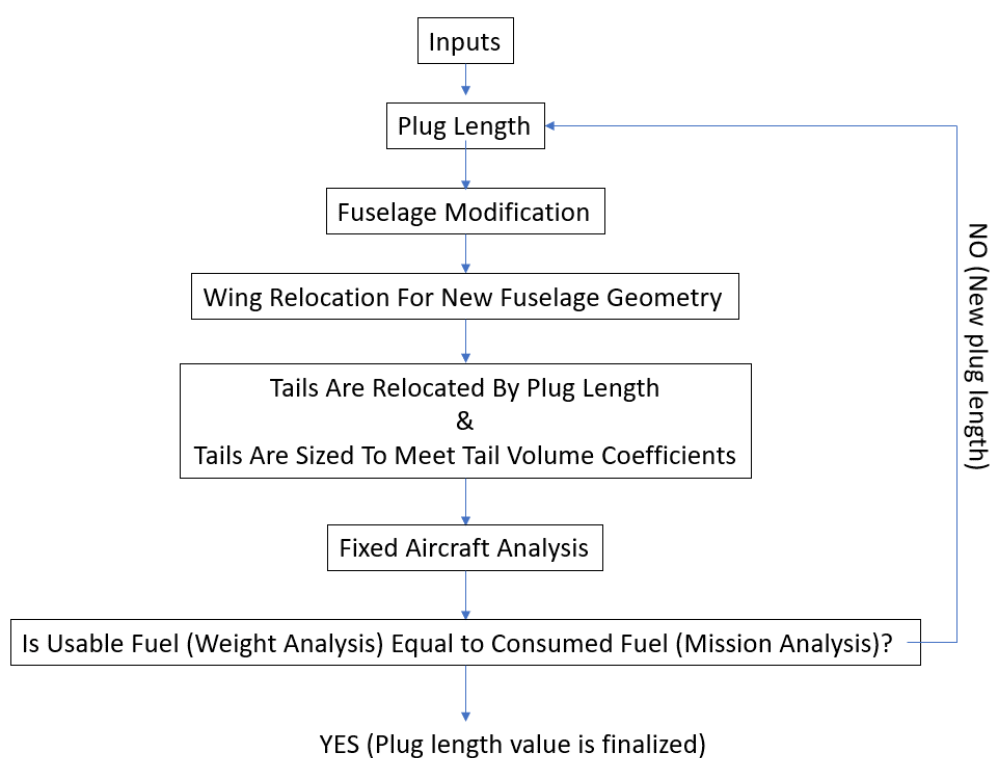
Figure 4.1. Fixed wing sizing process

4.1.1.1. Fuselage Geometry Sizing

The fuselage geometry is sized by displacement of the selected fuselage cross-sections with the parameter plug length. This results in larger or smaller fuselage geometry. The modification is carried through changing the fuselage cross-section inputs with the estimated values. Fuselage geometry sizing is presented in Figure 4.2, fuselage cross-sections (blue) highlighted by the green rectangle is displaced by the plug length to create new fuselage (red).
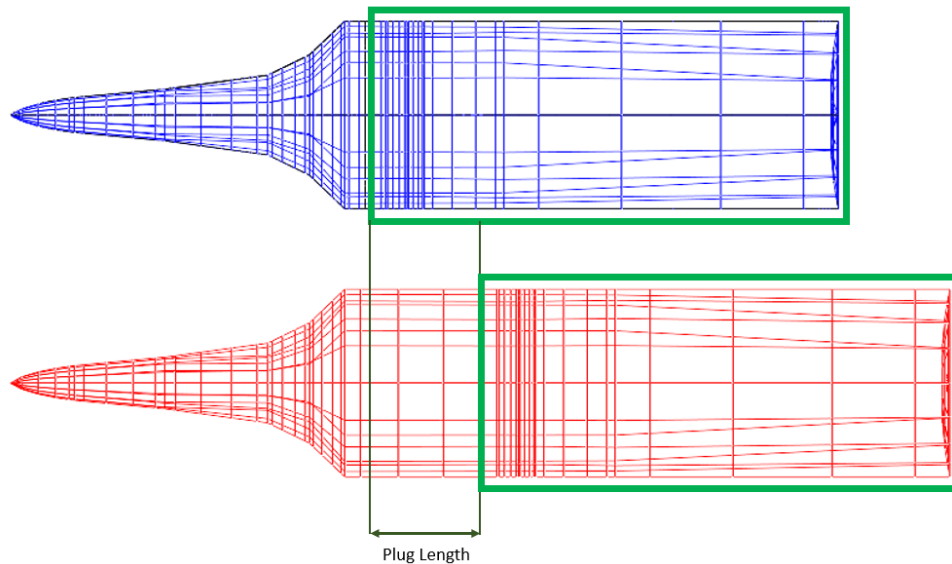
Figure 4.2. Fuselage geometry sizing by variable plug length

4.1.1.2. Wing Geometry Relocation

In order to logically place the wing during sizing process, wing must be relocated to a proper position. The wing position of the aircraft is predetermined in the design inputs as wing location parameter which is the percentage of mean aerodynamic chord distance with respect to the center of gravity position. Since the center of gravity position of the aircraft is a parametric value with variable fuselage length (design input

as percentage of the fuselage length), the new wing location are estimated with respect to the new center of gravity location. The process is presented in Figure 4.3.
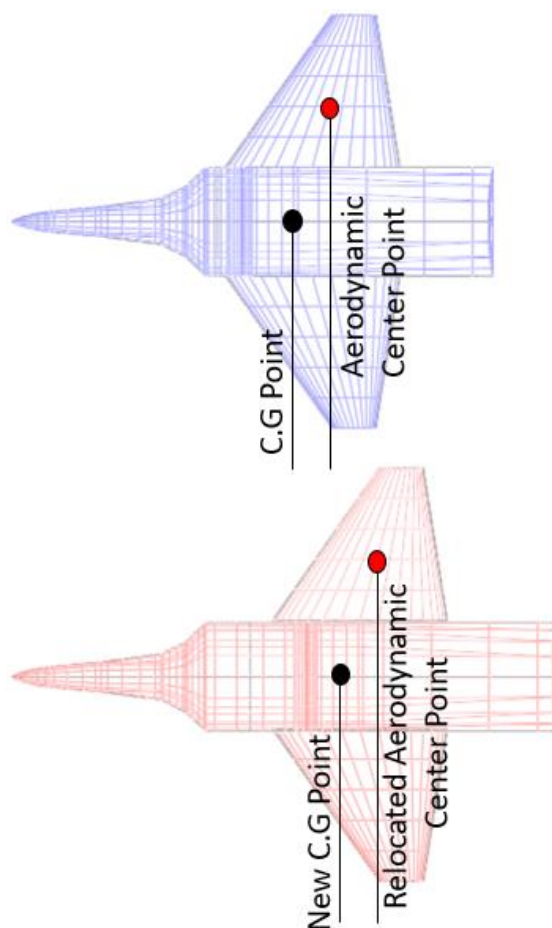
Figure 4.3. Wing relocation with new center of gravity location

4.1.1.3. Tail Geometry Sizing

Last segment of the fixed wing aircraft sizing process is the sizing of tails to maintain constant tail volume coefficient. The leading-edge point location of the exposed tail geometry is changed according to the same distance as the fuselage plug length parameter in the design inputs. Tail sizing algorithm is created as a function of tail

span. The geometry inputs are modified to increase or decrease the span of the component. The result of this function is the absolute difference of the actual tail volume coefficient and the required tail volume coefficient. This function is minimized iteratively by varying the span so that the final tail geometry matches the initial tail volume coefficient after the geometry analysis.

4.2. Multidisciplinary Design Optimization

4.2.1. Independent Design Variables

Independent design variables are selected among the parameters that create unique set of characteristics of the design problem. In the present thesis, the wing geometry and its parameters are selected as the independent design variables. List of these variables are exposed span length, exposed root chord length, exposed taper ratio and leading-edge sweep angle. These independent design variables are changed within the predetermined limits during optimization. These changes have been applied to the geometry by modification of the geometry input parameters for the wing (wing sizing) before the analysis.

4.2.2. Objectives

Objectives are set of solutions that are minimized or maximized during optimization process. These solutions can be anything that is changed with the variation of the independent design variables. In the present thesis, maximization of two parameters that challenge each other [10] are selected; subsonic sustained turn load factor and supercruise Mach number. These objectives are critical performance parameters of the aircraft because the subsonic sustained turn load factor is fundamentally defining a fighter aircraft's maneuverability. The supercruise Mach number defines the fighter aircraft's fast cruising capability with low observability through the enemy defense systems. More slender aircraft tend to have less subsonic sustained turn load factor while maintaining higher supercruise capability. As the slenderness ratio decreases,

the subsonic sustained turn load factor increases while the supercruise Mach number drops. The slenderness ratio is presented in equation .

$$Slenderness\ Ratio = \frac{Aircraft\ Length}{Aircraft\ Maximum\ CrossSectional\ Area} \quad (71)$$

4.2.3. Constraints

When there are constraints present in the optimization procedure, there is a limit to the solutions that define the feasible design space. Solutions that have results outside the limits determined by the constraints are tagged as infeasible solutions. When there are no constraints to the optimization, all solutions are considered feasible. In the present work, absolute value of wing trailing edge sweep angle constraint and the wing tip chord length constraint are the constraints of the design problem.

4.2.4. Multidisciplinary Design Optimization Method

The list of multidisciplinary design optimization (MDO) methods and their convergence performance have been studied in [10] for research on the improvements in aircraft conceptual design process. It was observed as a key conclusion that all the MDO methods produced reasonable results.

In the current study, in order to generate pareto-fronts quickly, constrained nondominated sorting genetic algorithm II (NSGA-II) is used during optimization as proposed in [27]. The optimization procedure is presented in Figure 4.4. The parent population (P_t) of size N and off-spring population (Q_t) of size N is sorted into ranks (nondominated sorting) in combined population (R_t) of size 2N. Then depending on the ranking groups, a new population is created with the highest ranks until the new population reaches the size of N. However, in case where there are designs within the same rank group that increases the size of the new population size higher than N, then crowding distance sorting is used to eliminate enough results from that rank group to construct the new population to the size of N. This process is iterated until the maximum number of evaluations are reached. The off-spring populations are

generated using the usual binary tournament selection, recombination, and mutation operators.
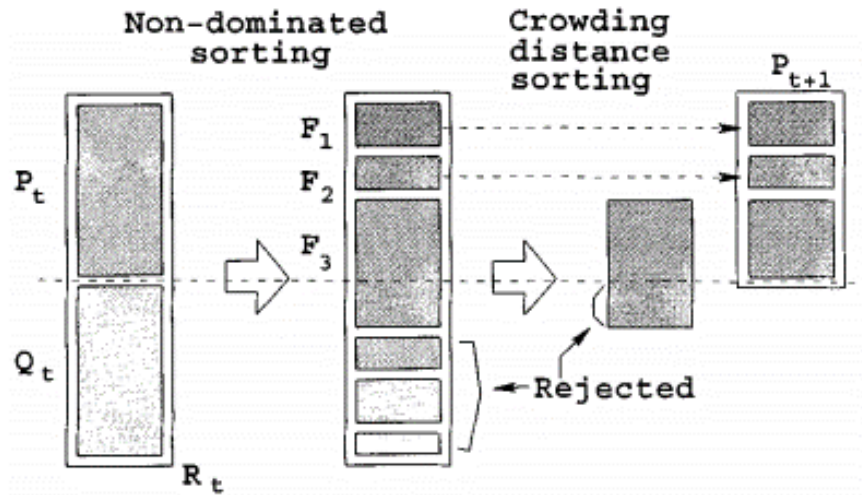
Figure 4.4. NSGA-II procedure [27]

A fast non dominated sorting approach is introduced as presented in Figure 4.5 [27]. For each solution (p) a domination count (n_p) and the number of solutions which dominate the solution p and list of solutions (S_p) that solution p dominates are calculated. In case the size of the population that dominate the solution p is 0, then this solution is tagged as $n_p = 0$ and added to the first set of non-dominated (ranked F1) solutions. For each solution p with n_p equals 0, all members of S_p is visited (q) and their domination count is reduced by 1. During this process, in case any q reaches domination count of 0, it is added to the second non-dominated set of solutions (ranked F2). Then this process is repeated for the F2 population. This process is continued until all rankings are sorted out with maximum of N ranks.

```
fast-non-dominated-sort(P)
for each p ∈ P
    S_p = ∅
    n_p = 0
    for each q ∈ P
        if (p ≺ q) then                    If p dominates q
            S_p = S_p ∪ {q}                 Add q to the set of solutions dominated by p
        else if (q ≺ p) then
            n_p = n_p + 1                    Increment the domination counter of p
    if n_p = 0 then                         p belongs to the first front
        p_rank = 1
        F_1 = F_1 ∪ {p}
i = 1                                       Initialize the front counter
while F_i ≠ ∅
    Q = ∅                                   Used to store the members of the next front
    for each p ∈ F_i
        for each q ∈ S_p
            n_q = n_q − 1
            if n_q = 0 then                 q belongs to the next front
                q_rank = i + 1
                Q = Q ∪ {q}
    i = i + 1
    F_i = Q
```

Figure 4.5. Fast non-dominated sorting [27]

Crowding distance calculation requires the procedure shown in Figure 4.6 [27]. For each objective, every solution belonging to each rank group is assigned a distance depending on their normalized objective result. Solutions with maximum values towards each objectives are given an infinite distance value. Therefore these solutions are always selected before the crowding distance calculations takes place.

```
crowding-distance-assignment(I)
l = |I|                                             number of solutions in I
for each i, set I[i]_distance = 0                   initialize distance
for each objective m
    I = sort(I, m)                                  sort using each objective value
    I[1]_distance = I[l]_distance = ∞               so that boundary points are always selected
    for i = 2 to (l − 1)                            for all other points
        I[i]_distance = I[i]_distance + (I[i + 1].m − I[i − 1].m)/(f_m^max − f_m^min)
```
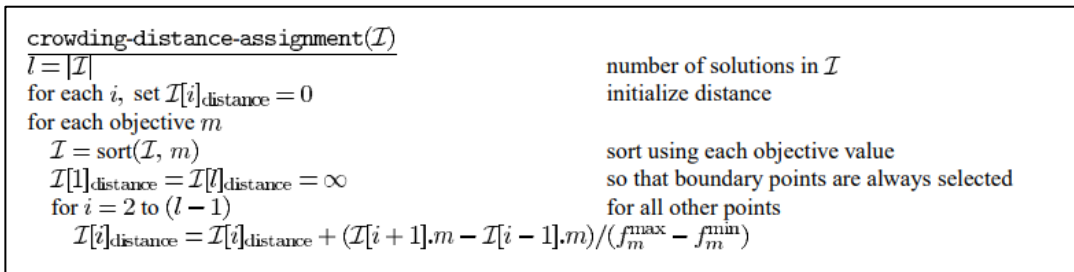
Figure 4.6. Crowding distance assignment [27]

In case there are no constraints to the problem, all solutions are feasible. However, if there are constraints, solutions violating these are infeasible solutions. In NSGA-II, constraint handing is implemented into the domination procedure by following the definition: A solution i is declared to be constrained-dominate solution j, in case any of the following conditions is valid [27]:

- Solution i is feasible and solution j is infeasible,
- Solution i and j are both infeasible, however solution i has overall less constraint violation (closer to being feasible),
- Solution i and j are both unfeasible and solution i dominates solution j.

A python module for multidisciplinary optimization with parallel computing capability called platypus [28] and its NSGA-II implementation is used for the optimization purposes of this thesis.

4.3. Aircraft Conceptual Design Synthesis

Aircraft conceptual design synthesis that has been constructed using the methodologies presented in previous chapters is presented in Figure 4.7. The requirements and preparation work conclude initial engine sizing. The internal systems have been selected and laid out depending on the design decisions. Parametric model has been generated around the system layout respecting the design decisions. Then the optimization module randomly generated independent design variables (with in the lower and upper bounds range) creating new wing geometry for the model. Then the aircraft has been sized to meet the design mission profile. Once the usable fuel and the consumed fuel has been equal to each other, fixed aircraft results have been processed through optimization algorithm until the maximum number of calculations have been reached.
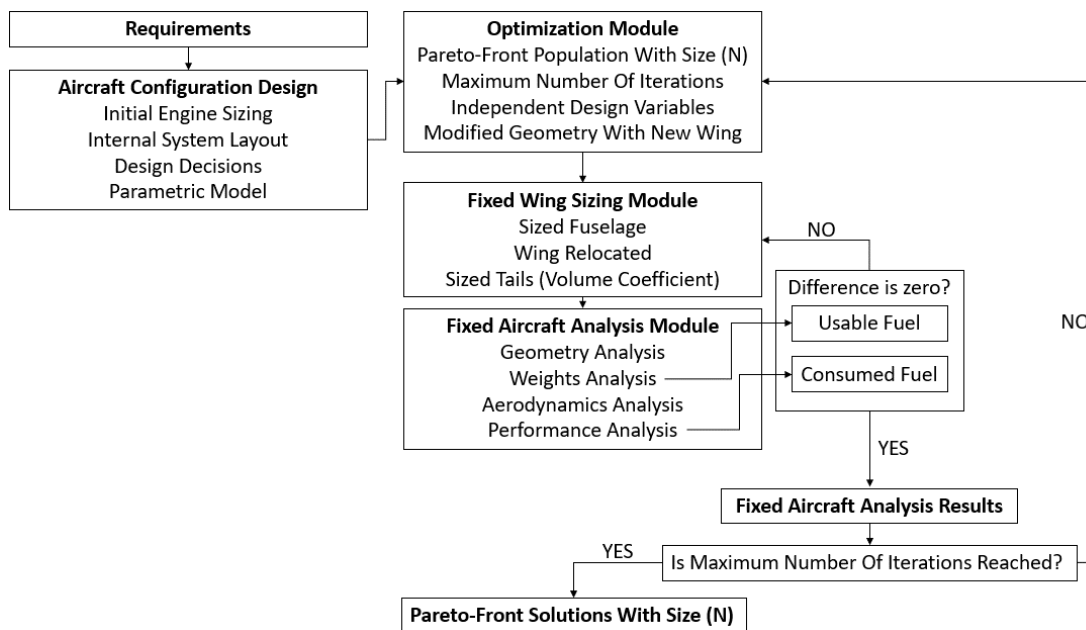
Figure 4.7. Proposed aircraft conceptual design synthesis

Result of the design synthesis is a pareto-front against two selected objectives with predeclared population size. Each solution within the pareto-front has its own unique geometry, weight, aerodynamics and performance characteristics.

4.3.1. Multi-Criteria Decision Analysis

One of the simplest decision-making theories called weighted sum model is used for the multi-criteria decision making analysis during configuration selection from the pareto-front solutions [29]. Once all the criteria are weighted, all alternatives have their normalized (by the best solution or the requirement) criteria multiplied by the weighting factor and summed up resulting in the parameter called weighted quality. The alternative with the most weighted quality is the selection. Example of selection methodology is presented in Table 4.1. With alternative 1 with weighted quality of 6.94 and alternative 2 with weighted quality of 7.04, it is estimated by the method that the selection of alternative 2 is favorable. There are more complex and well-constructed multi-criteria decision analyses methods [29], however those methods are beyond the scope of this thesis.

Table 4.1. *Example of weighted sum multi-criteria decision method*

	Criteria 1	Criteria 2	Criteria 3	Weighted Quality
Weighting	*0.10*	*0.50*	*0.40*	
Alternative 1	1.8	5.2	10.4	6.94
Alternative 2	2.5	3.9	12.1	7.04

CHAPTER 5

RESULTS

In order to evaluate a fighter aircraft design using the proposed synthesis, two unique aircraft configurations are designed to meet the modified version of Advanced Tactical Fighter (ATF) program's final requirements as presented in [11]. These configurations are sized and optimized following the proposed synthesis.

5.1. Requirements

Top-level requirements of present study are presented in Table 5.1.

Table 5.1. *Modified top-level requirements* [11]

Criteria	Requirement
Mission radius	650 km
Weapons payload	6x AIM-120, 2x AIM-9, gun with 600 rounds casing retained
Total takeoff distance	1500 m
Total landing distance	1500 m
Max. Mach number	2.0 at 9000 m in combat configuration*
Supercruise Mach number	1.4 at 9000 m in combat configuration*
Specific excess power	125 m/sec, Mach number = 1.15 at 9000m in combat configuration*
Sustained load factor	3.8-g at Mach number = 0.9 at 9000m in combat configuration*
Acceleration	From Mach number = 0.8 to 1.4 in 50 seconds at 9000m with combat configuration*

*Combat configuration is the aircraft weight with 50% internal fuel and full internal payload.

Design mission profile of the analyses is shown in Table 5.2.

Table 5.2. *Design mission profile: Modified offensive counter-air mission* [11]

Segment	Description
1	Take-off and acceleration allowance (computed at sea level. 59º F). a. Fuel to accelerate on the ground to takeoff speed, rotate, and lift off. b. Fuel to accelerate to climb speed at take-off thrust (no distance credit).
2	Climb and accelerate from sea level to M = 0.9 and 9000m or higher (distance credit allowed).
3	Cruise out 600 km total (including previous leg) at M = 0.9 ending at 9000m or higher.
4	Accelerate to M = 1.4 and supercruise 50 km at 9000m or higher.
5	Supercruise Air Combat: Fuel required to perform two 4g 360-degree turn at 9000m or above and at least M = 1.2.
6	Weapons Delivery: Fire all missiles.
7	Egress: Accelerate and climb from M = 1.2 to M = 1.4.
8	Supercruise back 50 km.
9	Cruise back 600 km at M = 0.9 at or above 9000m.
10	Descent to sea level (no distance credit allowed).
11	Reserves: fuel required to loiter at 3048 m and speed for maximum endurance for 20 minutes.

Configuration: 6x AIM-120 AMRAAM, 2x AIM-9, MA1A2 rotary cannon with 600 rounds

5.2. Design 0

Design 0 is the initial aircraft design that is created to be analyzed. The initial engine sizing declares the size and the weight of the engine. Positioning the engines sets the basis for system layout determination and configuration creation. Once the aircraft surface is created, the design synthesis is followed to obtain a pareto-front solution set corresponding to the Design 0.

5.2.1. Engine Selection and Scaling

An afterburning turbofan engine data available from literature [10] for max dry and max reheat settings is used to generate an engine deck. Original engine data and the way the data is generated for different engine settings is given in appendix A. Initial engine sizing methodology depends on competitive aircraft aerodynamic dataset. Aerodynamic drag of F-15 for Mach number = 1.4 at 40000 ft is presented in Figure 5.1 [11]. It is observed that F-15 with speed of 1.4 Mach number at 40000 ft has 7625 kg drag force. The engine scale factor is estimated by changing the engine scale factor until the drag and the net propulsive force at Mach 1.4 and 40000 ft altitude are equal.
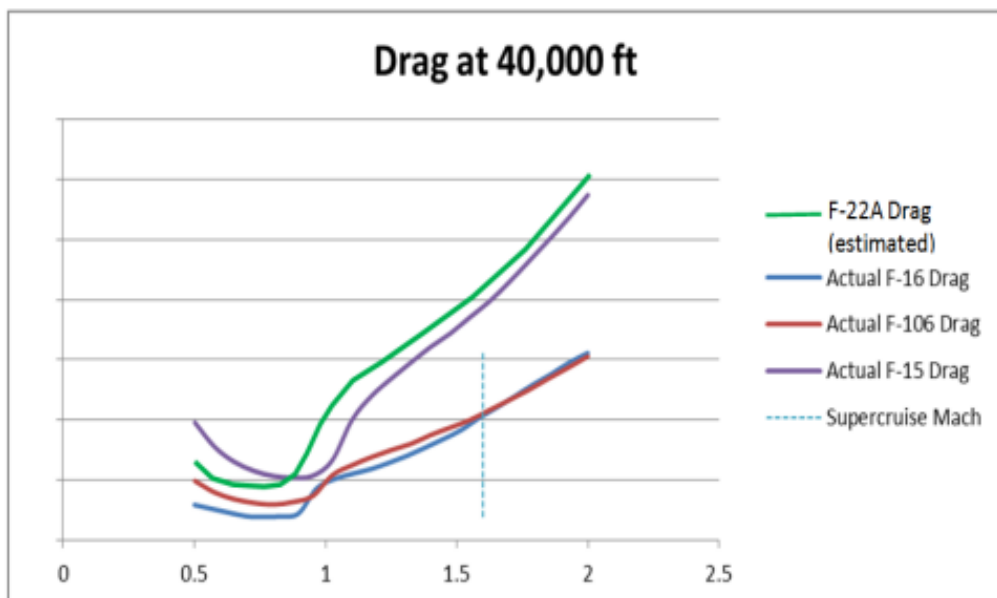
Figure 5.1. Variation of drag vs Mach number for four fighter aircraft at 40000 ft [11]

Estimation of capture area is done with a preliminary method presented in [3]. It is observed that the capture area to mass flow ratio for engines with design Mach number of 2.0 is 3.875 in^2/lb/s from Figure 5.2. The capture area then can be estimated with the engine mass flow value.

69
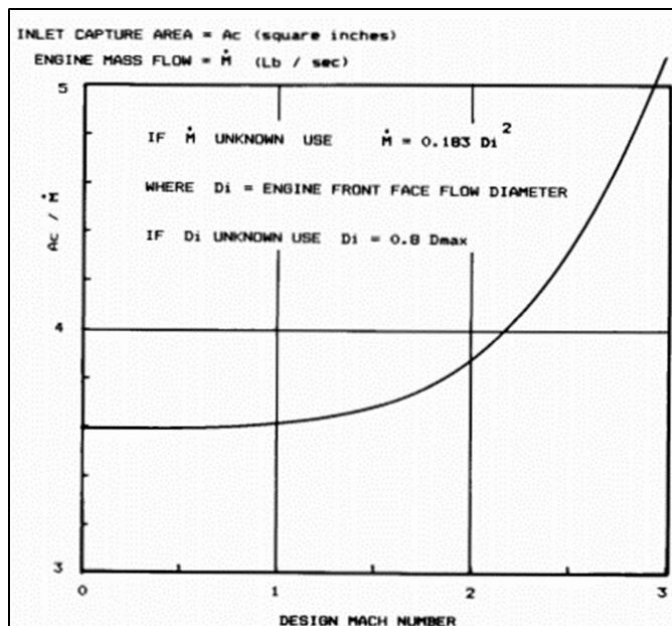
Figure 5.2. Preliminary capture area sizing [3]

The engine maximum diameter is used to estimate engine mass flow using equation 72 taken from [3]. The maximum engine diameter (D_{max}) is estimated by equation 2 with the engine scale factor and the initial engine's maximum engine diameter.

$$\dot{m} = 0.183 \ (0.8 \ (39.37 \ D_{max}))^2 \qquad (72)$$

The capture area (in inches) is then found by multiplying the mass flow in lb/s with the capture area to mass flow ratio of 3.875 in^2/lb/s obtained from Figure 5.2. Spillage drag has been added based on the capture area as presented in Figure 2.3. For addition of nozzle drag contribution Table 2.1 is used. With this process, engine scale factor result is presented in Table 5.3.

Table 5.3. *Engine scale factor estimation for the engine presented in appendix A*

Aircraft	Drag @ 1.4/40k ft (kg)	Engine Net Propulsive Force @ 1.4/40k ft (kg)	Engine Scale Factor
F-15	7625	7670	1.15

The slight difference between the drag and the net propulsive force can be neglected for the purposes of the initial design study. Resulting engine performance data for engine scale factor (ESF) of 1.15 is given in for max dry and max reheat throttle settings in Figure 5.3 to Figure 5.6.
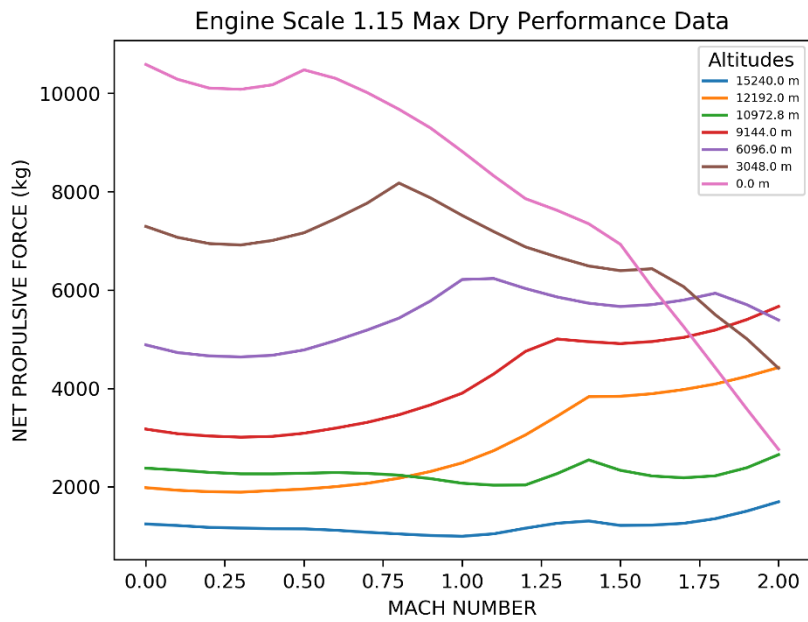
Figure 5.3. Net propulsive force (kg) for max dry setting vs Mach number (ESF = 1.15)
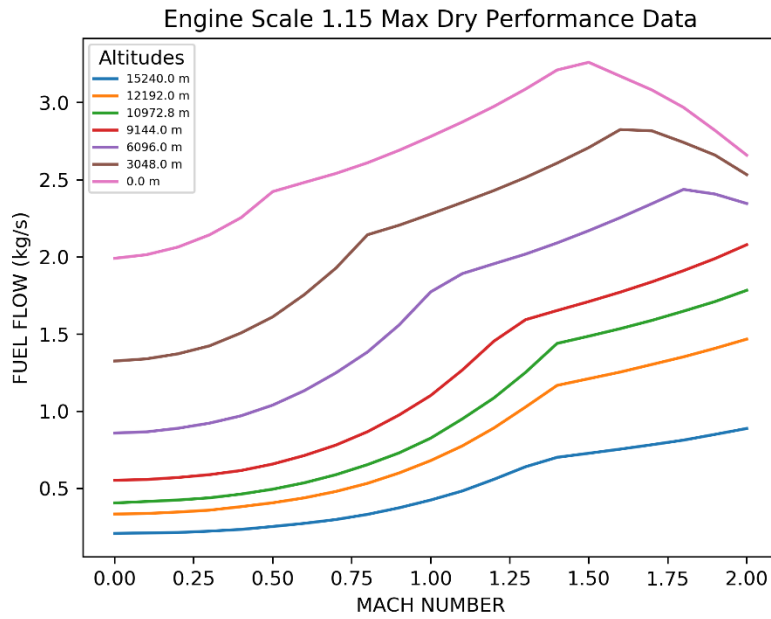
Figure 5.4. Fuel flow (kg/s) for max dry setting vs Mach number (ESF = 1.15)
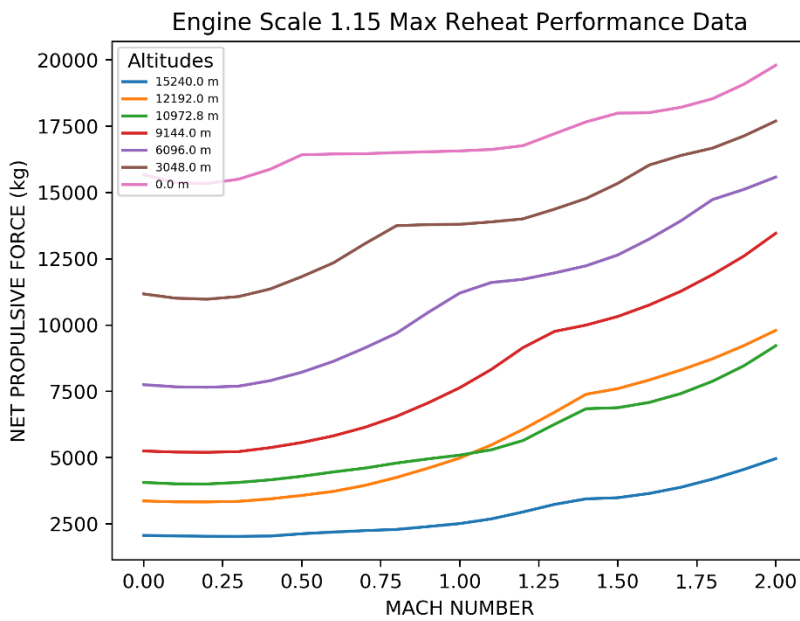
Figure 5.5. Net propulsive force (kg) for max reheat setting vs Mach number (ESF = 1.15)
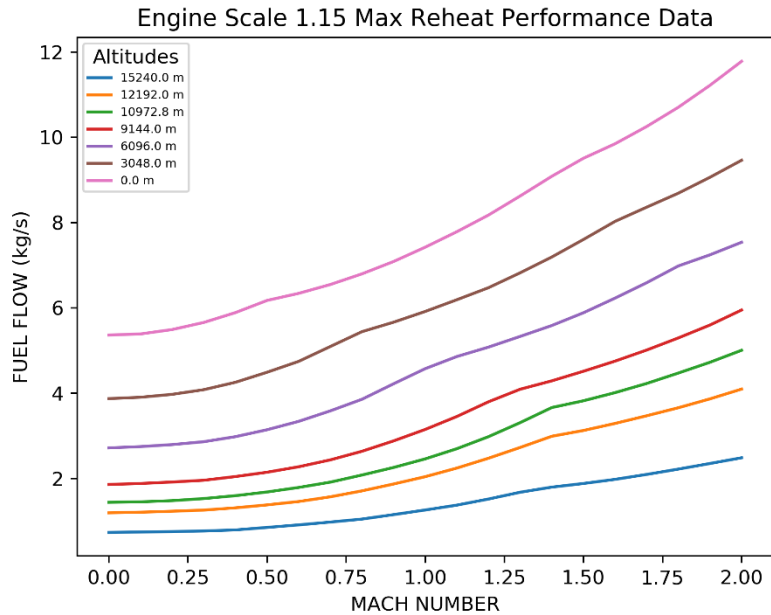
Figure 5.6. Fuel flow (kg/s) for max dry setting vs Mach number (ESF = 1.15)

10, 30, 50, 80% throttle setting of the max dry power is estimated for flight performance calculations. The installed net thrust at max dry is simply multiplied by the throttle setting to calculate corresponding installed net thrust. Then the net propulsive force is calculated by adding spillage and nozzle drag contributions. SFC at these throttle settings is calculated using equation 5. SFC and net propulsive force results of engine performance is presented in Figure 5.7 to Figure 5.14.
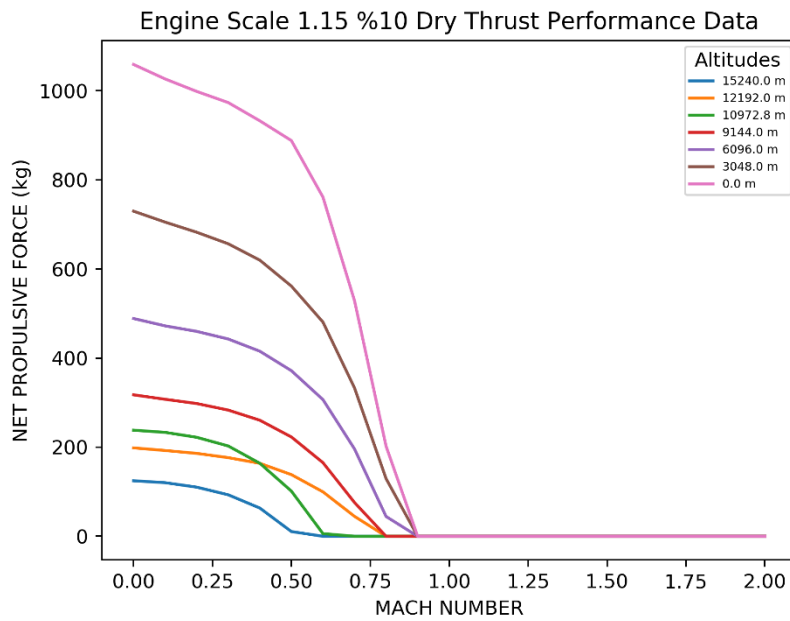
Figure 5.7. Net propulsive force (kg) for 10% dry setting vs Mach number (ESF = 1.15)
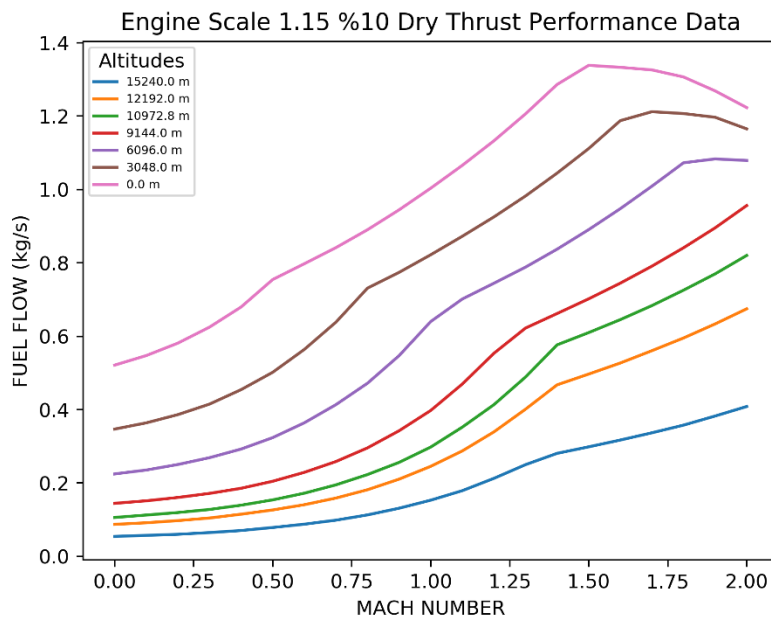
Figure 5.8. Fuel flow (kg/s) for 10% dry setting vs Mach number (ESF = 1.15)
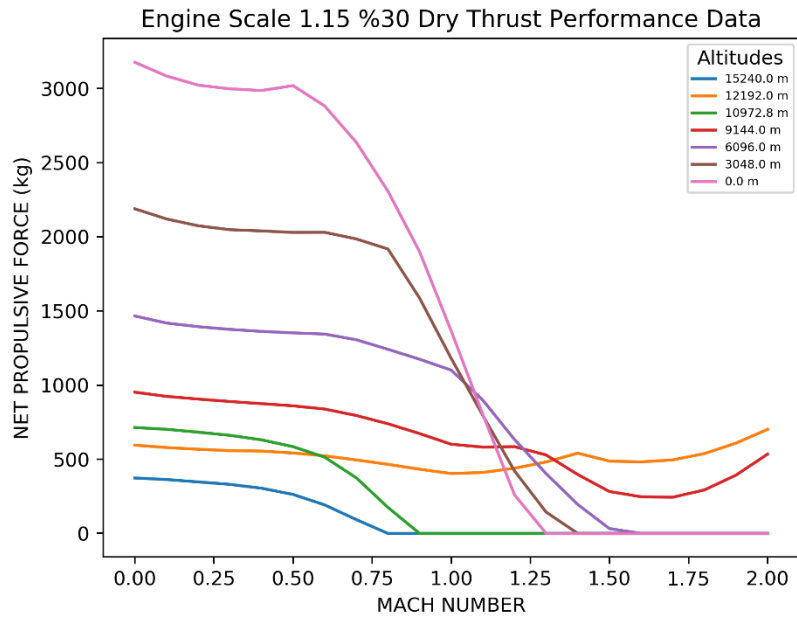
Figure 5.9. Net propulsive force (kg) for 30% dry setting vs Mach number (ESF = 1.15)
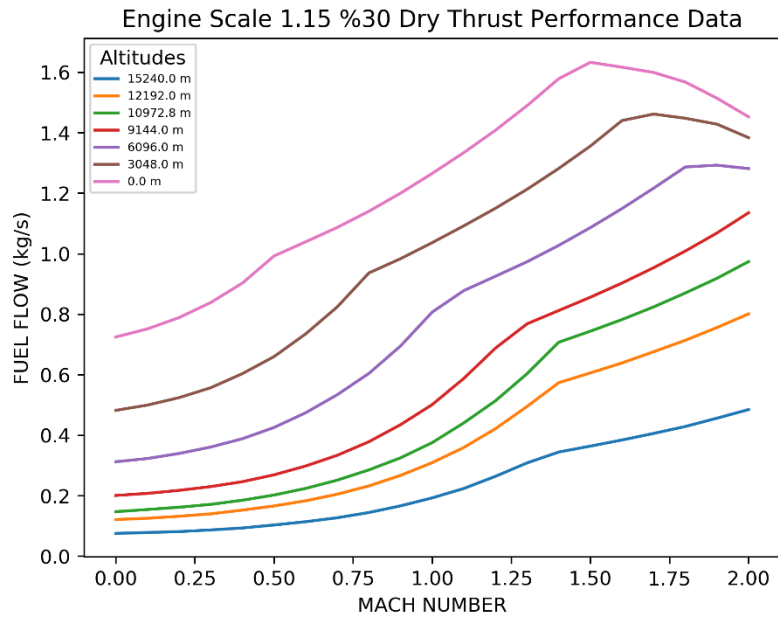
Figure 5.10. Fuel flow (kg/s) for 30% dry setting vs Mach number (ESF = 1.15)
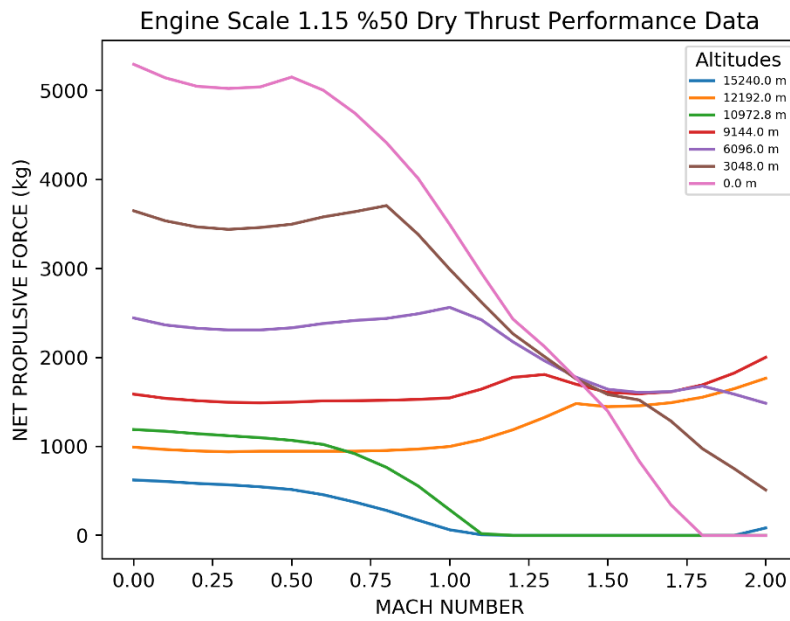
Figure 5.11. Net propulsive force (kg) for 50% dry setting vs Mach number (ESF = 1.15)
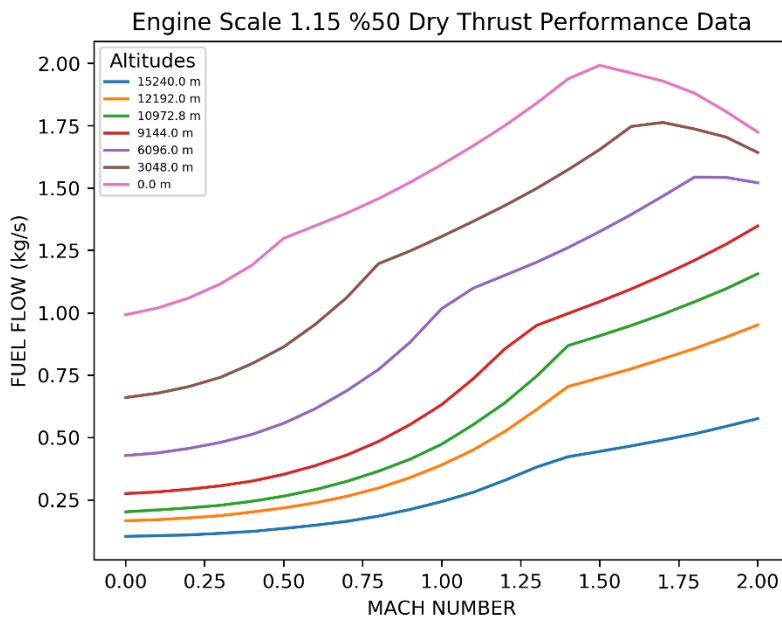
*Figure 5.12.* Fuel flow (kg/s) for 50% dry setting vs Mach number (ESF = 1.15)
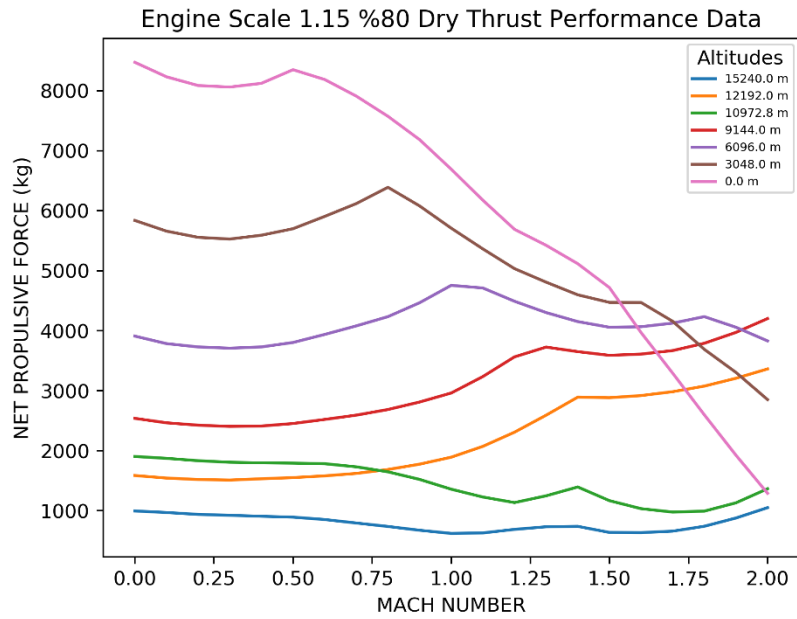
Figure 5.13. Net propulsive force (kg) for 80% dry setting vs Mach number (ESF = 1.15)
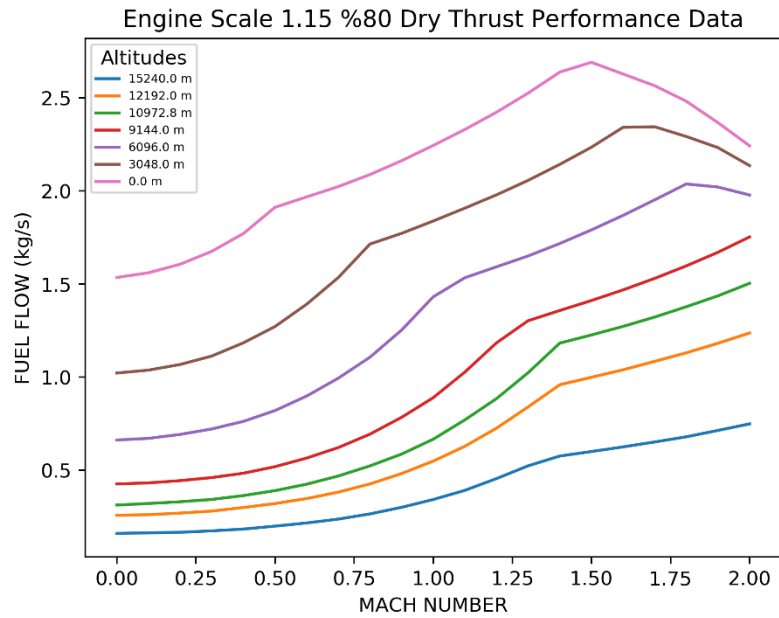
Figure 5.14. Fuel flow (kg/s) for 80% dry setting vs Mach number (ESF = 1.15)

77

Engine specifications corresponding the engine scale factor of 1.15 is presented in Table 5.4.

Table 5.4. *Engine specifications with engine scale factor of 1.15*

Specification	Value
Diameter (m)	1.09
Weight (kg)	1110.0
Length (m)	3.0

5.2.2. Configuration Design

Using generated engine geometry, the internal main systems such as radar, cockpit, weapons bay landing gears and engines are positioned and presented in Figure 5.15.
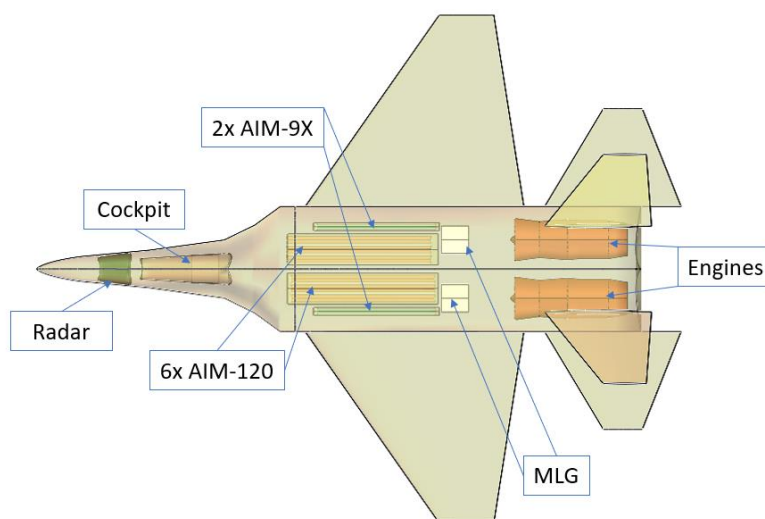
Figure 5.15. Design 0 systems layout

Radar is assumed to have a minimum diameter of 0.6 and maximum diameter of 0.8 meters. This assumption is made from the information presented in [3]. The cockpit is created conceptually from competitor aircraft scales to enclose enough space for a pilot, seat and necessary digital systems. Internal weapon bay clouds are generated

using the dimension of AIM-120 [30] and AIM-9X [31]. These clouds contain 6x AIM 120 and 2x AIM-9X. Landing gear clouds are generated using the initial tire sizes presented in [3] for military aircraft.

External fuselage surface, general wing and tail planform around these systems are generated using parametric geometry creation tool OpenVSP [7] and the surfaces are presented in Figure 5.16. The wing and tails are generated for initialization purposes of the design synthesis. During the optimization, the planform parameters are modified to a different value depending on the optimization algorithm.
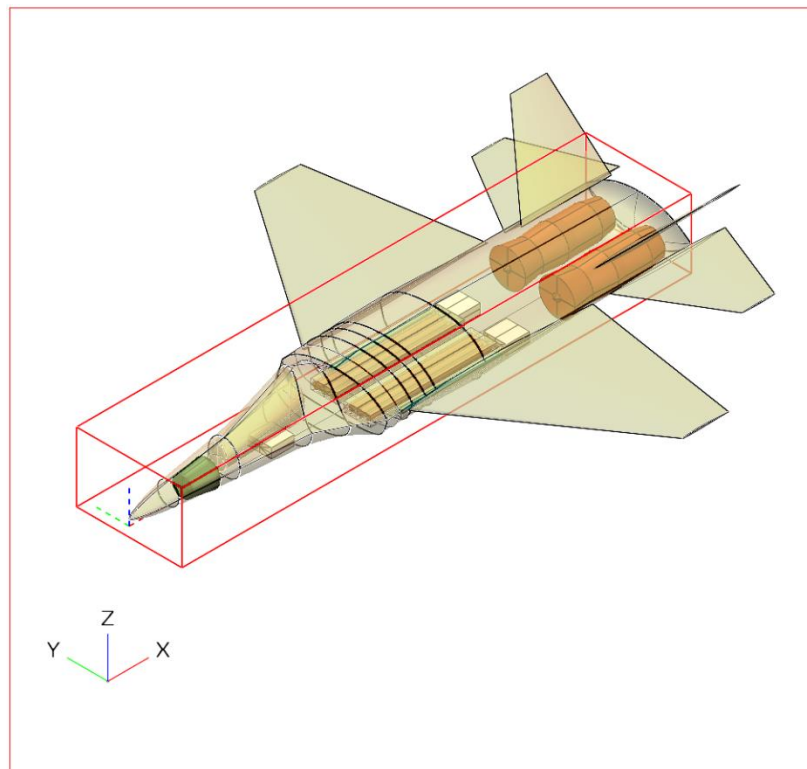
Figure 5.16. External surface generated around the system layout

5.2.3. Design Inputs

Design inputs for Design 0 has been presented in Table 5.5. Gun and ammo payload is added to the armament payload and their weights are taken from [3]. Design mission payload and the maximum payload are taken as equal and equal to the sum of 6x AIM-120 and 2x AIM-9X missile weights [30][31]. Design Mach number is taken from the maximum speed requirement of 2.0 Mach. Design lift coefficient, maximum load factor, ultimate load factor, base area, conceptual cg location, wing location, number of fuel tanks and exposed tail volume coefficients are selected from the competitor fighter aircraft as presented in [3]. System volume is calculated from the conceptual Design 0 created in the OpenVSP environment.

Table 5.5. *Design inputs of design 0*

Design Input	Value
Max. Mach Number	2.0
Design Lift Coefficient	0.2
Maximum Altitude	15000 m
Maximum Load Factor	9
Ultimate Load Factor	13.5
Flap Area Factor	0.3
Number of Engines	2
Armament (Gun & Ammo) Weight	500 kg
Design Mission Payload Weight	1228 kg
Maximum Payload Weight	1228kg
Paint Weight Per Square Meters	2.0 kg/m^2
Empty Weight Margin	10%
Fuel Density	802.83 kg/m^3
Number of Fuel Tanks	5
Fuselage Fuel Tank Volume Ratio	85%
Total of Main System Volumes	18.8 m^3
Base Area	0.25 m^2
Supersonic Drag Factor	2.0

Conceptual CG Location	52%
Wing Aerodynamic Center Location	CG Location-(5.0% MAC)
Exposed Volume Coefficients	HT = 0.2 VT = 0.05 (each tail surface for twin tail configuration)

Before running the design synthesis Design 0 is analyzed using fixed aircraft analysis methodology with these design inputs to understand the characteristics and differences to the requirements.

5.2.4. Geometry Results

Geometry analysis has been finalized and the summary of the parameters has been presented in Table 5.6.

Table 5.6. *Geometry parameters of design 0*

Parameter	*Value*
Fuselage Length (m)	15.46
Fuselage Maximum Depth (m)	2.04
Fuselage Maximum Width (m)	3.2
Wing Planform Area (m^2)	54.38
Wing Span (m)	13.0
Wing Aspect Ratio	3.1
Wing Pitch-up Tendency Transonic Aspect Ratio	1.81
Wing Leading-Edge Sweep (deg)	35.0
Wing Trailing-Edge Sweep (deg)	-8.92
Horizontal Tail Volume Coefficient	0.23
Vertical Tail Volume Coefficient (each)	0.04

5.2.5. **Weight Results**

Weight analysis is finalized and the results are given in Table 5.7.

Table 5.7. *Weight results of Design 0*

Weight Group	Value (kg)
Structure Group	5814
Propulsion Group	3348
Systems and Equipment Group	2931
Operating Empty Weight	13538
Payload Weight	1128
Total Usable Fuel Weight	5098
Mission Takeoff Weight	19764

5.2.6. Aerodynamic Results

Lift curve slope of Design 0 is estimated as shown in Figure 5.17.
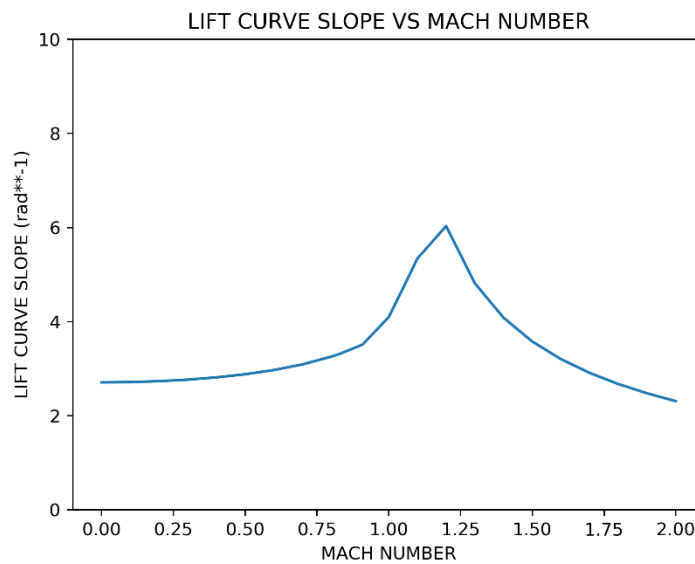
Figure 5.17. Lift curve slope of Design 0

Zero lift drag coefficient at sea level and 11250 m altitude is presented in Figure 5.18.
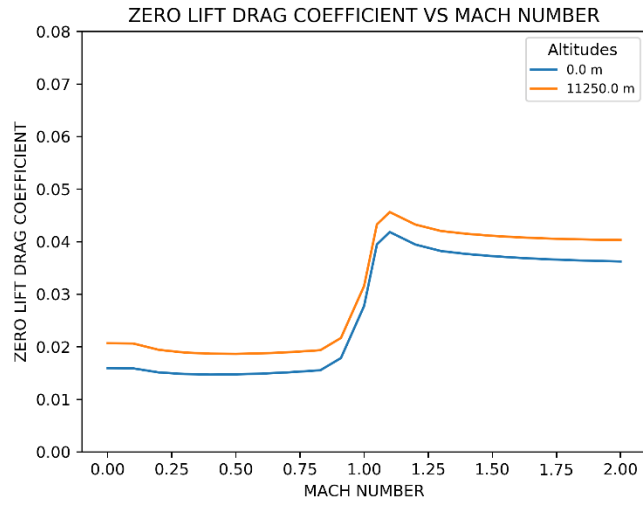
Figure 5.18. Zero lift drag coefficient curve of Design 0 at sea level and 11250 m altitudes

Drag due to lift factor with no suction and with full suction for Design 0 is shown in Figure 5.19.
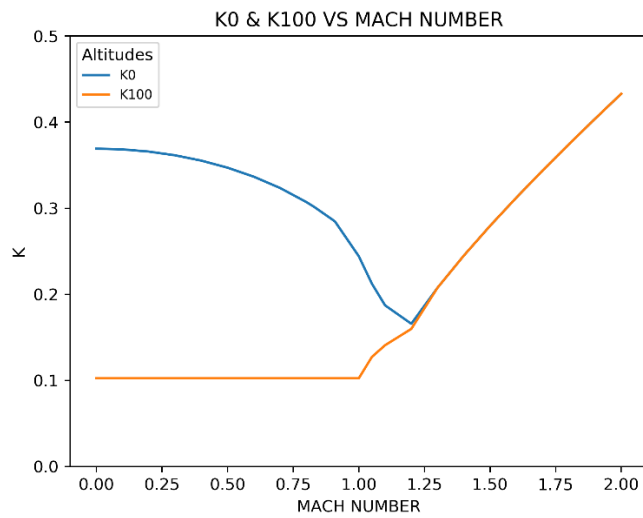
Figure 5.19. Drag due to lift factor (0 and 100% suction) for Design 0

83

Leading edge suction factor is presented for design lift coefficient of 0.2 in Figure
5.20.
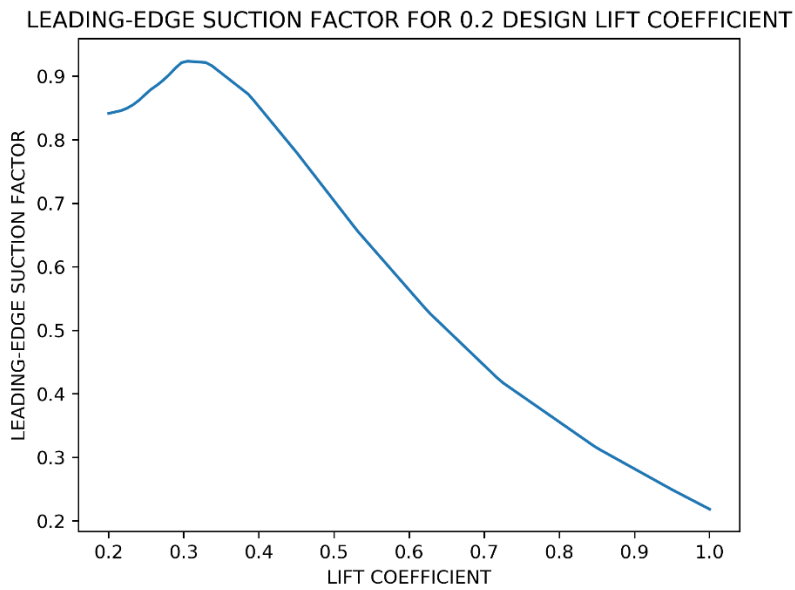
Figure 5.20. Leading-edge suction factor for design lift coefficient of 0.2

Drag polar at 0.9 Mach number, 9000m altitude (cruise conditions) for Design 0 is
shown in Figure 5.21.
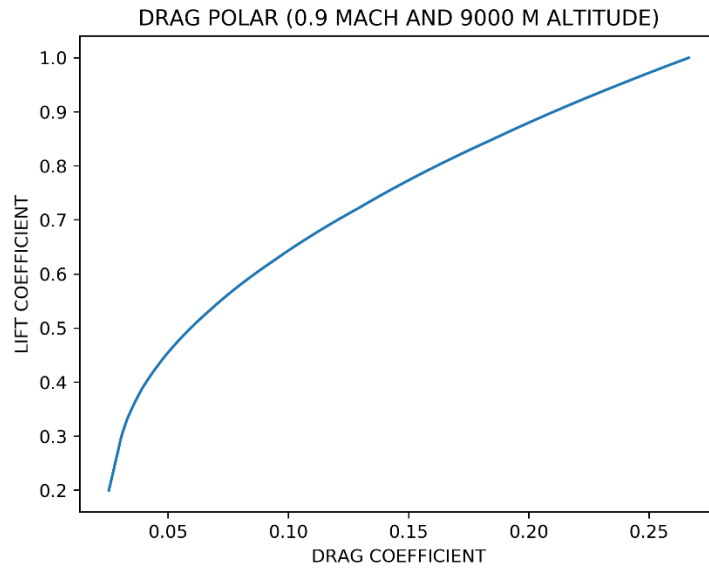
Figure 5.21. Drag polar of Design 0 at 0.9 Mach and 9000 m altitude

5.2.7. Performance Results

Mission performance results of Design 0 has been presented in Table 5.8. It is observed that the total usable fuel from weight analysis (5098 kg) is not enough to fly this mission as fixed aircraft mission performance fuel consumption is estimated as 7615 kg. In order to successfully fly the mission with the same range, this aircraft must be sized up to maintain more fuel. This is the essence of fixed wing aircraft sizing process presented in this thesis. In order to properly design an aircraft around a design mission profile, one must be able to size the aircraft geometry for including necessary fuel demand.

Table 5.8. *Mission performance details of Design 0*

Segment	Weight(kg)	Mach Number	Altitude (m)	Distance (km)	Total Time (min)	Total Fuel (kg)
Hangar	19764.12	0	0	0	0	0
Takeoff	19685.03	0.32	0	0.64	0.12	79.09

Accelerate	19530.88	0.90	0	4.76	0.35	233.23
Climb	19290.09	0.90	9000	12.74	1.18	474.03
Fly (distance)	16942.28	0.90	9000	612.74	37.76	2821.84
Accelerate	16796.36	1.40	9000	621.50	38.13	2967.76
Fly (max dry)	16413.17	1.41	9000	671.50	40.07	3350.95
Accelerate	16413.17	1.20	9000	671.50	40.07	3350.95
Sustained Turn	16140.30	1.20	9000	670.33	40.68	3623.82
Launch Weapons	15012.30	1.20	9000	670.33	40.68	3623.82
Accelerate	14945.55	1.40	9000	674.10	40.82	3690.57
Climb	14945.55	1.40	9000	674.10	40.82	3690.57
Fly (max dry)	14563.29	1.41	9000	724.10	42.76	4072.83
Accelerate	14563.29	0.90	9000	724.10	42.76	4072.83
Fly (distance)	12280.06	0.90	9000	1324.10	79.34	6356.06
Loiter	11020.76	0.50	3048	1324.10	99.34	7615.36

The point performance analysis has been completed and the results are given in Table 5.9. Results presented here are all compliant with the requirements, however since Design 0 cannot successfully fly the mission with the usable fuel it can contain, it is an unfeasible design point. Even if one were to size Design 0 with fixed wing aircraft sizing process and obtain results, one can never know whether it is the "best" design within the design space. That is the reason for acquiring a set of pareto-front designs and then selecting an aircraft that suits designer's intentions through multi-criteria decision analysis is essential.

Table 5.9. *Point performance analysis of Design 0*

Performance	Value
Maximum Mach number	2.0
Specific excess power (m/s)	209
Acceleration (s)	39.1
Takeoff distance (m)	1181
Landing distance (m)	802

Supercruise Mach number	1.4
Subsonic sustained G	4.38

5.2.8. Conceptual Aircraft Design Synthesis on Design 0

Conceptual aircraft design synthesis is applied to Design 0. Limits of the independent design variables is presented in Table 5.10. Constraints are defined as minimum of 1.0 meter tip chord length and the maximum of -15.0 degrees trailing-edge sweep angle for the wing in order to design cropped diamond wings. Optimization population (pareto-front) size is set to 100 aircraft and maximum number of design evaluations is set to 1500 aircraft. The runs are finalized successfully with the pareto front presented in Figure 5.22 in under 375 minutes with 3 processors with details shown in Appendix C. Results are observed to be non-dominated set of solutions. Conflict between both objectives are captured from the figure, which means that selecting an aircraft with increasing value of one objective cause to lose the value of the other objective. More slender aircraft are populated towards the higher supercruise Mach numbers as expected.

Table 5.10. *Independent design variables of optimization process*

Independent design variable	*Minimum*	*Maximum*
Exposed span (m)	8.0	12.5
Exposed root chord length (m)	5.0	8.0
Exposed taper ratio	0.1	0.25
Leading-edge sweep angle (deg)	35.0	50.0
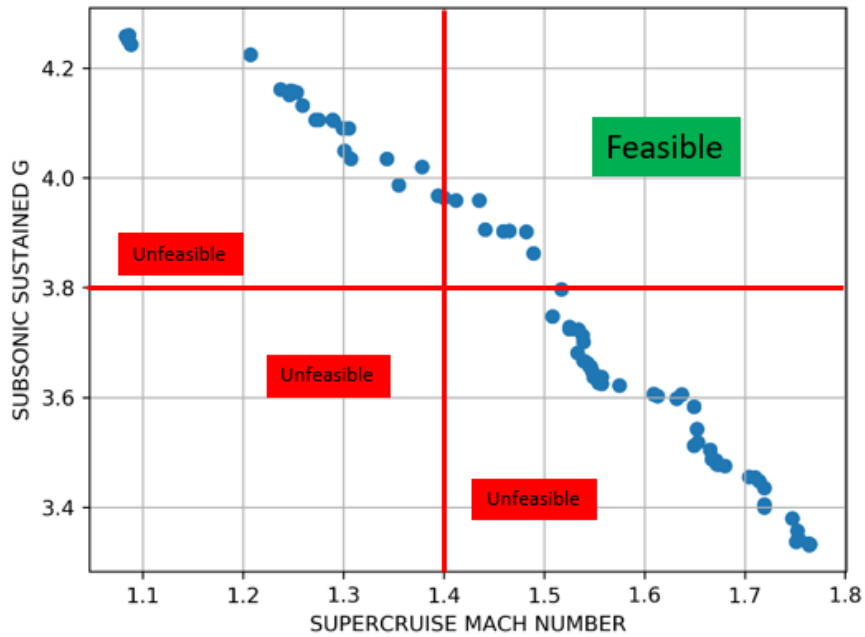
Figure 5.22. Sizing optimization of Design 0

The requirement filter is applied to the pareto-front, which were the supercruise Mach number of 1.4 and subsonic sustained g of 3.8. Total of 13 design results are observed to be compliant with these requirements and are presented in Table 5.11 below.

Table 5.11. *Filtered results of pareto-front for Design 0*

Design ID	Supercruise Mach Number	Subsonic Sustained G
5	1.517	3.797
6	1.489	3.863
11	1.441	3.906
13	1.435	3.959
16	1.394	3.968
21	1.482	3.902
27	1.465	3.904
30	1.412	3.959
40	1.4	3.964
71	1.435	3.959

73	1.482	3.902
88	1.459	3.903
91	o1.394	3.968

5.2.9. Configuration Selection by Multi-Criteria Decision Analysis

Maximum Mach number, specific excess power, acceleration, takeoff distance and landing distance requirement together with takeoff weight results for the filtered design solutions of Design 0 pareto front are presented in Table 5.12.

Table 5.12. *Requirement results for filtered Design 0 pareto front*

Design	Takeoff Weight (kg)	Maximum Mach Number	SEP (m/s)	Acceleration (m/s2)	Takeoff Distance (m)	Landing Distance (m)
5	23668.38	2.00	195.06	43.09	1357.06	865.02
6	23852.09	2.00	190.30	43.94	1327.13	867.51
11	24101.35	2.00	182.74	45.38	1266.44	836.22
13	24177.73	2.00	181.60	45.64	1267.11	855.09
16	24390.76	2.00	175.03	47.08	1214.27	820.51
21	23896.03	2.00	189.09	44.14	1326.35	880.20
27	23974.31	2.00	186.58	44.62	1302.32	862.69
30	24284.97	2.00	177.97	46.41	1236.11	831.74
40	24352.21	2.00	175.95	46.86	1219.78	821.83
71	24177.73	2.00	181.60	45.64	1267.11	855.09
73	23896.03	2.00	189.09	44.14	1326.35	880.20
88	23998.37	2.00	185.69	44.78	1293.06	854.65
91	24390.89	2.00	175.02	47.08	1214.28	820.52

Maximum Mach number is noted as 2.0 (same as the requirement) for all solutions, therefore this parameter has no effect on the multi-criteria decision making. SEP, acceleration, takeoff and landing distances are compliant with the requirements for all

designs. However, sizing and optimizing Design 0 has a negative effect on the specific excess power, acceleration, takeoff distance and landing distance performance.

In order to properly select and aircraft from the filtered set of solutions, one must apply the "design intentions" by selecting criteria weights for each property of the aircraft. For the purposes of this thesis, the takeoff weight is normalized to minimum takeoff weight within the filtered pareto solutions. Rest of the parameters are normalized to the requirements. User defined criteria weights, normalized criteria values and weighted qualities are presented in Table 5.13 for all filtered design solutions.

Table 5.13. *Multi-criteria decision making for Design 0*

Criteria Weight	0.2	0.2	0.2	0.05	0.05	0.1	0.1	0.1	
Design	Takeoff Weight	Supercruise Mach Number	Subsonic Sustained G	Maximum Mach Number	SEP	Acc	Takeoff Distance	Landing Distance	Weighted Quality
5	**0.00**	**0.08**	**0.00**	**0.00**	**0.56**	**0.14**	**0.10**	**0.42**	**0.110**
6	-0.01	0.06	0.02	0.00	0.52	0.12	0.12	0.42	0.106
11	-0.02	0.03	0.03	0.00	0.46	0.09	0.16	0.44	0.100
13	-0.02	0.03	0.04	0.00	0.45	0.09	0.16	0.43	0.099
16	-0.03	0.00	0.04	0.00	0.40	0.06	0.19	0.45	0.092
21	-0.01	0.06	0.03	0.00	0.51	0.12	0.12	0.41	0.105
27	-0.01	0.05	0.03	0.00	0.49	0.11	0.13	0.42	0.103
30	-0.03	0.01	0.04	0.00	0.42	0.07	0.18	0.45	0.095
40	-0.03	0.00	0.04	0.00	0.41	0.06	0.19	0.45	0.093
71	-0.02	0.03	0.04	0.00	0.45	0.09	0.16	0.43	0.099
73	-0.01	0.06	0.03	0.00	0.51	0.12	0.12	0.41	0.105

It is observed that design solutions with higher sustained g capability require more takeoff weight, have less specific excess power and accelerate slower. Weighted quality results show that Design 5 from the solution set is the "best" solution following the designer's goals. This indicates that with the design intentions (criteria weights

proposed here), aircraft in the pareto front towards the higher supercruise Mach number have increased weighted qualities.

5.3. Design 5

A more detailed look on the results of Design 5 is presented in this section. The geometry details, aerodynamics, weight and performance results are given.

5.3.1. Geometry Results

Visual definition of the aircraft helps the user to understand the component interactions and the feasibility of the model compared to competitors. Therefore, Design 5 geometry is recreated in the OpenVSP environment as shown in Figure 5.23.
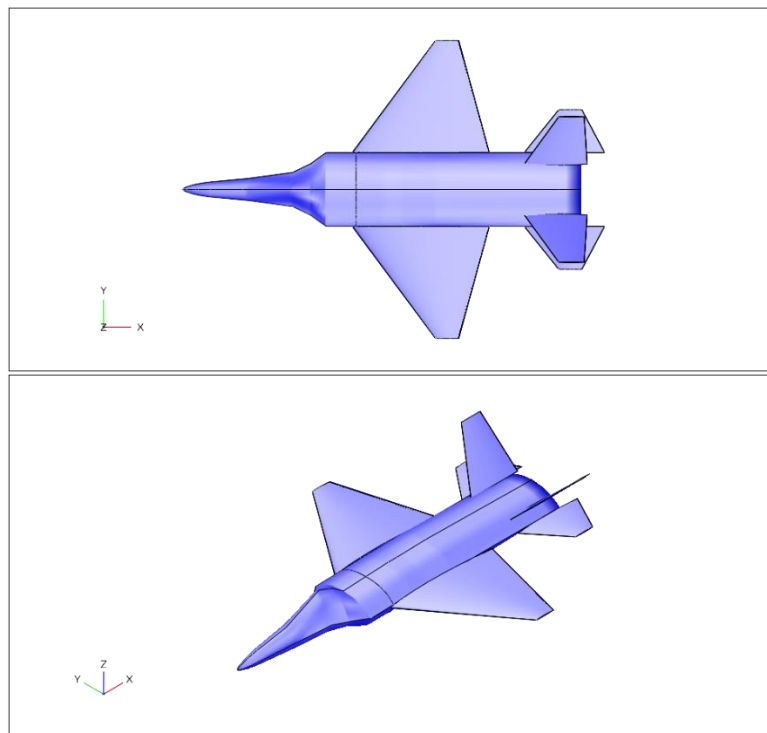
Figure 5.23. Design 5 CAD geometry

Summary of the geometry parameters are presented in Table 5.14. Compared to Design 0 (initial design), the fuselage length is increased by 12% and the wing area is increased by 1.9%.

Table 5.14. *Geometry parameters of design 5*

Parameter	Value
Fuselage Length (m)	17.31
Fuselage Maximum Depth (m)	2.04
Fuselage Maximum Width (m)	3.2
Wing Planform Area (m^2)	55.41
Wing Span (m)	12.9
Wing Aspect Ratio	3
Wing Pitch-up Tendency Transonic Aspect Ratio	1.53
Wing Leading-Edge Sweep (deg)	36.71
Wing Trailing-Edge Sweep (deg)	-15.31
Horizontal Tail Volume Coefficient	0.2
Vertical Tail Volume Coefficient (each)	0.05

5.3.2. Weight Results

Weight analysis results of Design 5 is shown in Table 5.15. Compared to Design 0, the weight results under the empty weight and the usable fuel weight have increased. Total of 19.75% increase in mission takeoff weight is observed.

Table 5.15. *Weight results of Design 5*

Weight Group	Value (kg)
Structure Group	6635
Propulsion Group	3371
Systems and Equipment Group	3143
Operating Empty Weight	14702
Payload Weight	1128
Total Usable Fuel Weight	7838
Mission Takeoff Weight	23668

5.3.3. Aerodynamic Results

Lift curve slope of Design 5 is estimated as shown in Figure 5.24. No significant change to the Design 0 lift curve slope is observed. This is caused by the fact that both designs have similar wing geometries, especially in terms of the aspect ratio.
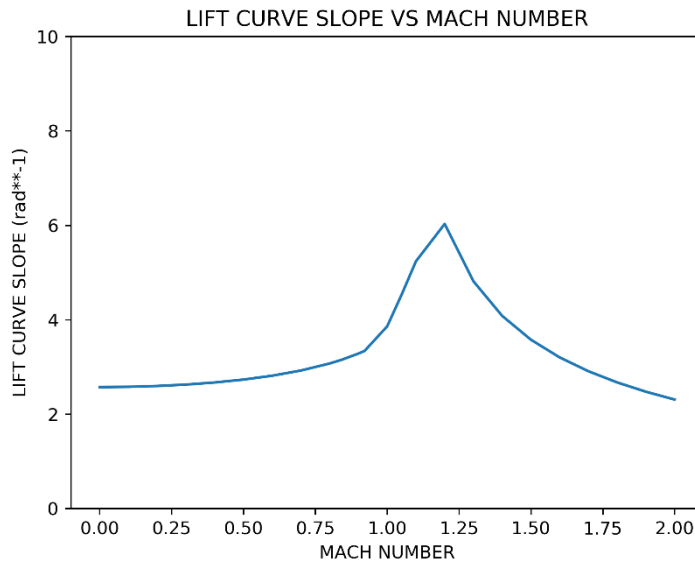
Figure 5.24. Lift curve slope of Design 5

Zero lift drag coefficient at sea level and 11250 m altitude is presented in Figure 5.25. It is observed that Design 5 has less "zero-lift" drag coefficient when compared to Design 0 at subsonic, transonic and supersonic Mach numbers.
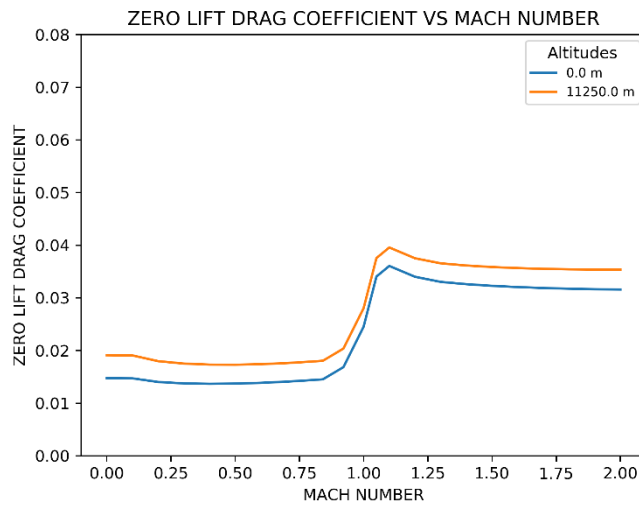
Figure 5.25. Zero lift drag coefficient curve of Design 5 at sea level and 11250 m altitudes

In order to properly compare the drag data between Design 0 and 5, the actual drags are computed at 9000 meters altitude and illustrated in Figure 5.26. Transonic and supersonic drag difference between Design 0 and Design 5 is observed. Design 5 is a more slender aircraft then Design 0, that is why its drag performance at high Mach numbers is more suited for supersonic flight.
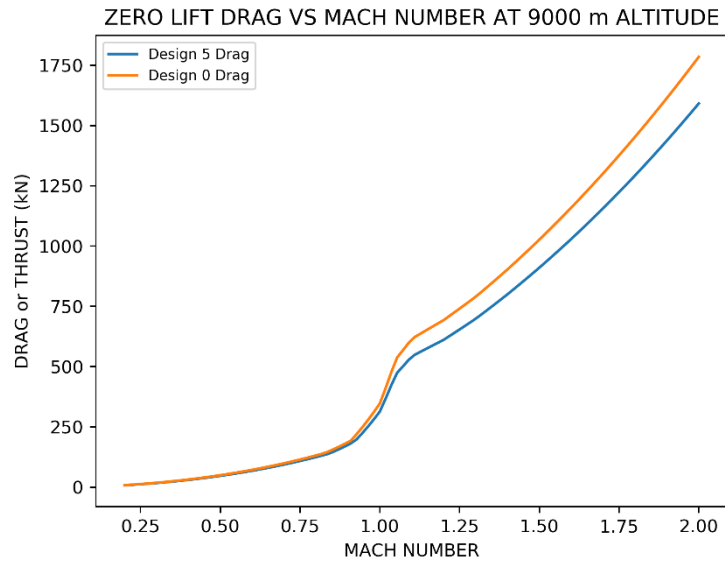
Figure 5.26. Zero-lift drag comparison for Design 0 and Design 5 at 9000 m altitude

Drag due to lift factor with no suction and with full suction for Design 5 is shown in Figure 5.27.
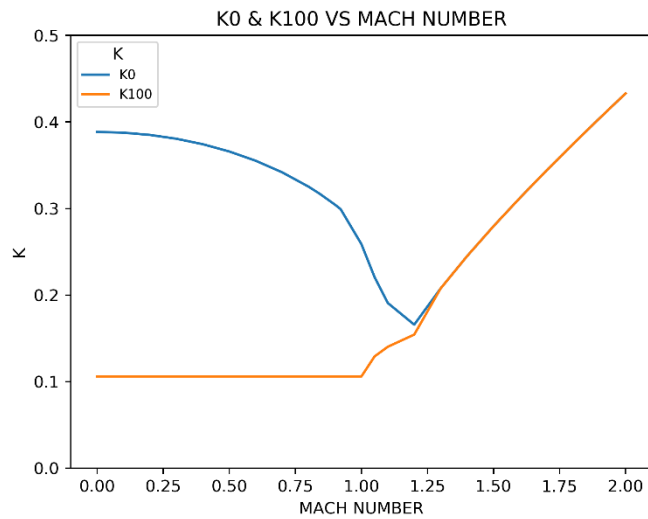
Figure 5.27. Drag due to lift factor (0 and 100% suction) for Design 5

Drag polar at 0.9 Mach number 9000 m altitude (cruise conditions) for Design 5 is shown in Figure 5.28.
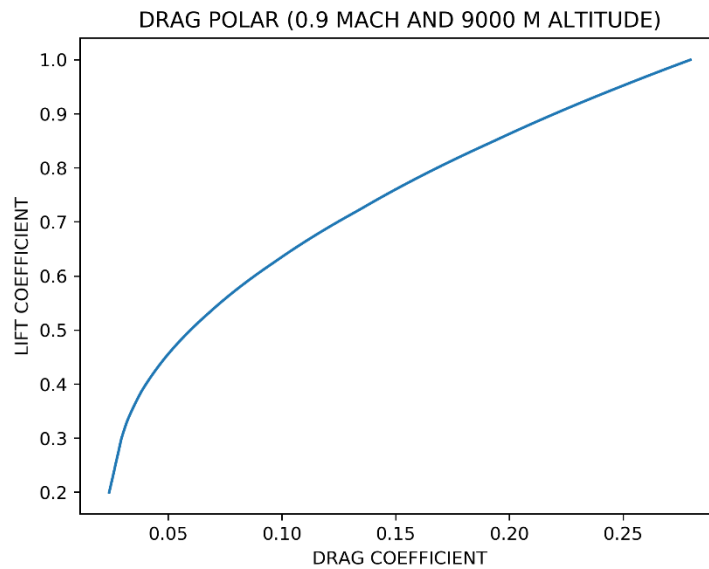
Figure 5.28. Drag polar of Design 5 at 0.9 Mach and 9000 m altitude

5.3.4. Performance Results

Mission performance results of Design 5 is presented in Table 5.16. It is observed that the total usable fuel from weight analysis (7838 kg) is within tolerance to fly this mission since fixed aircraft mission performance fuel consumption was estimated as 7841 kg (3 kg fuel difference can be neglected).

Table 5.16. *Mission performance details of Design 5*

Segment	Weight(kg)	Mach Number	Altitude (m)	Distance (km)	Total Time (min)	Total Fuel (kg)
Hangar	23668.38	0	0	0	0	0
Takeoff	23565.25	0.35	0	0.85	9.51	103.13
Accelerate	23383.78	0.90	0	5.52	25.10	284.59
Climb	23099.34	0.90	9000	16.79	83.55	569.04
Fly (distance)	20721.09	0.90	9000	616.79	2278.02	2947.29
Accelerate	20540.97	1.40	9000	627.34	2305.07	3127.41
Fly (max dry)	20171.12	1.51	9000	677.56	2415.13	3497.26
Accelerate	20171.12	1.20	9000	677.56	2415.13	3497.26
Sustained Turn	19852.55	1.20	9000	678.37	2457.39	3815.82
Launch Weapons	18724.55	1.20	9000	678.37	2457.39	3815.82
Accelerate	18646.84	1.40	9000	682.75	2467.70	3893.54
Climb	18646.84	1.40	9000	682.75	2467.70	3893.54
Fly (max dry)	18279.75	1.52	9000	732.87	2576.48	4260.63
Accelerate	18279.75	0.90	9000	732.87	2576.48	4260.63
Fly (distance)	15979.07	0.90	9000	1332.87	4770.95	6561.31
Loiter	14698.86	0.50	3048	1332.87	5970.95	7841.51

The point performance analysis is completed and the results are presented in Table 5.17. Results presented here are all compliant with the requirements.

Table 5.17. *Point performance analysis of Design 5*

Performance	*Value*
Maximum Mach number	2.0
Specific excess power (m/s)	195
Acceleration (s)	43.0
Takeoff distance (m)	1357
Landing distance (m)	865

Supercruise Mach number	1.51
Subsonic sustained G	3.8

Although specific excess power, acceleration, takeoff distance, landing distance and subsonic sustained G performance reduced in Design 5 compared to Design 0, it is designed so that it can successfully fly the design mission. Also, the amount of reduction in subsonic sustained G is coming from the multi-criteria decision-making analysis. The results with higher subsonic sustained g results are part of the pareto-front, however Design 5 being more slender design compared to rest of the solutions has the most weighted quality. Even though "best" solution is declared as Design 5, practically "best" solution can be any aircraft from the pareto-front, depending on the criteria weights assigned.

CHAPTER 6

CONCULUSION AND FUTURE WORK

6.1. Conclusion

A research on proposed fighter aircraft conceptual design synthesis by introducing initial engine scaling has been completed. Methodologies found from literature survey for geometry, weight, aerodynamics and flight performance analysis has been coded into the design framework. After completing the development of capability to analyze any given aircraft model, a fixed wing aircraft sizing algorithm has been developed. An optimization module that uses wing planform parameters as independent design variables has been introduced.

Initial engine performance data has been scaled with the competitor aircraft (F-15) aerodynamic drag performance at supercruise requirement conditions. System layout and the external surfaces have been generated using the parametric CAD design tools based on the scaled engine specifications. Fixed wing aircraft analysis has been conducted for initial concept (Design 0) and it has been observed that even though aircraft met all the other requirements, it could not successfully complete the design mission profile using the available fuel capacity. This has proven the importance of aircraft sizing. Without the present aircraft sizing methodology, remodeling of the aircraft manually would be inefficient. Using present sizing algorithms allows user to size the aircraft within seconds of computation time.

Using optimization algorithms, Design 0 has been modified and sized within the design space in order to obtain pareto-front solutions. Objectives have been selected as two trade-off performance figures of merit for modern fighter aircraft - supercruise Mach number versus subsonic sustained load factor. Optimization constraints have been applied for tip chord length and the trailing edge sweep angle to account for

decisions coming from competitor or historical aircraft. Then, the pareto-front solutions that are not compliant with the requirements have been eliminated. Thirteen design solutions have been left for reference aircraft selection. Within multi-criteria decision analysis, criteria weights have been introduced for each significant merit. Calculation of weighted quality has made reference aircraft selection possible. Even though Design 5 was chosen through this process, it has been observed that any of the thirteen aircraft could be selected depending on the assigned criteria weights. It has been found to be acceptable to make a subjective decision among aircraft that are compliant with the requirements.

Design 5 results have proven that starting with initial engine scaling improved the fighter aircraft conceptual design because a requirements compliant aircraft has been achieved with first configuration design generated with the scaled engine. Without the initial engine scaling, aircraft performance of configuration created with the original engine data would have to be analyzed first. Then by comparing the results, second round of configuration development would be necessary.

Characterizing each aircraft to its wing parameters resulted as a successful optimization since all independent design variable combinations produced unique aircraft specifications. Although the range of the independent design variables could be increased, for the purposes of the present thesis, the selected variables has been found to be sufficient.

6.2. Future Work

Aircraft design methodologies are developing each day by the improvements of the technology. All new-time consuming, higher fidelity methods could be applied during the design synthesis. High-end computing capabilities could made compute-intensive methods such as FEM or CFD to be able to support conceptual design. A methodology of these methods working with the parametric model generated for the design synthesis could be studied. It is useful to take close attention here that all the methods that have been presented in this thesis identify the advantages and the disadvantages

of the conceptual model, but these methods neglect the way how "bad" the aircraft has been designed. For example, the volume distribution of the aircraft is important for the drag calculations, but actual CFD results for conceptual parametric geometry could result in worse drag estimations due to aerodynamically inappropriate surface generation, which would be paid greater attention to at later design stages.

Another study could be the implementation of the design synthesis code here to a high-performance computing (HPC) systems. Since each design evaluation has been solved sequentially and population size must be solved until the next off-spring design, number of processors equal to the population size could be used to estimate the results fastest. For example, it takes 375 minutes to run 1500 designs with 3 processors with population of 100, using 100 processors 1500 design evaluations are expected to take 11.25 minutes which is 97% faster than the computation time spent in this thesis. Usually, the relationship is not linear.

REFERENCES

[1]   S. N. Mullin, "The Evolution of the F-22 Advanced Tactical Fighter," *AIAA Pap. 92-4188*, 1992.

[2]   M. J. Hirschberg, A. C. Piccirillo, and D. C. Aronstein, *Advanced Tactical Fighter to F-22 Raptor: Origins of the 21st Century Air Dominance Fighter*. American Institute of Aeronautics and Astronautics, Inc., 2012.

[3]   D. Raymer, *Aircraft Design: A Conceptual Approach, Sixth Edition*. 2018.

[4]   E. Torenbeek, *Advanced Aircraft Design*. John Wiley & Sons, Inc., 2013.

[5]   A. H. Robin S. Lineberger, "Program management in aerospace and defense," *Deloitte*, 2019. [Online]. Available: https://www2.deloitte.com/content/dam/Deloitte/us/Documents/manufacturin g/us-manufacturing-program-management-aerospace-defense.pdf. [Accessed: 29-Jun-2019].

[6]   E. M. Botero *et al.*, "SUAVE: An Open-Source Environment for Conceptual Vehicle Design and Optimization," 2016.

[7]   R. A. McDonald, "Advanced Modeling in OpenVSP," 2016.

[8]   H. Feng, M. Luo, H. Liu, and Z. Wu, "A knowledge-based and extensible aircraft conceptual design environment," *Chinese J. Aeronaut.*, 2011.

[9]   D. P. Wells, B. L. Horvath, and L. A. McCullers, "The Flight Optimization System Weight Estimation Method," *NASA/TM-2017-219627*, vol. 1, 2017.

[10]   D. P. Raymer, "Enhancing Aircraft Conceptual Design Using Multidisciplinary Optimization," Kungliga Tekniska Högskolan Royal Institute of Technology, 2002.

[11]   S. A. Brandt, "The Effect of Initial Engine Sizing on Fighter Aircraft Final Optimized Size and Cost," in *AIAA 2018-3834*, 2018.

[12]   M. Ayar, K. M. Güleren, and M. Cavcar, "Application Of Analytic Network Process In Evaluating Initial Training Aircraft," in *9th Ankara International Aerospace Conference*, 2017.

[13]   R. D. Finck, "USAF Stability and Control DATCOM," 1978.

[14]   MIL-STD-3013, "Glossary of Definitions, Ground Rules, And Mission Profiles To Define Air Vehicle Performance Capability," 2003.

[15]   C. A. Crawford and S. E. Simm, "Conceptual Design and Optimisation of Modern Combat Aircraft," in *Aerodynamic Design and Optimisation of Flight Vehicles in a Concurrent Multi-Disciplinary Environment*, 1999.

[16] E. W. Weisstein, "Bézier Curve," *From MathWorld--A Wolfram Web Resource.* [Online]. Available: http://mathworld.wolfram.com/BezierCurve.html. [Accessed: 26-May-2019].

[17] M. Hepperle, "JavaFoil." [Online]. Available: https://www.mh-aerotools.de/airfoils/javafoil.htm. [Accessed: 26-May-2019].

[18] Wikipedia, "Shoelace Formula." [Online]. Available: https://en.wikipedia.org/wiki/Shoelace_formula. [Accessed: 26-May-2019].

[19] E. W. Weisstein, "Convex Hull," *From MathWorld--A Wolfram Web Resource.* [Online]. Available: http://mathworld.wolfram.com/ConvexHull.html. [Accessed: 26-May-2019].

[20] T. E. Oliphant, "SciPy: Open source scientific tools for Python," *Comput. Sci. Eng.*, 2007.

[21] ESDU 76003, "Geometrical properties of cranked and straight-tapered wing planforms," 2012.

[22] N. Nigam, S. K. Ayyalasomayajula, X. Qi, P. C. Chen, and J. J. Alonso, "High-Fidelity Weight Estimation for Aircraft Conceptual Design Optimization," 2015.

[23] J. Roskam, "Part V: Component Weight Estimation," in *Airplane Design*, 1985.

[24] B. L. Horvath and D. P. Wells, "Comparison of Aircraft Conceptual Design Weight Estimation Methods to the Flight Optimization System," 2018.

[25] ESDU 77021, "Properties of a standard atmosphere," 2005.

[26] W. R. Sears, "On projectiles of minimum wave drag," *Q. Appl. Math.*, 1947.

[27] K. Deb, A. Pratap, S. Agarwal, and T. Meyarivan, "A fast and elitist multiobjective genetic algorithm: NSGA-II," *IEEE Trans. Evol. Comput.*, 2002.

[28] D. Hadka, "Platypus," 2015. [Online]. Available: https://platypus.readthedocs.io/en/docs/index.html. [Accessed: 07-May-2019].

[29] E. Triantaphyllou, *Multi-criteria Decision Making Methods: A Comparative Study*. 2000.

[30] Jane's, "AIM-120 Advanced Medium-Range Air-to-Air Missile (AMRAAM)," *Jane's Air-Launched Weapons*, 2019.

[31] Jane's, "AIM-9 Sidewinder legacy variants (AIM-9B to AIM-9S)," *Jane's Air-Launched Weapons*, 2018.

APPENDICES

A. Propulsion Data

Propulsion data that is required for the design synthesis calculations has been generated using the afterburning turbofan engine performance charts presented in [3]. Initial afterburning turbofan engine specifications have been shared in Table A.1. The specific fuel consumption and the thrust figures for max dry and max reheat has been shared in Figure A.1.

Table A.1. *Afterburning turbofan characteristics (installed)* [3]

| Specification	Value
Sea-level static thrust, lb	30000
Sea-level static TSFC, 1/hr	1.64
Sea-level static airflow, lbm/s	246
Bare-engine weight, lb	3000
Engine length (including axisymmetric nozzle), inch	160
Maximum diameter, inch	44
Fan-face diameter, inch	40
Overall pressure ratio	22
Fan pressure ratio	4.3
Bypass ratio	0.41
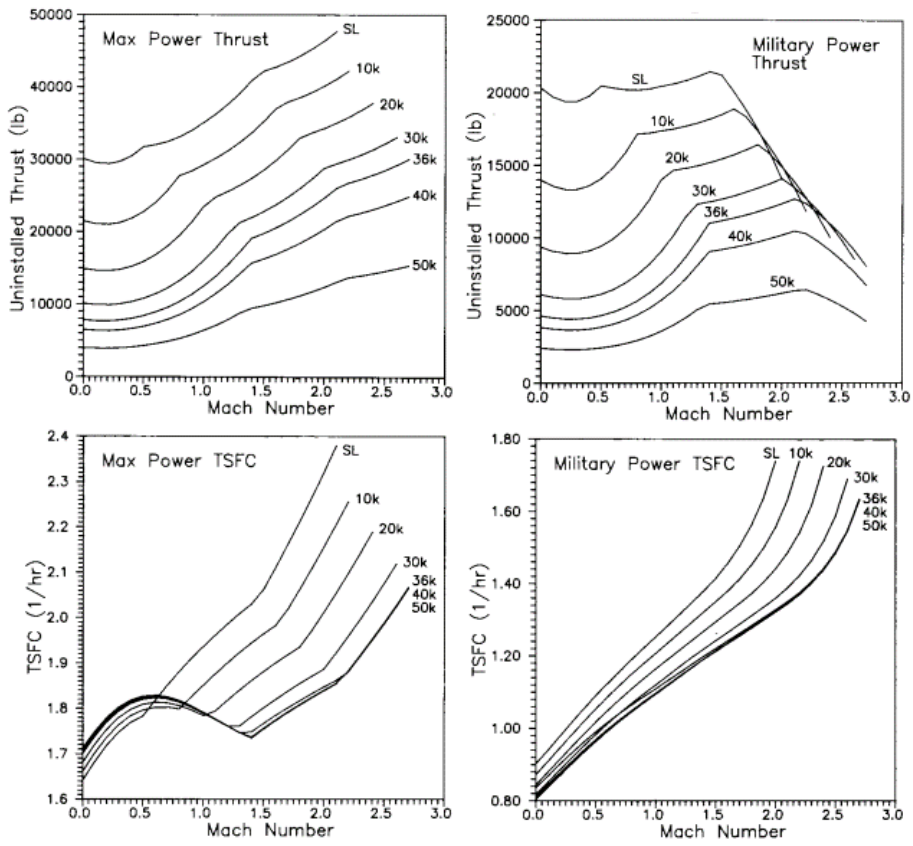
Figure A.1. Afterburning turbofan performance data for max dry and max reheat engine settings [3]

B. Weight Analysis Equations

Conceptual fighter aircraft weight estimations taken from FLOPS [9] are presented below :

Wing Weight Estimation

Equivalent bending material factor is estimated using equation below:

$$BT = \frac{\left(0.215(0.37+0.7TR)\left(\frac{SPAN^2}{SW}\right)^{EMS}\right)}{CAYL\ TCA} \tag{73}$$

Where BT is wing equivalent bending material factor. TR is the taper ratio of the wing. $SPAN$ is the wing span (ft). SW is the reference wing area (ft^2). TCA is the wing thickness to chord ratio (weighted average).EMS is the wing strut bracing factor and taken as equal to 0.0 for no wing strut. CAYL is the wing sweep factor for aeroelastic tailoring accounting and estimated by the equation presented below:

$$CAYL = (1.0 - SLAM^2)(1.0 + (C6)\ SLAM^2 + 0.03CAYA(C4)\ SLAM) \tag{74}$$

Where $C4, C6$ are factors and taken to be equal to 0.4 and 0.5 respectively to account for aeroelastic tailoring. $CAYA$ is another factor taken to be equal to 0.0 for wings with aspect ratio less than 5.0 and AR-5 for wings with aspect ratio greater than 5. $SLAM$ is the sine of the 3/4 chord wing sweep angle and estimated using equation below:

$$SLAM = \frac{TLAM}{\sqrt{1.0+TLAM^2}} \tag{75}$$

Total wing bending material weight is estimated using the equation below:

$$W1N1R = (A1)\ BT\left(1.0 + \sqrt{\frac{A2}{SPAN}}\right)(ULF)\ SPAN\ (1.0 - 0.4FCOMP)\ (1.0 - 0.1\ FAERT)(CAYF)VFACT\frac{PCTL}{10^6} \tag{76}$$

Where $W1NIR$ is the wing bending material weight (lb) without the inertia relief effects. $A1$ and $A2$ are constants presented in table below. ULF is the structural

ultimate load factor. $FCOMP$ is taken to be equal to 1.0 for maximum use of composites. $CAYF$ is equal to 1.0 for single fuselage. $VFACT$ is equal to 1.0 for lack of variable sweep. $PCTL$ is the fraction of load that wing is under with respect to all aircraft load.

Table B.2. *FLOPS wing weight constants for fighter aircraft* [9]

Consant	Value
A1	6.80
A2	0.00
A3	0.12
A4	0.65
A5	0.62
A6	0.80
A7	1.20

The wing shear material and control surface weight is estimated using the equation below:

$$W2 = A3\,(1.0 - 0.17FCOMP)SFLAP^{A4}DG^{A5} \tag{77}$$

Where $W2$ is the total shear material and control surface weight contribution of the wing (lb). $A3$ and $A5$ are constants presented in Table B.2. $SFLAP$ is the total movable wing surface area (ft²). DG is the design gross weight (lb).

Total wing miscellaneous items weight ($W3$) (lb) is calculated using the equation below:

$$W3 = A6\,(1.0 - 0.3FCOMP)SW^{A7} \tag{78}$$

Where A6 and A7 are constants presented in Table B.2.

Wing bending material weight inertia relief adjustment ($W1$) (lb) is estimated using equation below:

$$W1 = \frac{(DG)(CAYE)W1NIR + W2 + W3}{1.0 + W1NIR} - W2 - W3 \tag{79}$$

Where $CAYE$ is taken to be equal 1.0 because there are no wing mounted engines in the present thesis.

Total wing weight (W_{wing}) (lb) is calculated using the equation below:

$$W_{wing} = W1 + W2 + W3 \tag{80}$$

Horizontal Tail Weight Estimation

Horizontal tail weight (W_{ht}) (lb) is estimated using the equation below:

$$W_{ht} = 0.002 S_{ht}^{0.87} (ULF \, DG)^{0.66} \tag{81}$$

Where S_{ht} is the horizontal tail theoretical area (ft^2).

Vertical Tail Weight Estimation

Vertical tail weight (W_{vt}) (lb) is calculated using the equation below:

$$W_{vt} = 0.212 DG^{0.3} (TRVT + 0.5) NVERT^{0.7} S_{vt}^{0.97} \frac{ARVT^{0.5}}{\cos^{0.49}(SWPVT)} \tag{82}$$

Where $ARVT$ is the vertical tail theoretical aspect ratio, $SWPVT$ (deg) is the vertical tail sweep angle at quarter chord. S_{vt} is the vertical tail theoretical area per tail (ft^2). $NVERT$ is the number of vertical tails. $TRVT$ is the vertical tail theoretical taper ratio.

Fuselage Weight Estimation

The fuselage weight (W_{fuse}) (lb) is calculated using the equation below:

$$W_{fuse} = 0.15 XL^{0.9} DG^{0.61} (1.0 + 0.3 FNEF) * (1.0 + 0.33 VARSW) NFUSE^{0.3}$$

$$\tag{83}$$

$FNEF$ is the number of engines mounted on the fuselage. $NFUSE$ is the number of fuselages (1.0 in the present thesis). XL is the fuselage length (ft).

Landing Gear Weight Estimation

Main landing gear weight (W_{MLG}) (lb) is calculated using the equation below:

$$W_{MLG} = (0.0117 - 0.0012DFTE)(WLDG^{0.95})0(XMLG^{0.43}) \quad (84)$$

Where DFTE is a factor equal to 1.0 for fighter aircraft type. WLDG is the aircraft design landing weight (lb). XMLG is the length of the extended main landing gear oleo, in.

Nose landing gear weight (W_{NLG}) is calculated using the equation below:

$$W_{NLG} = (0.048 - 0.008DFTE)WLDG^{0.67}XNLG^{0.43}(1.0 + 0.8CARBAS)$$

$$(85)$$

Where $CARBAS$ is equal to 0.0 for land-based aircraft.

Paint Weight Estimation

Aircraft paint weight ($WTPNT$) (lb) is estimated by the equation below:

$$WTPNT = WPAINT(SWTWG + SWTHT + SWTVT + SVTFU) \quad (86)$$

Where $WPAINT$ is the area density of paint (lb/ft^2). $SWTWG$ is the wing wetted area (ft^2). $SWTHT$ is the horizontal tail wetted area (ft^2). $SWTVT$ is the vertical tail wetted area (ft^2). $SVTFU$ is the fuselage wetted area (ft^2).

Air Induction System Weight Estimation

Air induction system weight ($WAIS$) (lb) is calculated by the equation below:

$$WAIS = 1.06(THRUST\ NEF)^{0.23}(WF + DF)^{1.4}VMAX^{0.83} \quad (87)$$

Where NEF is the number of fuselage mounted engines. WF is the maximum fuselage width (ft). DF is the maximum fuselage depth (ft). $VMAX$ is the maximum Mach number.

Engine Controls Weight Estimation

Engine controls weight (WEC) (lb) is calculated by the equation below:

$$WEC = 0.106(NENG\ THRUST\ NFLCR)^{0.55} \tag{88}$$

Where $NENG$ is the total number of engines. $THRUST$ is the thrust of each engine (lb). $NFLCR$ is the number of flight crew.

Engine Starters Weight Estimation

Engine starters weight ($WSTART$) (lb) is estimated by the equation below:

$$WSTART = 11\ FNENG\ VMAX^{0.32}FNAC^{1.6} \tag{89}$$

Where $FNAC$ is the average diameter of each engine (ft).

Fuel System, Tanks and Plumbing Weight Estimation

The total fuel system weight ($WFSYS$) (lb) is calculated using the equation below:

$$WFSYS = 1.07FMXTOT^{0.58}FNENG^{0.43}VMAX^{0.34} \tag{90}$$

Where $FMXTOT$ is the aircraft total fuel capacity (lb).

Surface Controls Weight Estimation

The surface controls weight (WSC) (lb) is estimated using the equation below:

$$WSC = 2.95\ SFLAP^{0.45}DG^{0.36} \tag{91}$$

Where SFLAP is the total movable wing surface area (ft^2).

Auxiliary Power Unit Weight Estimation

The auxiliary power unit weight ($WAPU$) (lb) is calculated using the equation below:

$$WAPU = 54\,FPAREA^{0.3} + 5.4 \tag{92}$$

Where $FPAREA$ is the fuselage planform area (ft^2).

Instruments Weight Estimation

The instruments weight (WIN) (lb) is calculated using the equation below:

$$WIN = 0.09NFUSE\,XL\,DF * (1.0 + 2.5\,NFLCR + 0.1\,FNEW + 0.15\,FNEF) \tag{93}$$

Where $FNLCR$ is the number of flight crew.

Hydraulics Weight Estimation

The hydraulic weight ($WHYD$) (lb) is estimated using the equation below:

$$WHYD = 0.55\,(FPAREA + 0.27\,SW)\,(1.0 + 0.03\,FNEW\,0.05\,FNEF)\,VMAX^{0.01} \tag{94}$$

Where $FPAREA$ is the fuselage planform area (ft^2).

Electrical Weight Estimation

Electrical weight ($WELEC$) (lb) is estimated using the equation below:

$$WELEC = 10\,(XL + B)^{0.85}\,NFUSE^{0.27}\,VMAX^{0.1}\,(1.0 + 0.1\,NFLCR) \tag{95}$$

Avionics Weight Estimation

Avionics weight ($WAVONC$) (lb) is estimated using the equation below:

$$WAVONC = 0.43\,(NFUSE\,XL\,DF)^{1.3}\,VMAX \tag{96}$$

Furnishings and Equipment Weight Estimation

Furnishing and equipment weight ($WFURN$) (lb) is calculated using the equation below:

$$WFURN = 80\ NFLCR\ VMAX^{0.38}\ XL^{0.25} \qquad (97)$$

Air Conditioning Weight Estimation

Air conditioning weight (WAC) (lb) is estimated using the equation below:

$$WAC = 0.75\ WAONC + 0.37\ FNENG\ THRUST^{0.6}\ VMAX^{0.57} \qquad (98)$$

Flight Crew and Baggage Weight Estimation

Flight crew and baggage weight (WFLCRB) (lb) is calculated using the equation below:

$$WFLCRB = NFLCR\ 215 \qquad (99)$$

Unusable Fuel Weight Estimation

Unusable fuel weight (WUF) (lb) is estimated using the equation below:

$$WUF = 11.5\ FNENG\ THRUST^{0.2} + 0.04\ SW \qquad (100)$$

Engine Oil Weight Estimation

Engine oil weight ($WOIL$) (lb) is estimated using the equation below:

$$WOIL = 0.082\ FNENG\ THRUST^{0.65} \qquad (101)$$

Wing Fuel Capacity Estimation

Wing fuel capacity ($FULWMX$) (lb) is calculated using the equation below:

$$FULWMX = FWMAX\ SW^2\ TCA\ \frac{\left(1.0 - \frac{TR}{1.0 + TR^2}\right)}{SPAN} \qquad (102)$$

C. Optimization Procedure

Details of the optimization procedure towards maximum number of (1500) iterations are presented in this section by pareto-front results after 500 iterations and 1000 iterations.
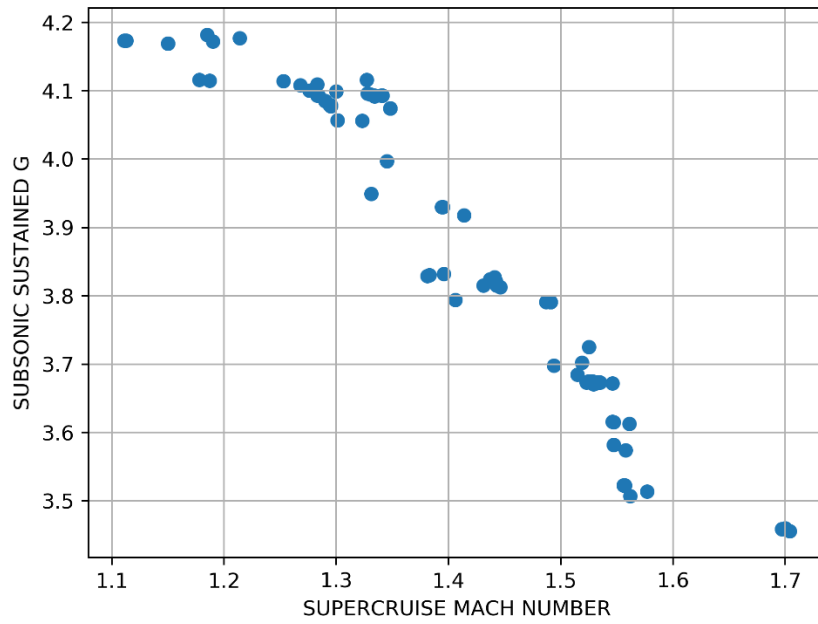
Figure A.2. Sizing optimization of Design 0 after 500 iterations
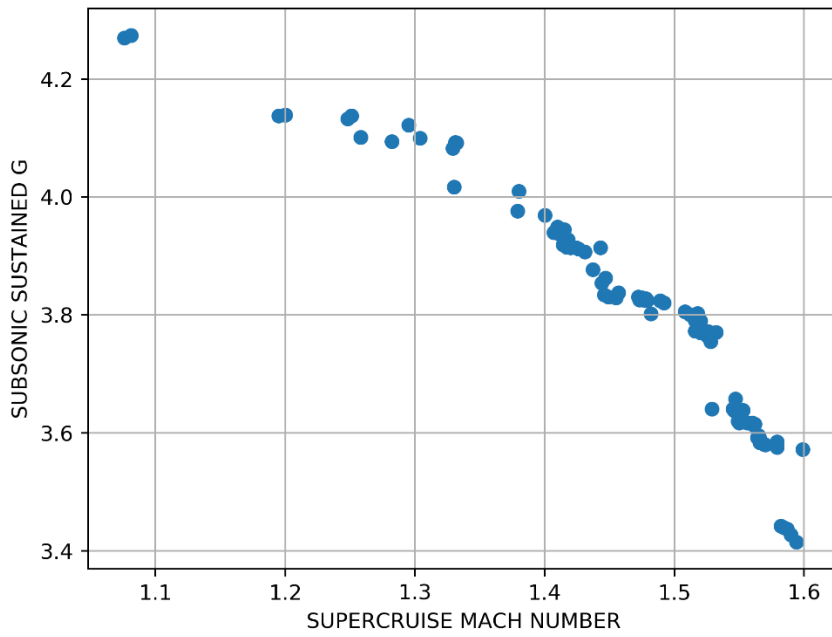
Figure A.3. Sizing optimization of Design 0 after 1000 iterations
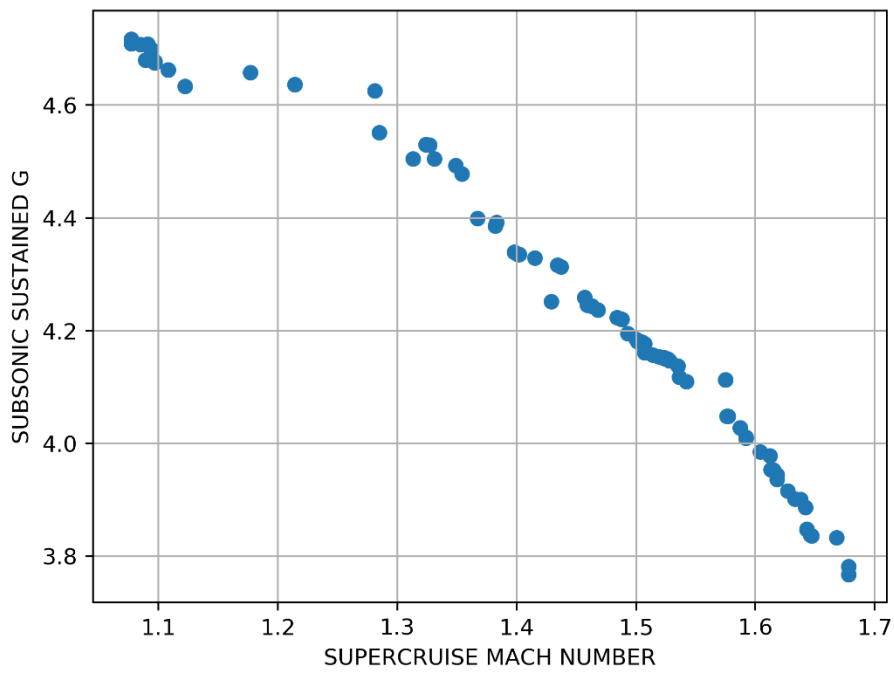

Figure A.4. Sizing optimization of Design 0 after 1500 iterations

116

D. Tool Validation: F-22 Class Aircraft Analysis

An F22 class aircraft geometry has been modeled in OpenVSP as presented in Figure A.5 [11].
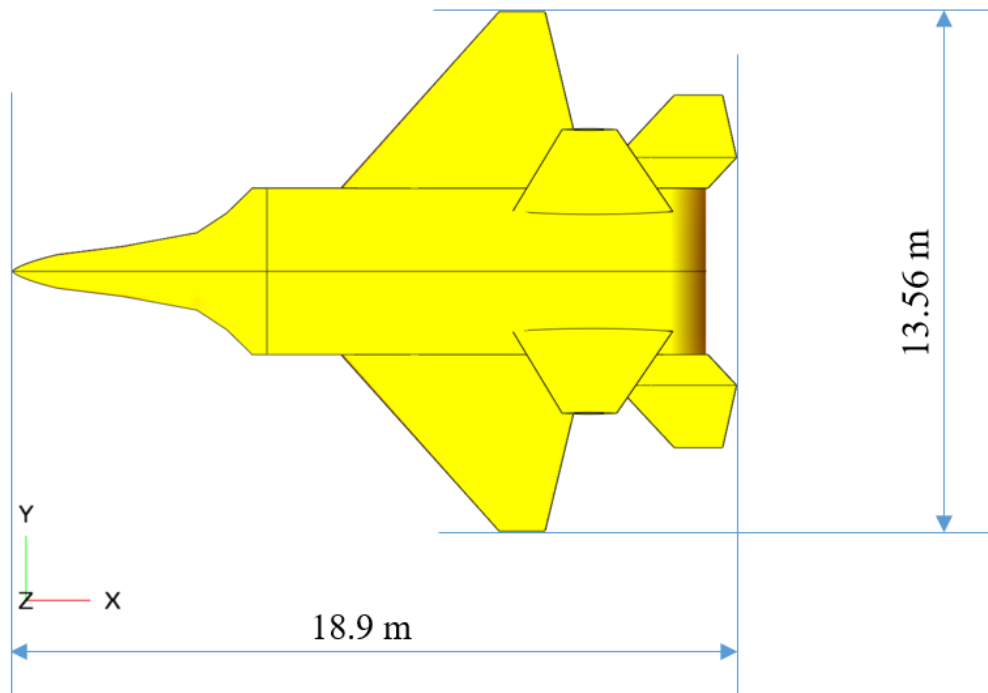

Figure A.5. F-22 class aircraft geometry modelled in OpenVSP

Same engine used in this study has been scaled by the same methodology in the engine scaling section to produce 22000 lb thrust at 40000 ft and 1.6 Mach (F-22 drag estimation [11]). Weight analysis results are shown in table below:

Table A.3. *Weight analysis comparison*

Weight	Analysis	Literature [11]
Operating Empty Weight (kg)	19298	19700
Total Usable Fuel (kg)	8288	8181

Flight performance requirements and results are presented in table below:

Table A.4. *Flight performance analysis comparison*

Flight Performance Merit	Analysis	Requirement [11]
Maximum Mach Number	2.0	2.0
SEP (ft/s)	670	400
Acceleration (s)	44.2	50.0
Total Takeoff Distance (ft)	3571	3000
Total Landing Distance (ft)	3024	3000
Supercruise Mach Number	1.66	1.6
Sustained Turn Load Factor	3.32	4.0

The geometry used for validation is created at low fidelity to represent an F-22 class aircraft. The engine is scaled from the engine dataset presented in [3]. Representative aircraft comparison to the F-22 requirements shows promising similarity, which support that the tool capability is sufficient to be used for conceptual design purposes.